NUMERICAL SIMULATION OF NON-LOAD BEARING LSF DOUBLE WALLS UNDER FIRE

Hiba Ben Ammar

A thesis submitted to the:

Université Libre de Tunis (ULT)

Instituto Politécnico de Bragança (IPB)

In Partial fulfilment of the requirements for the Degree of Master of
Construction Engineering

December 2020

NUMERICAL SIMULATION OF NON-LOAD BEARING LSF DOUBLE WALLS UNDER FIRE

Hiba Ben Ammar

A thesis submitted to the:

Université Libre de Tunis (ULT)

Instituto Politécnico de Bragança (IPB)

In Partial fulfilment of the requirements for the Degree of Master of
Construction Engineering

Supervised by:

Prof. Dr Paulo Alexandre Gonçalves Piloto
Prof. Dr Professor Issmail Yousfi

December 2020

Dedications

To my dear parents,

For their support during my school and student life,
For their unlimited sacrifices, for their incessant encouragement
And for their permanent benevolence ...

To my dear brother and all my family

Who always supports me and for their sacrifices
To all my dear friends

To all my IPB and ULT teachers for their support and encouragement

Acknowledgement

First of all, to God, it gives me the opportunity to have come this far to follow a dream and become a better and professional woman.

A special thank you to the Université Libre de Tunis (ULT) which guides me in this construction of knowledge in a human and technical way, and to the Polytechnic Institute of Bragança (IPB), which accepts me to broaden my horizons and receive.

Here, I would like to thank ***Professor Issam Khouzami***, ***Professor Yassin Mokadam*** and ***Professor Oussama Touati*** for their confidence in submitting a double degree.

At the end of this work, I have the honor to express my sincere thanks and my deep gratitude to my supervisor at the Instituto Politécnico de Bragança (IPB), who shared his experiences with me and helped to expand my knowledge, the Coordinating ***Professor Paulo Alexandre Gonçalves Piloto*** at the Polytechnic Institute of Bragança. I would like to thank him for his relevance, his comments and his valuable advice throughout this project.

I would particularly like to thank the members of the jury who did me the honor of judging this work. I hope this project deserves your consideration and please accept my sincere respect.

I would like to thank my supervisor of the Université Libre de Tunis (ULT), ***Professor Issmail Yousfi***, for his directives, encouragement and valuable advice. May he find my deepest gratitude here.

Finally, I do not forget to thank my family, specially my dear brother.

ABSTRACT

In recent years, light steel frame (LSF) structures, such as cold formed steel wall systems, have been used more and more, but there is a lack of adequate understanding of their fire performance. Traditionally, the fire resistance index of such non-loadbearing LSF walls, it is based on an approximate descriptive method developed on the basis of a limited fire test.

Building fire safety is generally viewed as very important by the construction industry and the community as a whole. Gypsum board is widely used around the world to protect thin gauge steel frame (LSF) walls. Gypsum contains free water, which is chemically bound in its crystal structure. Plasterboard also contains gypsum (CaSO4.2H2O) and calcium carbonate (CaCO3). The evaporation of the gypsum and the decomposition of the calcium carbonate absorb heat, thus protecting the LSF wall from fire.

[76] developed an innovative system of composite wall panels whose insulation of gypsum exterior walls and insulation of internal cavities (fiberglass) can improve the thermal and structural performance of LSF wall panels under conditions fire. In order to understand the performance of gypsum board and LSF wall panels under standard fire conditions, numerous experiments were carried out at the Fire Research Laboratory of the Queensland University of Technology [76] in (2018). Under standard fire protection conditions, Type X single plasterboard and non-load bearing LSF wall panels have been tested for fire protection.

However, no suitable digital model has been developed to study the thermal performance of LSF walls using innovative composite panels under standard fire conditions. It is inacceptable to continue to rely on expensive and time-consuming fire tests.

Based on laboratory tests, a review of the literature and a comparison of finite element analysis results of panel components, appropriate values for the important thermal properties of gypsum panels and insulating materials have been obtained [56], been proposed Sultan [56].The important thermal properties (thermal conductivity, specific heat capacity and density) of plasterboard and insulating materials were proposed [56] as a function of temperature and used in the digital model of non-load-bearing LSF wall panels.

Using these thermal properties, the developed finite element model can accurately predict the values. While there are many complexities in LSF fireless wall systems, the component temperature profile reasonably predicts the temperature distribution of the systems of non-loadbearing LSF walls.

This article presents some informations of the Finite Element Model of Gypsum Board and LSF Non-Loadbearing Wall Panel Components, including the Finite Element Model of Composite Panels developed [76] .

This article developed by [76] is based on 2 small-scale tests to verify and compare the thermal performance of composite panels made of different thermal insulation materials of different densities and thicknesses, and offers corresponding suggestions for improving LSF walls protected by these materials to composite panel. It also provides thermal performance data of LSF wall system and demonstrates the excellent performance of LSF wall system using composite panels, uses finite elements developed from the LSF wall model to provide a new LSF wall system with higher fire resistance.

The developed finite element model is particularly useful for comparing the thermal performance of different wall panel systems without the need for lengthy and expensive fire tests.

This thesis presents the numerical analysis to determine the thermal response of each model throughout fire exposure using ANSYS® Multiphysics. It was verified that the use of different experimental curves to represent the evolution of the temperature inside cavities or insulating blankets was essential to obtain better numerical results.

This thesis compares the fire resistance of two models (with insulating layer and without insulating layer) and come up with a parametric analysis.

Keywords: LSF Walls, Non Load-bearing LSF, Fire Resistance, Ansys Multiphysics, Numerical simulation .

Résumé

La sécurité incendie des bâtiments est généralement considérée comme très importante par l'industrie de la construction et l'ensemble de la communauté. Les panneaux de plâtre sont largement utilisés dans le monde entier pour protéger les murs à ossature en acier de faible épaisseur (LSF). Le plâtre contient de l'eau libre, qui est chimiquement liée dans sa structure cristalline. Les plaques de plâtre contiennent également du plâtre (CaSO4.2H2O) et du carbonate de calcium (CaCO3). La déshydratation du plâtre et la décomposition du carbonate de calcium absorbent la chaleur, protégeant ainsi la paroi LSF du feu.

[76] a développé un système innovant de panneaux muraux composites dont l'isolation des murs extérieurs en plâtre et l'isolation des cavités internes (fibre de verre) peuvent améliorer les performances thermiques et structurelles des panneaux muraux LSF dans des conditions d'incendie. Afin de comprendre les performances des panneaux de plâtre et des panneaux muraux LSF dans des conditions d'incendie standard, de nombreuses expériences ont été menées au fire research laboratory de l'Université de technologie du Queensland University of Technology [76] en (2018).

Dans les conditions standard de protection contre les incendies, des plaques de plâtre de type X monocouche et des panneaux muraux LSF non porteurs ont été testés pour la protection incendie.

Cependant, aucun modèle numérique adapté n'a été développé pour étudier la performance thermique des murs LSF utilisant des panneaux composites innovants dans des conditions d'incendie standard. Il est inacceptable de continuer à s'appuyer sur des tests au feu coûteux et longs. Par conséquent, cette recherche a développé un modèle numérique approprié pour étudier les performances thermiques des composants de plaques de plâtre et des panneaux muraux LSF non porteurs.

Sur la base d'essais en laboratoire, d'une revue de la littérature et de la comparaison des résultats d'analyse par éléments finis des composants des panneaux, des valeurs appropriées pour les propriétés thermiques importantes des panneaux de plâtre et des matériaux isolants ont été proposées par [76] . Le petit modèle en plâtre de cette étude et les résultats expérimentaux correspondants [76] . Les propriétés thermiques importantes (conductivité thermique, capacité thermique spécifique et densité) des plaques de plâtre et des matériaux isolants ont été proposées Sultan [56], en fonction de la température et utilisées dans le modèle numérique des panneaux muraux LSF non porteurs.

L’article développer par [76] présente certaines informations détaillées du modèle d'éléments finis des panneaux de plâtre et des composants de panneaux muraux non porteurs en LSF, y compris le modèle d'éléments finis de panneaux composites développé par [76] .

Le test expérimental développer par [76] basé sur 2 tests à petite échelle pour vérifier et comparer les performances thermiques de panneaux composites constitués de différents matériaux d'isolation thermique de différentes densités et épaisseurs . Il fournit également des données de performance thermique du système mural LSF et démontre les excellentes performances du système mural LSF utilisant des panneaux composites. Cet article utilise des éléments finis développés à partir du modèle de mur LSF pour fournir un nouveau système de mur LSF avec une résistance au feu plus élevée.

Le modèle d'éléments finis développé est particulièrement utile pour comparer les performances thermiques de différents systèmes de panneaux muraux sans avoir besoin d'essais au feu longs et coûteux.

Cette thèse présente l'analyse numérique pour déterminer la réponse thermique de chaque modèle tout au long de l'exposition au feu en utilisant ANSYS® Multiphysics. Il a été vérifié que l'utilisation de différentes courbes expérimentales pour représenter l'évolution de la température à l'intérieur des cavités ou des couvertures isolantes était essentielle pour obtenir de meilleurs résultats numériques.

Mots clés : Murs LSF, LSF non porteur, Résistance au feu, Multiphysique Ansys
Simulation numérique.

Contents

List of Figures

List of Tables

Notation

Latin letters:

Ai	Area of surface i
Aj	Area of surface j
c	Specific heat
C	Volumetric heat capacity
CFS	Cold-formed Steel
E	Integrity fire resistance criterion
FEM	Finite Element Method
FRR	Fire Resistance Rating
$\dot{g}$	Rate of heat generation or absorption per unit volume
hi	The thickness of the layer being considered
$\dot{h}_{c,n}$	Net conduction heat flux along n direction at the surface boundary
$\dot{h}_{c,x}$	One-dimensional conduction heat flux
$\dot{h}_{net,cv}$	Net convection heat flux
$\dot{h}_{net,r}$	Net radiation heat flux between any two grey surfaces
$\dot{h}_{r}$	Radiation heat flux emitted by a real surface
I	Insulation fire resistance criterion
kpos,exp,I	Position coefficient related to the layer (s) preceding layer i
kpos,unexp,i	Position coefficient related to the layer backing layer i
kpos,exp,n	Position coefficient related with the layer (s) preceding layer n
LSF	Light Steel Framing
LME	Liquid Metal Embrittlement
PID	Proportional Integral Derivative
R	Load-bearing fire resistance criterion
t	Time
tins	Insulation fire resistance of the assembly
tprot,0,i	Basic protection value of layer i
tprot,I	Protection value of layer i with protection function
tprot,i−1	Protection value of the layer preceding layer i
tins,0,i	Basic protaction value of layer n with insulation function
tins,n	Insulation value of layer n with insulation function
T	Temperature
$\dot{T}$	First temperature derivative with respect to time
T0	Ambient temperature
Tg	Gas temperature
Tm	Material surface temperature
U	Internal energy
$\vec{n}$	Normal unit vector

Greek letters

αcv	Heat transfer coefficient or film coefficient
ρ	Density
ρi	Desnity of the layer being considered
σ	Steffan-Boltzmann constant
λ	Thermal conductivity
εf	Fire emissivity
εi	Emissivity of surface i
εj	Emissivity of surface j
Δ	Variation
Δti	Correction time for layer I with protective function
Δtn	Correction time for layer n with insulation function
εm	Surface emissivity for a given material
ϕ	View factor
ϕij	View factor between surfaces i and j
Ω	Dominium
Ωe	Dominium of an element
ψk	Weighing function
∇	Gradient operator
∂	Del operator
∀	For all

CHAPTER 1

1. Introduction

Since prehistoric times, humans have improved their ability to construct buildings. These buildings started with stone buildings like the famous Stonehenge, and these building techniques have developed to this day. The original architectural art was designed to protect animals and climate change. Its main purpose was to improve it over the centuries, and these buildings also added new uses, such as artistic expressions, religious representations, and current buildings. It is designed to be beautiful. Even with these new goals, the search for safer structures has never ceased. Gas, electricity and sanitation in taller and more complex buildings increase the risk of fires, collapses, etc.

In order to achieve these objectives, various measures must be taken to comply with fire regulations. Although active measures have been taken to prevent or control fires (alarm systems, smoke detection, sprinklers, etc.), experience shows that fires can spread quickly in the building under the action of the heat given by the fire, the final heating of the structural elements will become apparent as the mechanical properties of building materials weaken with increasing temperature, the development of a fire can cause part or all of the structure to collapse.

Therefore, in order to ensure the safety of personnel, appropriate measures must be taken to prevent the fire from spreading and the building from collapsing. The resistance of these building elements must be determined according to three different standards, namely load Capacity (R), Integrity (E) and Insulation (I).

Usually, in order to provide protection against corrosion, the steel surface is cold formed galvanized steel with a thin layer of zinc coated on both sides this process significantly improves the durability of the entire structure, thereby reducing the number of diseases.

1.1.Objective

The primary objective of fire safety is to protect the lives of residents and emergency personnel on the premises. It also aims to protect the environment and limit material (structure and content) and economic (business continuity) damage. In order to achieve these objectives, various measures must be taken to comply with fire regulations. The main objective of this research is to develop a 2D-dimensional thermal model to study the fire resistance of LSF walls. For this, a two-dimensional model has been developed on the ANSYS 2020 software. The main focus of this research is to present the details of finite element of different type of insulations materials assemblies into both load-bearing and non-load bearing LSF walls panels including this with composite panels. However, this work presents a study across the fire effects on non-load bearing walls light steel frame LSF structure and makes a recommendation to improve the fire performance of stud walls panels to analyze the knowledge when using different configurations and materials.

This work presents a study across the fire effects on a non-loadbearing walls Light Steel Frame (LSF) structure, to improve the knowledge when using different configurations and materials. Specific tasks are included to be investigated: different types of insulation materials, position of insulation materials, (Gypsum Plasterboard, glass fibre).

The developed finite element models are particularly useful in comparing the thermal performance of different wall panel systems without time consuming and expensive fire tests.

To develop finite element models capable of simulating the thermal behavior of non-load bearing LSF wall panel, special numerical tasks are required to develop an accurate model to predict fire resistance using ANSYS Multiphysics.

ANSYS is a market leading digital simulation software used in the development of industrial products. It covers all the stages necessary for a simulation: processing of results and optimization, ANSYS offers a multiphysical computing platform integration the mechanics of fluids and structures, thermic as well as the simulation of systems and circuits.

The validation of 2D finite element model is presented using the results of experimental tests. The experimental tests should be developed to define the fire resistance of non-load bearing wall, according to EN1363-1 [1] and EN1364-1 **[**2].

1.2.LSF construction

LSF appeared at the end of the 20th century and its main advantages are: high load capacity, structural weight and a wide range of possibilities and configurations **[**3].

The definition of LSF given by **[**3] is increasingly used as a system of load-bearing and non-loadbearing elements in commercial and residential buildings, but LSF is an LSF composite wall system supported by studs and tracks.

The fire resistance of the LSF wall system is important in the emerging medium height cold formed steel structure. Therefore, detailed studies have recently been carried out to improve the acoustic, thermal (energy) and fire performance caused by non-load bearing LSF. It is necessary to develop a new LSF wall system with a higher fire resistance class to replace the traditional LSF system with cavity protection and insulating plasterboards. However, the thermal model of the LSF wall system has not been studied, in particular the new system developed by [77] .Therefore, this research will focus on the development of finite element models suitable for improving the knowledge of their thermal performance, while developing the time-temperature for these wall systems under standard fire conditions and studying the behaviour of these walls.

These panels must be rigid and secure to prevent sagging or warping of the section in between. There is a cavity on the panel, defined by the space between the interior panels and these spaces usually are used for placing ducts, ducts and cables, these spaces can be filled with protecting materials to improve fire resistance or acoustic and thermal performance. LSF with void cavities are generally used as partition walls and are the most common methods.

The requirement in these cases is a structure that will not collapse within a certain range of time between 30 and 240 minutes (or longer), depending on the national regulations.

Figure 1.1: Light Gauge Steel Framing (LSF) Systems [78, 79]

1.3.Single stud non load bearing LSF walls

Non-structural LSF is primarily used for internal partitions that do not support the external vertical or lateral load of adjacent structures. They can be assembled in different ways to provide adequate acoustic and heat insulation. Their typical frame is mainly composed of CFS studs arranged vertically and horizontally, which are connected, riveting screwing, riveting or powder fixing [5]. The frame is covered with a cover plate or a composite panel connected to the frame by self-tapping screws. If required, the insulation material can be placed inside (wall cavity) or outside (as in a composite panel), as shown in Figure 1.2.

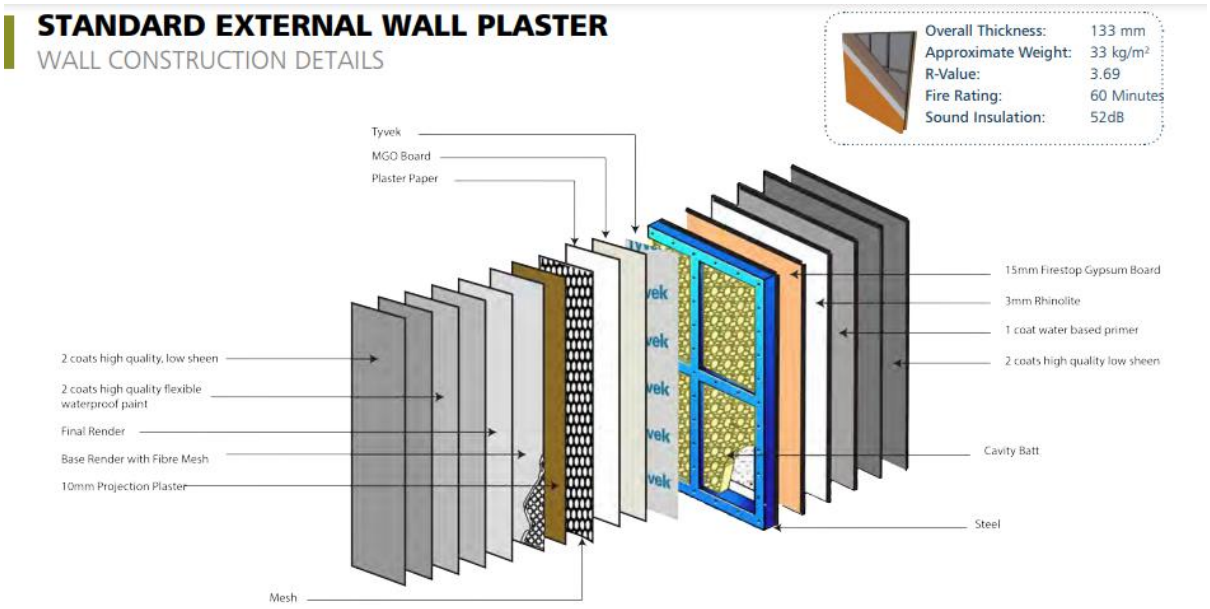

Figure 1.2: Typical single-stud LSF wall assemblies [80].

Depending on the floor-to-ceiling height, framing method, side restraint, and various design specifications, additional reinforcement using intermediate horizontal tracks may be required to provide stiffness and stability to the sides of the frame. These tracks are often called “noggin” or “blocking tracks”. The support system and the elastic profiles also improve the overall stability of the steel frame, especially in terms of supporting frames. However, when improved thermal and acoustic insulation performance and higher durability are required.

1.4.Thin -walled cold -formed steel

Steel frames are typically made from thin-walled CFS galvanized C-, U- or Z-shaped profiles with a thickness of 0.4 to 6.4 mm, depending on the application [6]. The geometry file can be configured in various forms to meet design requirements. For non-loadbearing, the most used steel profiles are C-shaped and U-shaped steels, which can be as thin as 0.46 mm for nonstructural purposes [7].

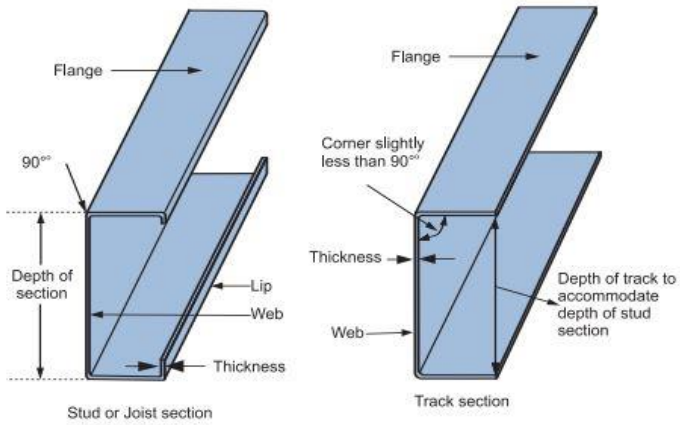

Figure 1. 3: Geometry of C-shaped studs and tracks for partition walls. Adapted from CSSBI [8].

Figure 1.3 illustrates the main geometric parameters of C-shaped and U-shaped cross sections, which are commonly used for wall studs and tracks. In addition, the web on the core and / or the rib on the flange can be used to reinforce the CFS element.

The steel frame is usually made of a thin-walled CFS galvanized C, U or Z-shaped profile and the thickness depends on the application range [6]. The geometry can be configured in various forms to meet design requirements. The most widely used steel profiles for partition walls are C-shaped and U-shaped steels [7].

1.5.Research objectives and scope

The research project developed by [76], provided large-scale results to study the structure and fire performance of both traditional and new non-loadbearing LSF composite walls systems under standard fire conditions to increase awareness of the effects, determine the parameters in today's cold formed steel structural and standard regulations used by fire engineers.

The specific tasks of this study are to,

1) Investigate the thermal behaviour of new composite LSF walls panels .

2) Present numerical model definition (convergence tests, material properties, boundary conditions, solution methods, convergence criteria). Comparison of results, validation of the numerical model.

3) Compare the fire performance (insulation) of the new LSF wall with the predictions of the full scale results developed by[76], based on full scale tests .

4) Present the details of the experimental test [76] . Present the specific heat and thermal conductivity of Gypsum plasterboards [56], Glass fiber [58], cold formed steel carbon steel [22], [52] .

5) Develop a parametric analysis with regard to different thickness of the insulation materials and increasing the thickness of the layers.

6) Present the discussion about the results and define the influence of the protection layer and the influence of LSF structure .

7) Present the main conclusion regarding to the experimental [76], and numerical simulation.

1.6. Plan of thesis

The outline of this thesis is as follows,

Chapter 1: Defines the objectives of this work and the study plan.

Chapter 2: Presents a detailed literature review to successfully conduct this research presents the cold formed steel members and light gauge steel frame (LSF) walls and explains the thermal behaviour LSF walls and introduces the new concept of cavities and composites LSF walls.

Chapter 3: Defines the Fire safety concept and explains the heat transfer theory, showing the main characteristics and the most used standard curves that quantify this event. Defines the need for fire resistant structures, further defines the heat transfer theory.

Chapter 4: Presents the details of the experimental analysis which was conducted investigate the thermal performance of non-load bearing walls lined with insulation [76]. Presents the material properties of several materials involved in the simulation, such as, the specific heat and thermal conductivity of Gypsum plasterboards, Glass fiber, cold formed steel carbon steel and air.

Chapter 5: Presents the numerical models (ANSYS 2020) validated by these experiments test [76].

Chapter 6: Present the parametric analysis, change the number of layers and test new thickness of insulating materials (increase the thickness of the cavity due to the modification of the dimension of the stud [74], through research, further discussion about the results is presented, in particular and define the influence of the protection layer and the influence of LSF structure.

Chapter 7: Presents the discussion of the results obtained . The last chapter presents also the main conclusions of this work.

CHAPTER 2

2. State of the art

The state of the art explores the current knowledge of the LSF wall panels on a time line basis taking into account the experimental and numerical investigation of LSF walls panels under fire conditions, including the behaviour of all the components. However, this behaviour depends on the level of restrains imposed to the studs and tracks, temperature fields (temperature level imposed) and displacement behaviour, failure modes. Due to the induced compressive stress caused by the thermal expansion coefficient of steel, local instabilities can be a potential failure mode of the LSF structure. Due to the definition of cross section steel members as a class 4, the compressive stress is generally less than the elastic limit. This behaviour depends on the degree of stress imposed on the studs and tracks and on the temperature level applied. This explains why the temperature field is very important during the event of a fire.

2.1.Literature review

Son and Shoub [81] carried out fire endurance tests on two load-bearing stud wall assemblies with glass fibre batt cavity insulation. Each assembly consisted of double module walls of gypsum board and steel studs. The outer plasterboards were type X Gypsum boards 15.9 mm thick while the inner ones facing the cavity between the walls were 12.7 mm in thickness. Studs used were lipped channel sections (76.2 x 44.5 x 12.7 x 1.21mm). The glass fibre insulation used in assembly two was thicker than the one used in assembly one. A uniformly distributed load of 15 kN/m was applied to each wall. On exposure to fire from one side, the structural failure of the fire exposed wall occurred in 42 minutes as compared to 67 minutes in assembly two. In both assemblies, the structural failure occurred only after the collapse of the exposed plasterboard. It was also observed, that as compared with assembly one the heat penetration in the second assembly was much slower. This was attributed to the thicker insulation used in assembly two.

The investigators recommended the use of two layers of plasterboard with staggered board joints to eliminate the direct passage of heat onto the steel studs when the joints open out in the fire.

Klippstein [82] carried out tests on ten wall panels exposed to ASTM E119 fire. The first seven of these tests were sponsored by American Iron and Steel Institute (AISI) and conducted at Underwriters' Laboratory (UL). The other tests were sponsored by U. S. Steel Corporation (USSC). The objective of these tests was to empirically determine the variation of the stud temperature and the lateral deflection of the stud during the test up to the failure of the wall, which would serve as inputs in predicting the structural behaviour of the studs when exposed to ASTM E119 or similar fires. All panels consisted of C–shaped steel studs of varying thickness and dimensions, spaced at 600 mm centres. One to three layers of (12.7 mm or 15.9 mm) gypsum boards were attached on the fire side. One gypsum board was attached to the cold side of the panels. Out of the ten wall panels, four wall panels had fibreglass insulation placed between studs and claddings as cavity insulation. The average load per stud ranged from 15.12 kN to 44.7 kN. The steel studs closer to the wall ends were seen to be at lower temperatures than the central ones, possibly due to the flow of cold air from outside into the furnace chamber caused by a negative pressure inside the furnace. The central studs being at a higher temperature than the studs at the wall ends, expanded more and consequently attracted more load during the initial phase of the fire test. In the later phase of the test the load was redistributed to the studs farther away from the central ones and the failure times of the wall panels varied from 37 minutes to 127 minutes, with the higher failure times generally seen associated with greater number of gypsum boards on the fire side and lower wall loads.

Sultan [83] ,conducted 41 full-scale wall fire resistance tests at the National Research Council of Canada, in accordance with ULC-S101 standard fire exposure, to determine the gypsum board fall temperatures from the wall panels. The tests used assemblies with wood and steel studs protected with either one or two layers of Type X gypsum board and with or without insulation in the wall cavity. The temperature criterion recorded for the fall off of the plasterboards was based on the sudden temperature rise measured on the back side of the fire exposed gypsum board caused by its failure.

The parameters studied included resilient channels, spaced either 406mm or 610 mm. installed between the gypsum board and framing for sound reduction purposes.

The insulation material used were glass and rock fibre batts and cellulosic fibre insulation either spayed wet or dry blown in the wall cavity, see Table 2.1.

Table 2.1 -Small Scale Assembly Parameters and Fire Test Results [66]

Assembly Number	Gypsum Board Layers (Exp/Unexp)	Gypsum Board Thickness (mm)	Gypsum Board Type	Insulation Type	Insulation Thickness (mm)	Point Failure (min)	Average Failure (min)
S - 09	1 X 1	12.7	X	None	-	46	46
S – 22	1 X 1	12.7	X	GF	90	46	48
S – 14	1 X 1	12.7	X	RF	40	69	72
S – 15	1 X 1	12.7	X	CF	90	69	71
S – 10	1 X 2	12.7	X	None	-	86	86
S – 23	1 X 2	12.7	X	GF	90	88	93
S – 26	1 X 2	12.7	X	RF	90	114	117
S – 18	1 X 2	12.7	X	CF	90	134	135
S – 12	2 X 2	12.7	X	None	-	129	129
S – 25	2 X 2	12.7	X	GF	90	139	139
S – 27	2 X 2	12.7	X	RF	90	160	162
S – 21	2 X 2	12.7	X	CF	90	157	163
S – 01	2 X 2	12.7	RL	None	-	82	84
S – 32	2 X 2	12.7	RL	GF	90	74	76
S – 33	2 X 2	12.7	RL	RF	90	98	101
S – 34	2 X 2	12.7	RL	CF	90	102	***

Plasterboards used were of Type X gypsum board 12.7 mm or 15.9 mm thick. The fall off temperatures for assemblies with a single layer of gypsum board, with and without insulation in wall cavity, and with different screw spacing was observed to be in the range of 755 °C to 785 °C. The fall off temperatures for both single and two layers of gypsum board was observed to havevery little difference.

Performed several small-scale fire resistance tests on gypsum board clad steel stud wall assemblies using glass fibres, rock fibres and cellulose fibres as cavity insulation. The test specimens were 914 mm in height and 914 mm in width with depth depending upon the number of layers of gypsum board used. The small-scale wall assemblies were constructed using two types of gypsum boards (regular and Type X). Details of the test specimens are as shown in Table 2.1 and Figure 2.1.

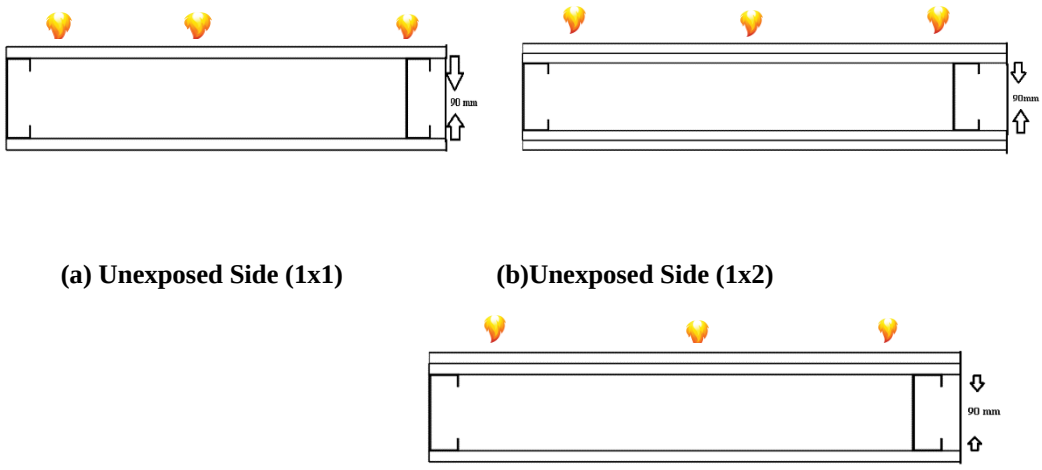

(a) Unexposed Side (1x1) **(b)Unexposed Side (1x2)**

(c) Unexposed Side (2x2)

Figure 2.1:Fire Resistance of Typical Floors, Walls and Partitions Comprising Cold-formed Steel Sections and Planar Board Protection, and Heated from One Side Only [84,5] .

The authors also observed that compared to uninsulated wall assemblies, the cavity side of the exposed gypsum board of insulated wall assemblies heated up more rapidly reaching temperature levels of 700°C far earlier as compared to the temperature rise of the exposed gypsum board in an uninsulated wall assembly. Compared to the uninsulated assemblies, the assemblies with cavity insulation recorded much higher temperatures on the exposed side of the cavity just after the calcination of the exposed board. The authors also observed that, in the case of type X gypsum board, the temperature increase was primarily due to the burning of combustible material used in the insulation, whereas with regular gypsum boards the temperatures on the exposed side of the cavity were comparable to the furnace temperatures implying a rapid and extensive failure of the gypsum board. The advantage gained in the use of cavity insulations was that, the board on the ambient side remained at a much lower temperature for a longer time as compared to the board in the uninsulated wall assembly.

After the failure of the gypsum board on the exposed side, the cavity insulation helped in providing some initial protection against fire to the gypsum board on the ambient side. This protection offered was around 5 – 10 minutes with glass fibres, 10 – 15 minutes with rock fibres and 25 - 30 minutes with cellulose fibre insulation. The increase in temperature of the unexposed gypsum after the initial protection period was found to be most rapid in case of assembly with glass fibre insulation in the cavity. The temperature in the cavity was seen to exceed even those measured in the uninsulated assembly, thus giving a neutral effect on the fire resistance of assemblies constructed with type X gypsum board. For regular gypsum board assemblies, this increased temperature led to

an earlier failure of the boards, thus in fact, lowering the fire resistance rating of the assembly below that of the uninsulated assembly.

The authors remarked that the Rock and Cellulose fibre cavity insulations, gave approximately a 30-minute improved fire resistance when compared with uninsulated wall assemblies.

SCI Publication [84,5], presents guidance for the fire resistance of protected sections in floors or walls acting as compartment boundaries, it is means planar protection. In this case, heat is applied from one side only and the floors or walls must satisfy the necessary insulation criterion. Design tables are presented for typical materials and section sizes. Table 4 of this publication defines the fire resistance time in respect of different parameters such as the number of plasterboards, protection thickness, type of plasterboard and insulation.

Alfawakhiri [69], used the thermal properties gained from literature review and calibrated them to produce a good match of numerical and test results.

It was believed that these apparent thermal properties, to some degree, implicitly account for physical phenomena other than heat transfer, such as mass transfer, and phase change.

The presence of the steel frame was neglected in the heat transfer simulations, because, due to the light weight of thin gauge members, they play a minor role in the heat transfer mechanism.

Another parameter that has a major effect on simulated temperature histories is the fall-off time of gypsum board layers. The spalling of gypsum boards was modelled by removing it from the simulation at a user-specified time. The fall-off time is the beginning of layer spalling based on visual test observations.

In the retrospective simulations, these times were slightly adjusted in order to represent a time when a significant portion of the layer had fallen off. In both simulated and measured temperature histories, the fall-off of gypsum board layers is usually manifested in respective time-temperature curves by sudden shifts in temperature closely approaching the furnace temperature.

In the study of Zhao et al[85] ,different computer codes such as ABAQUS, ANSYS and FLUENT were used to investigate the validity of heat transfer analysis. The results obtained from these different computer codes showed a good agreement between them and it was considered that all these computer codes are available for heat transfer analysis if one of them is validated against tests.

It was assumed that conduction is the main heat transfer mechanism in the steel studs and plasterboards of LSF walls. Convection and radiation act essentially for heat transfer from fire to plasterboards. As simplification, radiation effects within the plasterboards were neglected. In numerical models, on-linearity due to temperature dependency of material properties and boundary conditions were taken into account. The height and the cross-section size of the stud were considered as parameters affecting the thermal behaviour. However, the mass transfer in materials such as moisture movement was not simulated, physical experiments have shown that as the porosity of glass fibre insulating material increases, the amount of glass fibre decreases and the effective heat transfer coefficient of the material also decreases.

This is in accordance with the fact that the coefficient of thermal conductivity of glass is quite large compared to that of air.

Mathematical and numerical analyses of dehydration of gypsum plasterboards exposed to fire was carried out by [86], and it was found that the radiative heat transfer between the unexposed surface and the surrounding cannot be neglected.

In numerical simulations, stress-free thermal bowing deflections were assumed to remain constant when temperature difference across the depth of the steel stud decreased. The total horizontal deflection at stud mid-height was calculated by adding the thermal bowing deflection to the deflection due to the average stud load.

An iterative procedure was used to determine the applied critical temperatures, at which predicted steel stud capacities were equal to the applied load. These critical temperatures were then compared with compression flange temperature histories to find failure times.

The temperature distribution in the flat elements such as walls, floors, and ceilings are essentially one-dimensional, with a gradient only across the thickness Opening of joints, cracking, and ablation of fire exposed gypsum-board lining caused an accelerated rise in measured temperatures.

Gunalan [87], have produced extensive thermal performance data of a range of LSF wall systems in terms of time-temperature profiles under standard fire conditions. However, there is a need to develop a validated numerical model that can simulate the observed time-temperature profiles. Once a validated numerical model is available a combination of experimental and numerical results can be used to develop time-temperature profiles for various LSF wall systems in particular for the new LSF wall system with a composite panel. There is also a need to investigate the effect of various LSF wall components on their thermal performance under both standard and more realistic fire condition. Designers can determine fire resistance of typical floors and walls see table 2.2.

Table 2.2- Fire Resistance of Typical Floors, Walls and Partitions Comprising Cold formed Steel Sections and Planar Board Protection, and Heated from One Side Only [84,5]

Form of construction	Number of layers of board	Protection thickness (mm)	Fire resistance (hours)		Notes
			Plasterboard	Fire resistance board	
Floor with ceiling protection	1	12.5	----	0.5	----
	2	12.5	0.5	1.0	+60mm glass wool mat **
	2	12.5	----	1.5	----
Non-Load-bearing walls (partitions number of layers per surface)	1	12.5	0.5	0.5	------
	1	12.5	0.5	1	+25mm glass wool mat *
	1	15	0.5	1.0	----
	2	12.5	1.0	1.5	----
	2	12.5	1.0	2.0	Box section depth >60mm
	2	12.5	1.5	2.0	----
Load bearing walls	1	12.5	----	0.5	----
	2	12.5	0.5	1.0	-----
	2	15	----	1.5	-----

Glass wool mat is required for insulation purposes for more than 30 minutes fire resistance for floors, the glass wool mat is only necessary for fire resistant suspended ceilings.

2.2.Single stud LSF Walls

Sultan and Kodur [9] analysed the parameters that affect the fire resistance of conventional full-size empty drywall components under standard fire conditions. Tests 1 to 4 were clad with one type X gypsum board on the fire side, while the unexposed side was clad with two type X gypsum boards. Tests 2, 3 and 4 used insulating materials. made of glass fibre rock fibre and cellulose fibre (wet blown) with a thickness of 90 mm, respectively. Test 1 was not used, not isolated. The results show that the performance of test 3 is better than that of test 1 (fire resistance is improved by 54%), because the insulating material can delay the average temperature rise in the cavity on the unexposed side of the gypsum board, even after the fire-side gypsum board collapsed Still kept intact.

However, the thermal behaviour of test 2[9] is the same as that of test 1, mean that the glass fibre insulation appears to have little effect on the thermal behaviour of the LSF wall at high temperature. May be due to the loss of its integrity.

In a standard test performed by Keerthan and Mahendran [10], the fiberglass insulating material sandwiched between two refractory plasterboards melted as the temperature of the insulation interface of the cavity approached. 700ºC, regardless of the thickness and density of the insulating layer. The thermal behaviour of Test 4 is similar to that of Test 1, because when the fire-side plasterboard falls off, the cellulose fibres are wet sprayed and no longer provide insulation to the cavity, the author also pointed out. the importance of fixing the insulating material in the cavity between the studs to prevent it from falling at high temperatures.

Feng et al. [11] studied the experimental and numerical behaviour of small-sized LSF wall panels under standard fire. The symmetrical components are neither insulated nor insulated with 100mm thick mineral wool, and coated with 1 or 2 layers of 12.5mm thick fireproof plasterboard. The steel frame is made of CFS half-timbered lip pieces, but not. Overall, the assembly with two plasterboards (with and without cavity insulation) showed no insulation and integrity defects even after being exposed to fire for 2 hours. Components insulated with gypsum flakes and mineral wool also work well at temperatures up to 1 hour. As expected, the cavity insulation increases the thermal gradient across the steel section due to the 'insulation.

Regarding the numerical simulations carried out, the thermal properties of the plasterboards were verified using ABAQUS, and the properties of the steel and the mineral wool are taken from Eurocode 3 Part 1-2 [45] and manufacturer's specifications. The comparison between the results obtained in the experiment and the results of the simulated surface temperature and the thermal gradient of the steel shows that this is a good agreement for the non-isolated specimens. However, the thermal insulation test performed in the cavity showed a high simulated steel thermal gradient, which may be due to the assumed perfect contact between the thermal insulation layer and the steel interface and the uncertainty welding.

Thermal performance of insulation. In the actual assembly, the space between the insulation and the steel interface and the ablation of the insulation will increase the radiation effect in the cavity, thus making the temperature change in steel more uniform. In addition, for all samples separated in the cavity, the mineral wool remained intact throughout the test.

In addition, through the analysis of the parameters, it is found that the high thermal conductivity of the steel significantly affects the heating rate of unexposed panels, thus reducing the time required to achieve insulation failure. This contradicts the assumptions of the thermal model of Sultan [13] and Alfawakhiri and Sultan [14].

Dias and others [15], subsequently confirmed this hypothesis. Their research shows that for non-porous insulated walls, the breakdown time of the insulation should be determined as a function of the temperature of the panel. Unexposed gypsum at the base of the column, rather than on its overall surface. The analysis of the parameters developed by Feng et al. [11] allows the author to conclude that the thickness of the cross section and the small width of the lips hardly affect the temperature variations on the unexposed side of the LSF wall panel. Therefore, the presence of insulating materials in the temperature of the wall, rather than its shape and thickness, tends to significantly affect the temperature of the steel.

Poologanathan and Mahendran [16] evaluated the effects of various parameters on the thermal performance of full-scale and full-scale CFS frame wall configurations subjected to curves by experimental and numerical studies using SAFIR. Standard lighting AS 1530.4 [17]. The model they proposed makes it possible to predict the average temperature distribution of the wall Compared to the experimental results, even at higher temperatures, the insulation and coating materials encounter integrity problems (which have an impact negative on the thermal model). Precise precision compared to experimental results.

As shown by the studies of Sultan and Kodur [9] and Feng et al. [11] , based on a series of experimental results and previous research, the loss of integrity of gypsum board and insulation materials was modelled with appropriate effective thermal properties, which helped improve the modelling results.

In addition, their finite element analysis also confirmed the destructive effect of cavity insulation on the structural performance of LSF walls. Through the analysis of the parameters, it is confirmed that the shape and depth of the CFS element will not affect its temperature curve and have little effect on the overall thermal performance of the non-insulated LSF wall panel.

Recently, Chen et al. [19] proposed an alternative method to solve the integrity problem of fire-retardant plasterboard in LSF walls and composite panels.

In their analysis, the gypsum board was preheated and then a transient thermal conductivity measurement was taken instead of the direct thermal conductivity which is usually measured by heating methods.

Experimental tests have been carried out and two plasterboards are coated on both sides of the steel nail assembly with a partially insulated cavity, in which the 35mm thick rock wool is in contact with the exposed face.

The local buckling of the nail net and the fall of the plasterboard in the fire were observed. Using similar boundary conditions proposed by Rusthi et al [18].

Rusthi et al.[18] developed 3D finite element models to better evaluate the fire performance of LSF walls exposed to ISO 834 [21] standard fire curve. According to the authors, a 3D model would contribute to fully comprehend parameters that are not regularly accounted for in 1D and 2D simulations, such as the influence of noggin tracks, diverse steel and cavity shapes, service holes and mixed boundary conditions.

The thermal properties used included the thermophysical behaviour of gypsum plasterboards and insulation at high temperatures, i.e. integrity loss, dehydration, ablation and fall-off. Steel thermal properties were taken from Eurocode 3 Part 1-2 [22]. Conduction was defined using the thermal properties of the materials.

The emissivity was 0.9 constant for all enclosures throughout the simulation and as for convection, film coefficients of 10 and 25 $W/m^2/K$ were assigned for the unexposed and exposed sides, respectively. Perfect contact between the plasterboards and the steel elements was assumed. For non-insulated assemblies, as radiation tends to be the major heat transfer mechanism in air cavities, conduction and convection were negligible in that region.

The plasterboard transient time-temperature history showed a remarkedly good agreement with experimental tests, even for cavity-insulated assemblies. The model also provided accurate steel temperatures, allowing the prediction of failure modes and the critical temperature of the hot flange. The thermal model was effectively implemented in a coupled thermo-mechanical parametric analysis, yielding adequate results for various load and non-load-bearing models.

A 2D model using ABAQUS was developed [18], except for emissivity equal to 0.8. In order to simulate the plasterboard falling, the author used stillborn element technology which involves removing the exposed plasterboard from the fire side when the surface temperature reaches 690-750 ° C (critical temperature). With the exception of the temperature around the cavity, the simulation results are in good agreement with the fire resistance test, indicating that the measured thermal conductivity of the plasterboard after heating can be fully utilized for the digital simulation.

In addition, Chen et al. (2018; 2019) [19,20] also mentioned that under the same fire conditions and the same configuration, aluminium silicate-based mineral wool has better thermal insulation properties than rock wool.

The accuracy of the simplified method of predicting thermal and structural damage of LSF walls under fire conditions is based mainly on experimental data and the fact that the wall cavity is filled with insulating materials.

In this sense, a broader approach is needed to study the effects of voids, the location of each layer in the module, and common integrity issues associated with LSF building structures.

2.3.Cold-formed Steel Members

Steel members are widely used in buildings due to their advantages of high strength, good ductility and fast fabrication and erection. Two types of structural steel are used in the building industry, i.e. hot-rolled and cold-formed steels.

In cold-formed steel products, the strength comes from the material and from geometry.

The load bearing capacity of a thin flat sheet of steel can be greatly increased if it is formed into an efficient multi-sided cross-section.

The strength to weight ratio of cold-formed steel products is very favourable in comparison to the thicker hot-rolled steel products. Figure 2.2 shows some commonly used cold formed steel structures. The depth of the element is generally between 50 mm and 300 mm and its thickness is of the order of 0.75 to 3 mm.

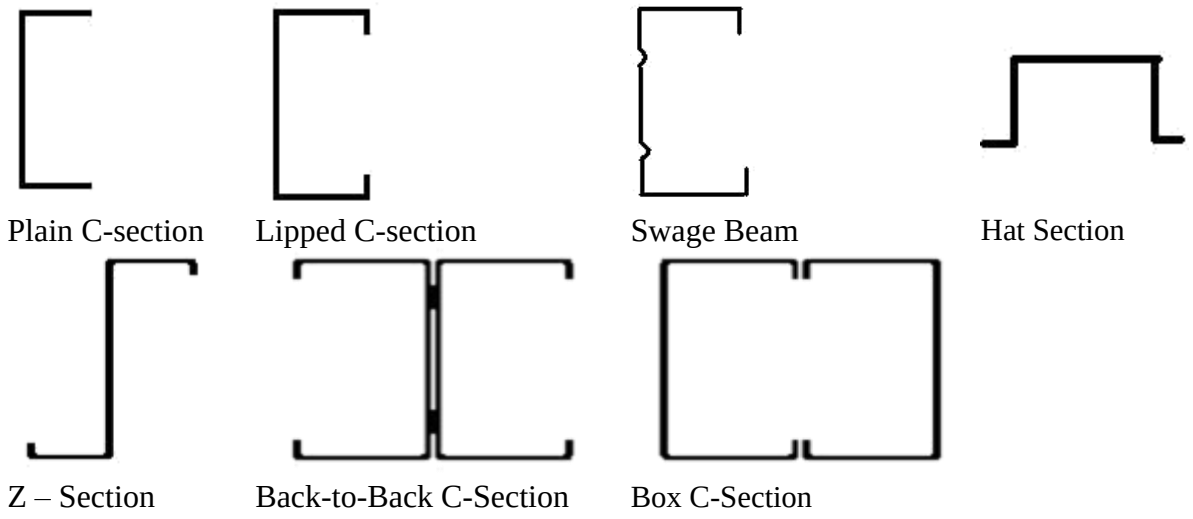

Figure 2.2: Commonly Used Cold-formed Steel Structural Shapes [88] .

Cold-formed products are products of various shapes, the open section of which or the parts connected to the edges are constant over the entire length. They consist of hot or cold rolled flat products (coated or not) and their thickness is only slightly modified by cold forming processes (for example: forming, stretching, press forming, wooden planks, etc. etc.). These products may be distinguished in general or special products. General or standard products: such as L, U, C, Z shaped products, see Figure 2.2. Special products: products corresponding to specific uses, such as cold formed sheet piles, guardrails and building frame profiles.

Cold-formed steel sections are usually manufactured up to a length of 12 meters [23]. The main applications of cold-formed steel products have been in elements such as purlins and sheet rails, cladding and decking, pallet racking and shelving. Their strength, lightweight, versatility, non-combustibility, ease of prefabrication and handling has made cold-formed steel members very popular in the building industry.

Trusses, wall Frames, posts and beams made of cold-formed steel as shown in Figure 2.3 are being regularly used. As shown in Figures 2.4 and 2.5, cold formed steel is an attractive material to replace all building materials.

(a) Trusses (b) Wall Frames

(c) Studs (d) Beams

Figure 2.3: Applications of Cold-formed Steel Products [89] .

Figure 2.4: Transportable Houses [89] .

Figure 2.5: House Frames [89] .

2.4. Light steel frame studies

Faced with the increasing use of LSF in construction, research on fire resistance has been carried out to improve the reliability of construction methods. In 1996, Gerlich et al. [24] used the finite element model from TASEF software to study the fire behaviour of load-bearing walls, focusing on the deformation of steel structures caused by high temperatures. The study of the parameters was also carried out by modifying the thickness of the pads and of the track to minimize the deflection.

In 2006, Telue and Mahendran [25] carried out a numerical study of the effect of gypsum on the structure of LSF walls, the model only covered one side and the author had also analysed it in experimental studies, compare limit load, load deformation Destroy curves and models. The author has developed a design method based on numerical results, which is proposed as an improvement of the standard method.

In 2007, Manzello et al. [26] conducted research and standard tests on non-loadbearing LSF walls under real fire conditions, compared these experimental results with each other and compared them to simulations, and greatly contributed to the accuracy. The prediction of damage to the walls by the calculation method is related to the damage of plasterboard.
Once unpredictable, these failures will increase errors in the calculation model. In 2011, Park et al. [27] also performed non-standard tests on real instrument walls under real fire conditions to improve the reliability of the parameter fire curve. The set fire temperature curve may very well approach the maximum value. The temperature and the arrival time are overestimated. The temperature in the cooling phase varies considerably, but this study provides valuable experimental data.
The Lightweight Steel Frame System (LSF) is recognized as one of the most effective methods in residential, commercial and industrial construction. Its constituent parts are assembled in load-bearing and non-load-bearing building structures, such as walls, floors, ceilings and roofs, and because the steel frame is mainly composed of light weight, strength ratio -High weight and dimensional stability, cold galvanized. LSF is a member of the steel section (CFS). Compared to traditional building technologies such as lumber and masonry, LSF has many advantages including a significant increase in construction speed, durability and performance. Environmental and physical characteristics, as well as improved aesthetic appeal and reduced maintenance costs [8]. With the increasing demand and popularity of LSF components, special attention has been paid to their safety requirements, especially safety requirements related to fire behaviour.

Therefore, the correct evaluation of the performance of the light steel frame building structure under fire conditions is essential to ensure correct fire safety design and compliance with the requirements of standards and operating specifications. This is the basis for the prevention and reduction of fire risks [8]. In this sense, non-load-bearing walls made of thin-walled CFS profiles are one of the main components of the LSF system. As these walls are primarily used as partitions, they play an essential role in protection against fire and the spread of fire. Each compartment extends the overall integrity of the building [29,30]. Therefore, a wall without LSF should be carefully assessed against fire protection requirements (that is mean its fire resistance, expressed in the Fire Resistance Index (FRR)). During the evaluation period, the building components failed to meet one or more specified standards when exposed to standard fire scenarios [8]. In this regard, improving the fire resistance of LSF walls is mainly based on various assembly methods and flame-retardant materials, including various types of sheathing panels and cavity wall insulation materials, which will greatly affect the fire resistance of concrete.

Therefore, although the behaviour of conventional LSF walls in standard fire scenarios is well known, experimental tests and verification of analytical models are still needed to assess the fire and thermal insulation performance of different partition components LSF.

With improved FRR (e.g, double columns and bulkheads), it can help improve performance and fire protection design rules based on LSF building code to ensure their safety at high temperature.

2.4.1. Classification of LSF construction element

With regard to thermal behaviour, LSF building components are generally classified according to the location of the insulating layer [31]. Figure 2.6 shows the three types of LSF constructions: cold frame construction, hybrid construction and hot frame construction. In the cold frame structure, the insulation material is placed in the wall between the steel nails. Therefore, given the lower temperature of steel nails, this solution may be more prone to pore condensation, mainly in cold climates. In addition, the steel frame thermal bridge is more expressive in this type, resulting in higher heat losses and gains.

When the insulating material is distributed between the outer surface between the steel nails and the wall cavity, the LSF structure is classified as a hybrid structure, in this type, at least 1/3 of the thermal resistance should be placed outside of the wall cavity to reduce the risk of thermal bridges and interstitial condensation [32].

Finally, in the thermal frame building system, all thermal insulation materials are placed outside the steel frame, which has the best thermal insulation performance. However, this type of wall thickness can result in a smaller net floor area. See figure 2.6

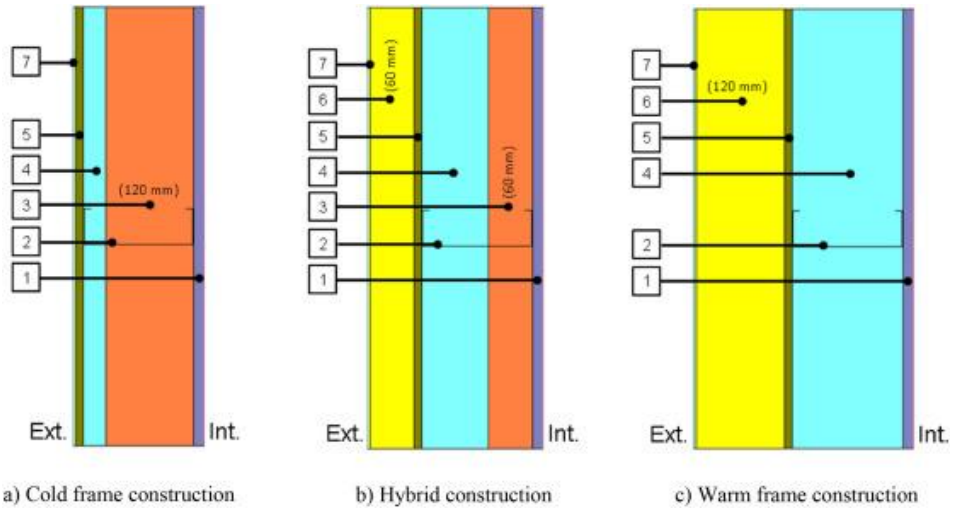

Figure 2.6:Classification of LSF constructions depending on the position of insulation materials (1- Gypsum; 2- LSF; 3- Mineral wool; 4- Air gap; 5- OSB; 6- EPS; 7- ETICS) [32].

2.4.2. Elements used in LSF

In the construction of the LSF wall, steel components of small size are used. On the wall panel, the upright studs (vertical elements) and tracks (horizontal elements) are generally used. Nail wear Vertical load, tracks with connecting studs to make the frame see Figure 2.7and Figure 2.8. These members made of cold-rolled steel strip, so the fire resistance should be based on in terms of protective materials, plasterboard is by far the most common.

Fire resistance of drywall is better than most drywall moisture in gypsum crystals can lead to similar materials.

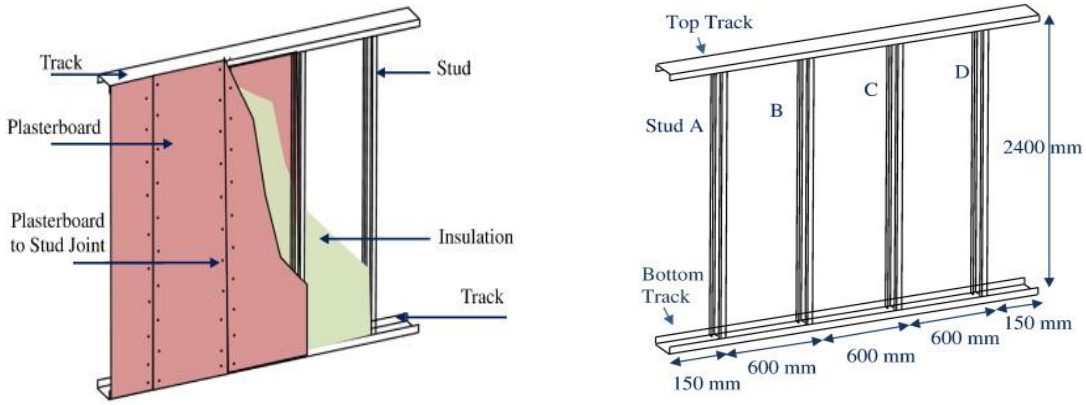

(a) (b)

Figure 2.7 (a): LSF Wall System[90]. (b) : LSF Wall System Stud cross section[90].

Figure 2.7:LSF Wall system [90].

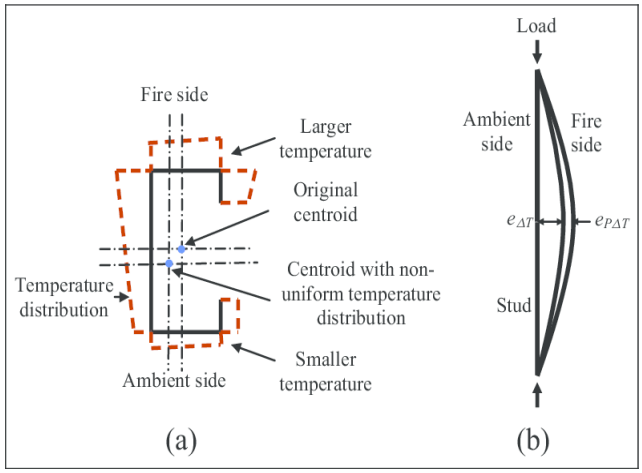

Figure 2.8: LSF Wall and the steel stud cross section[91] .

2.4.3. Cavities and composites: the new concept

Holes in walls that were initially filled with air are one of the most promising objects of research because filling these holes with material changes heat flow, fire resistance, and the acoustic performance through the wall.

In 2012, Balachandren Baleshan [33] developed the LSF system based on a composite panel in innovative insulating material for experiments and digital research related to floors and ceilings. The authors concluded that the structural and thermal performance of this innovative solution is better than traditional LSF floor systems with and without cavity insulation. The hybrid simulation uses the experimental results of temperature as input and simulates and tests under stable and transient conditions. According to the equations proposed by Dolamune, Kankanamge and Mahendran [34], the mechanical properties at high temperature are considered. The results confirmed the excellent performance of the innovative solution and developed a set of parametric simulations. Kolarkar and Mahendran [35] studied the insertion of fiberglass, rock fibre and cellulose fibre in the cavity and between two plasterboards. This model of composite plate is an innovative construction method designed to reduce heat transfer and improve fire resistance. The result is used to verify the digital model of the composite board by time-temperature measurement.

Research such as Kontogeorgos et al. [36] not only considers heat transfer, but also considers the mass transfer effect caused by dehydration of gypsum at high temperature and its impact on the LSF wall, as a method to improve the accuracy of the simulation, and it is recommended to include this effect in future mathematical models to improve reliability. In any case, the search for the new configuration continues. Kesawan and Mahendran [37] ,[38] suggested changing the profile of the steel column, which is usually "C" shaped, and then switching to a welded profile to create two "C" shaped shells to improve performances. When the LSF wall caught fire.

Rusthi et al. [38] A digital study of the 3D model using plasterboard, the results showed a good and accurate result of the temperature field. The author also presented the properties of the new material measured on plasterboard and of magnesium. Preliminary digital analysis shows that the fire resistance is poor when magnesium plasterboard is used. In a similar study using calcium silicate boards, it was found that calcium silicate boards have similar fire resistance results, as shown by Ariyanayagam and Mahendran [39].

In this work, the single-layer mixture of different materials and gypsum mixtures is a new direction of research. In the research for the design of floors in LSF, Jatheeshan and

Manhendran [40], a study was carried out to analyse the fire resistance of floors with and without insulation, considering each single- and double-layer plasterboard.

They also analysed the fire resistance of the new gasket. In the design, the effect of using welded hollow flange channels and web openings. They concluded that in this case the fire resistance only depends on the thickness of the steel and the yield strength reduction factor of the cold formed steel used to fabricate these joists. Current research should help develop new formulations to avoid experimental testing and provide accurate fire resistance ratings based on cross-sectional thermal analysis.

Experiments were performed on three different LSF steel structures from four different walls and infill cavities, to increase the influence on the thickness of the gypsum board and the understanding of the influence of the gypsum board. influence of the thickness and structure of steel and wall materials on fire resistance. Burning non-loadbearing walls tend to generate compressive loads on the steel structure and usually reach instability mode as the failure mode. Due to the thermal gradient of the large wall cavity, the stud will bend toward the exposed side of the wall. Local buckling and deformation buckling will occur in the reduced wall. Changes in the tightness of the cross section will cause the neutral axis of the cross section to shift, which is the effect contained in the current version of the Eurocode.

2.5. Thermal Behaviour of LSF Wall Elements in Fire

The behaviour of LSF walls at elevated temperatures depends on their thermal and structural properties, which can be assessed by exposing the wall to thermal loads and evaluating its time-temperature curve, integrity and load bearing capacity.

Kesawan and Mahendran [41] concluded on the basis of extensive research that the main parameters affecting the thermal behaviour of LSF walls are: composition, thermal performance, the combined effect of drip and slabs. plaster; and cavity insulation, CFS and its thermal properties. These factors will affect the mechanism of heat transfer to determine the appropriate experimental and modelling methods.

2.5.1. Gypsum Plasterboard

Gypsum wallboards have been in use since the mercial buildings. The core of these wallboards or plasterboards is made up of Gypsum i.e. calcium sulphate dihydrate ($CaSO_4.2H_2O$), a naturally occurring non-combustible mineral. The core is sandwiched between two layers of paper (see Figure 2.9), which are chemically and mechanically bonded to the core to form flat sheets available in a range of sizes. The papers provide sufficient tensile strength to the board to assist in handling and transportation. Gypsum plasterboards have become very popular due to their non-combustible core and fire resisting properties. Most gypsum boards are made with a thickness between 10 and 20 mm.

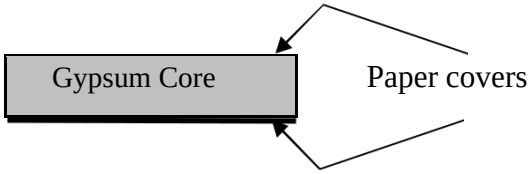

Figure 2.9: Gypsum Plasterboard

The plasterboards are generally available in three main varieties i.e. Regular, Type X and Special Purpose Boards. Regular Plasterboards generally do not have any fire resistance rating and are made up of low-density Gypsum core without use of reinforcing fibres. They are mostly used in constructing non-load-bearing walls. When exposed to fire the regular boards tend to crack up and fall off soon after the burning up of paper facings, which takes place at around $300^{O}C$.

Type X Board is a generic term that describes a Gypsum board with a specially formulated core to provide a greater fire resistance than a regular board of the same thickness. All type X boards contain some additives such as Vermiculite and Glass fibre reinforcing to enhance the fire resisting properties.

Vermiculite expands when exposed to heat and thus partly helps in compensating the shrinkage of the Gypsum core during calcination (i.e. dehydration).

Glass fibres improve the mechanical properties of the board, reduce shrinkage and ablation and thus enhance the stability and integrity of the board, when exposed to fire. Special Purpose Boards (some called as Type C Boards) are proprietary products made by manufacturers to obtain superior fire or structural performance over Regular or Type X boards.

For the Gypsum boards to stay in place, in the stud wall assembly they should possess sufficient tensile ductility to accommodate the thermal strain incompatibility with steel studs i.e. as the boards tend to shrink and the studs tend to elongate with rise in temperature. Special additives are used in proprietary formulations to reduce shrinkage and enhance strength and ductility characteristics of the Gypsum core.

Gypsum contains approximately 21% by weight chemically bound water of crystallization and about 79% calcium sulphate, which is inert below a temperature of $1200^{o}C$. In addition to water of crystallization it is found that approximately 3% free water is also present inside Gypsum plaster, depending upon the ambient temperature and relative humidity, Buchanan [59].

The fire retarding property of the gypsum board primarily stems from this water content (Free water and water of crystallization). When the gypsum board is exposed to fire, the free water and water of crystallization is gradually released and evaporated. The dehydration i.e. release of water occurs in two phases. In the first phase also known as calcination, Gypsum dehydrate loses some amount of water to yield Gypsum hemihydrate ($CaSO_4.1/2H_2O$) commonly known as Plaster of Paris.

$$CaSO_4.2H_2O \longrightarrow CaSO_4.1/2H_2O + 3/2H_2O \qquad (2.1)$$

The above reaction (calcination) is endothermic in nature occurring between $100^{o}C$ to $120^{o}C$ and consumes large amounts of energy in order to evaporate the free water and release as steam the chemically bound water of crystallization.

This absorption of energy delays the heat transmission through the board and causes a temperature plateau on the unexposed face of the lining. The length of this plateau is a function of the lining thickness, density and composition and is commonly referred to as the ‘Time Delay’ ,Gerlich et al[41] .

Calcination leads to shrinkage and loss of strength of the sheet material. The progress of calcination through the sheet thickness is retarded by the exterior layer of calcined Gypsum on the fire exposed side which acts as a protective layer and adheres well with the inner uncalcined layers. The second phase of dehydration, i.e. complete dehydration occurs when the Gypsum hemihydrate is transformed to Gypsum anhydrite.

$$CaSO_4.1/2H_2O \longrightarrow CaSO_4 + \tfrac{1}{2} H_2O \qquad (2.2)$$

This reaction occurs at about 210 ^{o} C and at about 600 ^{o}C according to Sultan [13] and at about 225 ^{o}C. The temperature at which the second phase occurs much depends upon the rate of heating.

Gunawan [42] and Keerthan and Mahendran [43] studied changes in the literature regarding thermal properties of plasterboard and, from their results, specific thermal values tend to be consistent. Dehydration (~ 125 ° C), but the temperature of the second dehydration is not consistent. It should be noted that if the water vapor pressure is negligible, the second dehydration peak is unlikely to occur, and vice versa [44]. According to the results of Keerthan and Mahendran [43], no significant difference was observed for the decomposition temperature of calcium carbonate or magnesium carbonate and plasterboard containing CaCO3. Tend to stay at ~ 670 ° C.

Regarding thermal conductivity, the value found to be consistent below 400 ° C, the difference thereafter is due to the shrinkage behaviour of the plasterboard and the fact that the ablation and landing effects are correctly taken into account. Consider or don't consider. In terms of density, different types of drywall have different densities, but in general, it is found that the density value decreases significantly at the temperature where the first dehydration reaction occurs, and remains roughly constant by the after.

In LSF walls, due to the variability in the composition of plasterboard and the different types of heat transfer that occur during a fire, their thermophysical properties (such as specific heat) are determined at a certain temperature, high density, emissivity and thermal conductivity. And convection coefficient.

For modelling purposes, precise or careful calibration should be performed, including calcination, cracking behaviour, ablation and dropping of plasterboard under standard fire conditions.

2.5.2. Glass Fibre Insulation

Glass fibre insulation materials (see Figure 2.10) play an important role in energy conservation in buildings.

Figure 2.10: Glass Fibre [95] .

These insulation materials are made in the form of thick rectangular plates and installed on the wall. Physical experiments show that when the porosity of this insulating material increases, i.e. when the number of glass fibres decreases, the effective heat transfer coefficient of the material also decreases. In fact, the thermal conductivity of glass is greater than that of air. But this phenomenon continues only up to a certain degree of porosity. If the porosity exceeds this level, the heat transfer coefficient of the insulating material begins to increase again with the porosity. This shows that the quality of fiberglass insulation can be improved by reducing the uneven density of glass fibre as much as possible . In terms of fire protection, insulating materials are used to prevent extreme temperature rise on the unexposed side of the LSF wall, thus improving the insulation performance. However, due to the low thermal conductivity of insulating materials, hot flanges heat up faster than cold flanges and the insulating layer of the cavity tends to increase the thermal gradient along the cross section of the steel frame. Thermal deformation deflection and higher temperature. Stress, which will reduce the fire resistance of the wall in terms of structural performance.

In addition to a sufficient load capacity, according to the test of Ariyanayagam and Mahendran [39], when the fibre cavity of the LSF wall is insulated, the fire resistance of the LSF wall on a large scale is improved by 12 minutes. Glass is used, but the insulating material begins to melt after being placed at 650 ° C for 45 minutes, which shows that using insulating materials with higher melting points can achieve better insulating properties (rock wool and ceramic fibres).

2.6. Researche review finding

According to Feng et al. [11], internal insulation (cavity) has a positive effect on the fire resistance of the steel cladding. However, in studies by Kodur and Sultan [9], and Alfawakhiri [14], wall components without cavity insulation have a higher fire resistance than insulated cavity components. Therefore, previous studies cannot conclude that the traditional method of placing insulating materials in the cavity is effective. Recently, Kolarkar and Mahendran [12],developed a new composite panel system in which the insulation material was placed on the outside of the steel frame and its fire resistance was found to be significantly improved. However, the study by Kolarkar and Mahendran [12], is limited to experimental studies with a charge ratio of 0.2.

Therefore, further experimental studies with a higher charge ratio are needed. To fully understand the improvements brought by the new system, numerical and theoretical analyzes must also be carried out.

Research by Gerlich et al. [70,63], was limited to steel grades 300 and 450 with thicknesses of 1.15 mm and 1 mm. Kodur and Sultan [9], used nominal metal thicknesses of 0.84 and 0.912 mm. In the study by Alfawakhiri [14], a thin steel plate with a metal thickness of 0.912 mm was used and the yield strength of the steel was very low 228 MPa. Research by Feng et al. (2003b) The thickness limit is 1.2 mm. Feng and Wang [71], extended their research to S350 steel of 1.2 mm and 2 mm thickness. In the research of Zhao et al. [85] ,steel thicknesses of 0.6, 1.2 and 2.5 mm were considered. The yield strength of the steel used is 402 MPa and the steel grade is S280 and S350 are used for the search parameters.

Therefore, it can be concluded that in previous studies the behaviour of low-grade steel and finished thickness LSF wall panels at high temperature has been investigated. Therefore, further study is needed LSF steel wall systems with different thicknesses and steel grades.

In the research of Alfawakhiri [14] and Zhao et al. [85] the studs broke towards and away from the furnace. In the test of Gerlich et al. [70,63] , The crampons failed at medium to high altitudes. However, according to the opinions of Alfawakhiri [14], and Zhao et al. [85], the stud broke halfway near the bracket. In most previous studies, the location of the test failure was poorly predicted, and the behaviour of steel nails at elevated temperatures was not fully understood, hence further experimental numerical and theoretical studies are necessary in the field of LSF components exposed to fire to fully understand their behaviour and failure modes during fire tests.

CHAPTER 3

3. Introduction

This chapter includes detailed information on fire safety, LSF wall systems and different types of insulating materials. In addition, it explores the current state of knowledge on fire performance, fire resistance of LSF walls and thermal models. Finally, the review of the literature summarizes the current state of knowledge and the contributions to current research.

3.1.Fire Safety

Unnecessary fires [4] are destructive, causing many deaths and billions of dollars in property damage each year. All over the world, people want their homes and workplaces to be protected from unnecessary fires. Unfortunately, fires can occur in almost any type of building (Figure 3.1), which is usually the least desirable situation.

Figure 3.1:Fire Damaged Lebanon: Zaha Hadid's building in Beirut in flames [92].

The safety of the occupants depends on several factors in the design as well as the construction of the buildings. In most cases, the verification of the fire resistance of light frame structures is carried out in the time domain, in this time domain the level of exclusivity is compared to the fire resistance specified by the code or to the equivalent time. Failure criteria for fire safety may be defined for load bearing (R), integrity (E) or insulation (I).

Integrity is defined in AS 1530.4 (SA, 1997) [57], as the ability to resist fire or smoke passing through the area. When the walls are used in fire-resistant buildings, they must meet the three requirements of fire resistance, stability, insulation and integrity.

The LSF wall is made of a thin plate of steel, so it loses its resistance to high temperatures. Therefore, LSF walls are usually covered with plasterboard and insulation materials to form wall assemblies capable of withstanding the required fire exposure. Integrity assessment should be done as part of a large-scale test, as the small-scale test cannot assess factors such as large-scale plasterboard shrinkage or cracking due to structural deformation.

According to ISO 834 [21], and AS 1530.4 (SA, 1997), when the average temperature rise on the unexposed surface exceeds 140 or at the highest temperature at any point increases more than 180 ° C above the initial average temperature, the component is considered to have failed by insulation.

3.2. Need for Fire Resistant Structures

Fire barriers play an important role in maintaining the integrity of the building and reducing the spread of fire from the original room to adjacent compartments.
However, there has been an increasing demand for prefabricated lightweight steel (LSF) frame systems. Due to its high strength and good forming properties, the material generally used is galvanized mild steel. Steel tracks and uprights are considered an environmentally friendly and recyclable alternative to the wood stud system. Replacing wood with steel is becoming more prevalent in areas where wood resources are scarce and also in commercial or community applications where other advantages such as speed of assembly and flame retardancy are more important. One or two-sided claddings (eg plasterboard) have been widely used in building construction since the 1940s. Panels are generally constructed by connecting panels. studs with rivets and guide rails to form the frame, then use self-drilling screws to connect the duct panel to the frame.

These panels can be easily assembled in load-bearing and non-load-bearing partition walls. In the event of a fire, due to its small thickness, the CF-TW steel profile will heat up quickly, resulting in a rapid decrease in strength and rigidity. However, if the gypsum board and thin-wall steel channels are combined to form a half-timbered steel wall as shown in Figure 3.2

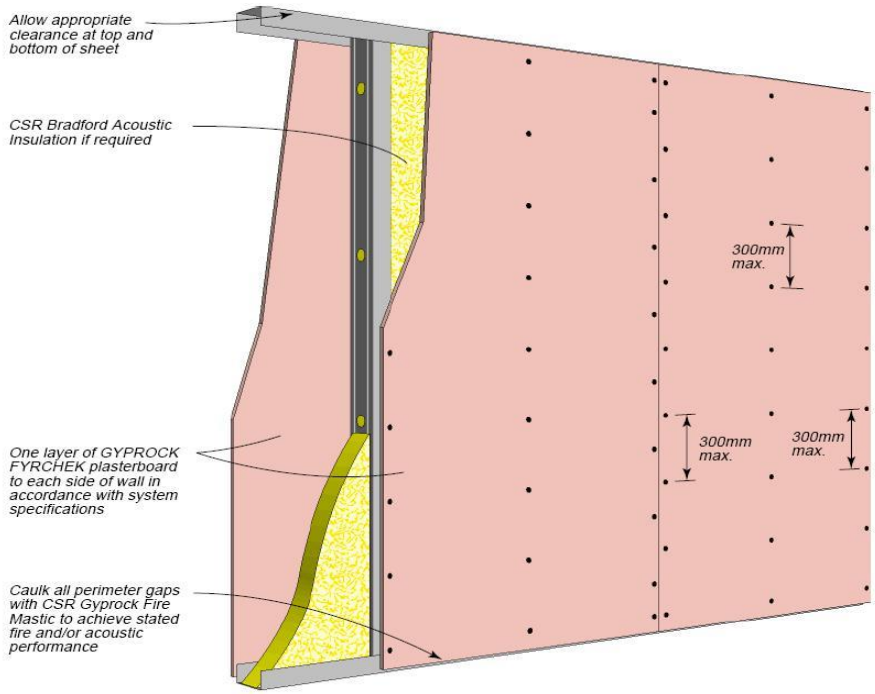

Figure 3.2:Steel Stud Wall System [93] .

Since the 1940s, partition wall panels made of cold-formed steel frames have been coated with a coat of paint (like plasterboard) on one or both sides. First connect the studs and rails with rivets to form a frame, then use self-drilling screws to connect the duct panel to the frame. These panels are easy to assemble and can be made into load-bearing and non-load-bearing partition walls Cold rolled steel for thin-walled steel profiles (CF-TW) is the main part of load-bearing wall nails in light metal structure. In the event of a fire, CF-TW steel heats up quickly due to its small thickness, thus rapidly reducing its strength and rigidity.
In terms of experimental analysis and according to EN 1363-1 [1], the fire resistance of LSF walls can be determined by submitting one side of the wall specimen to a standard fire load that behaves according to the heating curve specified by ISO 834 [21]. Under a standard fire test, the FRR of a building component is then defined according to the following failure criteria.

3.2.1. Integrity (E)

Integrity is defined in AS 1530.4 (SA, 2005) as the ability to resist flame or smoke. Integrity assessment should be performed at large scale testing, as small-scale testing cannot assess factors such as drywall shrinkage or cracks due to structural deformation. high- Scale tests are also needed to assess the effect of drywall falling from the wall into the fire.

3.2.2. Insulation (I)

According to ISO 834 [21], and AS 1530.4 (SA, 2005), this criterion is met when the average the temperature rise of the unexposed surface exceeds 140 ° C, or the when the maximum temperature exceeds 180 ° C, above the initial average temperature.

3.2.3. Load-bearing capacity (R)

the rating period in which the specimen sustains its load-bearing ability until failure. Failure is deemed to have occurred when both: specified deflection or rate of deflection are exceeded.

3.2.4. Structural Adequacy

The structural fit criterion has already occurred when: Crash or when the deviation exceeds the limit. Advantages of LSF the connection is mainly in the steel element itself, not in the finishing material. The coating material is essential to ensure the lateral stability of structural elements, but their contribution to the overall strength and rigidity is small.

Evaluate the fire resistance of LSF walls in terms of insulation, integrity and endurance load-bearing endurance should be based on large-scale testing due to heat distribution when assembled, the appearance cracking and shrinkage resistance of the gypsum sheath will be different and it all depends on the size of the wall and the structural performance of the steel frame depends on its geometric characteristics, stresses and support conditions. However, the scale is small, so the specimens can be used for standard fire resistance tests as they still provide heat transfer effect.

3.3. Fire curves

A fire occurs when there are three factors: the heat source (responsible for the initial ignition), fuel (such as paper, oil and wood), and oxygen. Regardless of the presence or absence of these factors, the fire will not ignite or reach a high level. Although composed of complex random events, fires can be represented by temperature-time curves. In structures subjected to high temperatures, these curves make it possible to determine the highest temperature reached on the element and its corresponding fire resistance. The following subsections will briefly discuss some fire curves.

3.3.1. Standard Fire Curves ISO 834

In 1975, the International Organization for Standardization (ISO) introduced the standard fire curve through the international standard ISO 834: 1975 - “Fire resistance tests - Construction elements of buildings”. In 1999 this version of the standard was replaced by the first edition of ISO 834-1 [22], modifying the tolerances applied to the deviation of the average furnace temperature curve from the heating curve. standard.

This fire curve has a logarithmic relationship between temperature and time and is one of the most widely used nominal fire curves for the determination of the fire resistance of structural members (see Eq. 3.1 and Figure 3.3). Eurocode 1, other standards have also adopted standard fire protection curves, such as the Brazilian standard NBR 14432: 2000 - “Fire Protection Requirements for Building Components” [75], Fire test - Part 20: Method for determining the fire resistance of building elements (general principles) ". The standard fire model is a natural fire curve method, independent of space and thermal load density.

These curves are generally close to "flashover" and the fire continues, which is the most critical and high temperature fire period. Eurocode 1 on fire protection structures [45] proposes three types of nominal fire protection curves: the standard curve (also called ISO834), the curve of exterior elements and the ignition curve caused by hydrocarbons.

This work uses a standard curve, as shown in Equation (3.1) and Figure 3.3

$$\theta_g = T_0 + 345\ log_{10}\ (\ 8t + 1\ ) \qquad (3.1)$$

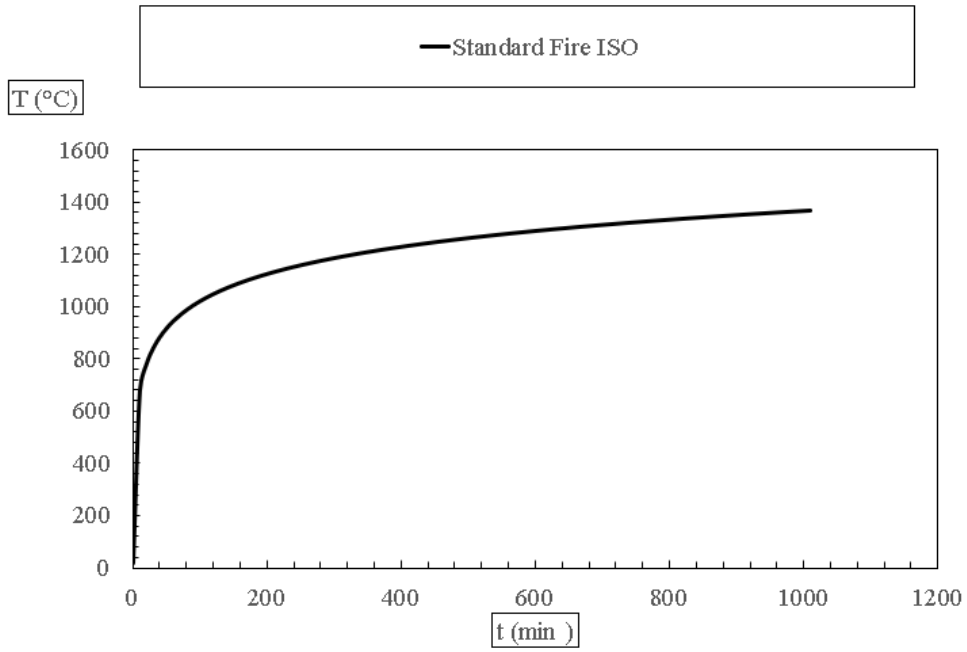

Figure 3.3:ISO 834 Standard Curve [22].

The equation describing this curve is shown below, where θg represents the gas temperature (° C) and t represents the time (min).

3.4. Behaviour of LSF Walls in Fire

Composite structures are widely used in construction engineering, because when the properties of each constituent material are combined, improved performance can usually be achieved. However, under fire conditions, the composite structure can undergo complex models of heat transfer and thermal behaviour, which can make it difficult to obtain the overall thermal response of the composite during the modelling process, particularly in due to nonlinear time-temperature equations and materials addiction.

Irregular thermal characteristics and boundary conditions. However, in addition to defining appropriate limit values, simplified assumptions can also be derived by identifying associated heat transfer modes and their assumptions.

For this reason, it is necessary to fully understand the basic heat transfer mechanism and the effect of heat on the LSF wall under fire.

This section provides the necessary background for numerical studies of the thermal performance of the Single-stud LSF wall related to the objectives of this research, including a brief study of the heat transfer mechanism and thermal effect of the panel wall.

In addition, it also considers experimental and numerical aspects and explores the knowledge, latest findings and contributions of load-bearing and non-load-bearing LSF walls exposed to standard fire scenarios. Provides a detailed review of the literature on the ignition behaviour of double-stud wall assemblies.

3.5. Heat Transfer Theory

Heat transfer theory attempts to predict the energy transfer that can occur between materials due to temperature differences. This energy transfer is defined as heat. In fact, heat can be transferred from one place to another by the following three modes: conduction, convection and radiation.

A thermodynamic analysis deals with the amount of heat transfer as an energy system undergoes a process from one equilibrium state to another. The heat transfer is the science which concerns the determination of the rates of these energy transfers. The heat transfer between two substances requires the existence of temperature differences and occurs from the high-temperature medium to the lower-temperature medium . This energy transfer is defined as heat. In fact, heat can be transferred from one place to another by the following three modes: conduction, convection and radiation. In order to calculate the rate of temperature increase in structural components, it is fundamental to determine the amount of heat which affects these components.

The Eurocode 1 – Part 1-2 [52] presents thermal actions for temperature analysis, which are given by the net heat flux $\dot{h}_{net}$ (W/m^2) to the boundary surface of the element.

On the fire exposed surfaces, the net heat flux is divided into two components: the first considers heat transfer by convection ($\dot{h}_{net,cv}$) and the second by radiation ($\dot{h}_{net,r}$), as presented below.

$$\dot{h}_{net} = \dot{h}_{net,cv} + \dot{h}_{net,r} \tag{3.2}$$

The following subsections present the formulation used to determine each component of the equation above and give a brief description of the three modes of heat transfer.

3.5.1. Conduction

Is the ability of a material to conduct heat without moving things. It is directly related to the physical and thermal properties of the material. According to Fourier's law, the one-dimensional conductive heat flux hx [W/m²] through a fixed medium along the direction of infinity dx [m] is proportional to the temperature gradient dT [K] which exists in this direction.

$$\dot{h}_x = -\lambda \, dT / dx \qquad (3.3)$$

[3.3] this Equation, the thermal conductivity of a material λ [W /mK] is a physical property which measures the thermal conductivity of a substance and depends mainly on the composition of the medium, temperature and pressure conditions.

Metals tend to have high thermal conductivity due to the movement of free electrons, while insulators and most non-metallic building materials exhibit low thermal conductivity because heat is only conducted by molecular vibration. In addition, for non-metals, the density, network structure, porosity and moisture content will significantly affect its thermal conductivity. It should be emphasized that the heat transfer zone should always be perpendicular to the direction of heat flow, which is towards the lowest temperature [46].

When modelling a composite building structure subjected to fire, because the gas temperature changes over time, a transient method should be used, in which the transient conduction heat flux can be discretized through the model and time, as well as the appropriate initial limits and limits. Conditions, considering the range and effective thermal properties of composite materials and their interaction with fire, environment, adjacent surfaces and voids.

3.5.2. Convection

Convection also includes conduction, but heat is also affected by the overall movement of the fluid. An example is the transfer of heat between the moving gas and the boundary surfaces at different temperatures. In addition, in some cases, convection occurs due to the exchange of latent heat, which is usually related to the phase change of the material, such as for example the evaporation and condensation of fluids [47, 48].

Regardless of the mechanism used, the flow of heat by convection is proportional to the temperature difference. Therefore, according to Newton's law of cooling and EN 1991-1-2

[49], the net convective heat flux $\dot{h}net, conv$ [W/m²] between the surrounding gas and the surface at temperature Tg [K] $\dot{h}net$ [W / m²] at temperature Tm [K] is expressed as:

$$\dot{h}_{net,cv} = \alpha_{cv} .(Tg - Tm) \quad (3.4)$$

Equation (3.4), refers to the standard fire scene in the building, Tg is the gas temperature near the surface of the element exposed to the fire, which is consistent with the respective ambient temperature, and αcv is the heat transfer coefficient or coefficient of film [W / m²K], and its value is often the same as the surrounding fluid Thermal conductivity is directly proportional and is affected by temperature, surface geometry and thermophysical properties of the fluid, in particular the behaviour of motion . For surfaces exposed to fire, Tg according to the standard nominal time-temperature ignition curve specified in ISO 834 [21].

Determining the appropriate film coefficient (convection coefficient) at the fluid-solid interface is a fairly complex procedure.

Nevertheless, under fire conditions, since radiation tends to be the most relevant heat transfer mechanism, the temperature distribution in an element exposed to fire will not be too sensitive, even at large changes in the coefficient. heat transfer [50].

3.5.3. Radiation

Includes long-distance energy exchange between the human body through electromagnetic waves. It depends on the fire emissivity εf and the surface emissivity εm element. The thermal radiation flux $\dot{h}r$ [W/m²] emitted by a real surface area at temperature Tm [K] is given by:

$$\dot{h}_r = \sigma \epsilon_m {T_m}^4 \quad (3.5)$$

In order to calculate the heating rate of structural components, it is important to determine the heat affecting these components. Eurocode 1-Part 1-2 [52] describes the thermal effects used for temperature analysis. These effects are given by the net heat flux ḣnet (W / m2) at the boundary surface of the element.

On a surface exposed to fire, the net heat flux is divided into two components: the first considers heat transfer by convection ($\dot{h}_{net,cv}$), and the second considers radiative heat transfer ($\dot{h}_{net,r}$), as shown below.

$$\dot{h}_{net} = \dot{h}_{net,cv} + \dot{h}_{net,r} \quad (3.6)$$

Among them, the Stefan-Boltzmann constant σ is equal to 5.67 × 10−8 [W / m²K4], and is the emissivity of the surface. Emissivity is an attribute of the value contained in the interval 0 ≤ 1 ≤ 1, which indicates the capacity of the surface to emit radiant energy with respect to the black body (εm = 1).

Both are performed at the same temperature and depend on the surface emission, finish and temperature of the material, as well as the wavelength and direction of the radiation [54,46]. When the electromagnetic waves reach the surrounding surface, the received radiant energy is partially reflected and transmitted, while the rest is absorbed. In the event of a fire, the surface of the construction element is surrounded by flames and hot air. For practical reasons, the exchange of radiant energy between any two surfaces in the enclosed space is brought together by the transfer of heat between the opaque and scattered gray surfaces. Multiple reflections and partial absorption occur there [53,51]. This is called gray body radiation.

This means that the surface is not transparent and its emissivity is considered independent of temperature, wavelength and direction of radiation, and the average emissivity of the surface is equal to its average absorbance. (Kirchhoff's law) [53,47].

In this case, the radiant heat generated from the temperature-emitting surface [K] to the temperature-receiving surface θg [K], regardless of the transmission effect, is called the net transfer rate. Radiant heat, $\dot{h}net$ [W / m²], is given in the following formula (3.7)

$$\dot{h}_{net,r} = \frac{1}{\frac{1-\varepsilon_i}{\varepsilon_i} + \frac{1}{\phi_{ij}} + \frac{A_j}{A_j}\left(\frac{1-\varepsilon_i}{\varepsilon_i}\right)} \sigma\left(T_g{}^4 - T_m{}^4\right) \quad (3.7)$$

Where Ai, Aj are surfaces, εi, the emissivity of two surfaces, and ϕij is the view or shape factor (dimensionless), which means that the direction of the surface and the shadow to the heat radiated between the two opposite surfaces are considered. The exchange effect is defined as the ratio of the radiation leaving the surface i and directly reaching another surface j, where $0 \leq \phi ij \leq 1$ [53,51].

When the radiation from the radiation source is uniform in all directions and the medium between the surfaces is considered transparent to radiation, i.e. when (3.7) does not affect the radiation, is an effective housing radiation internal. Moreover, the equation. As shown in equation (3.7) can be adjusted to quantify the net radiant heat affecting the building (3.8). In this case, the fire and the exposed surface are considered to be two distant gray bodies, so that the radiation reflected from the exposed surface will be lost to the environment without being absorbed by the fire [46].

According to EN 1991-1 [52], (3.8) become

$$\dot{h}_{net,r} = \phi \varepsilon_f \varepsilon_m \sigma({T_g}^4 - {T_m}^4) \quad (3.8)$$

Where εf and εm are respectively the emissivity of the fire and the bare surface, Tg [K] is the gas temperature, Tm [K] is the surface temperature of the bare surface.

On the unexposed side, the net heat flux Must assume αc = 9 [W / m2]. This value includes the influence of heat by radiation.

If the standard does not specify the surface emissivity of the element (ε_m), this value can assume that ε_m = 0.8. The emissivity to fire is generally considered to be εf = 1 [55]. The gas temperature (Tg) can be used as a nominal temperature-time curve. This one This work uses a standard temperature-time curve, which is presented in section (3.1).

Moreover, EN 1363-1 [1] requires that $T0$=20 $°C$.

3.5.4. Thermal actions on Partition LSF Walls

In a typical uninsulated LSF wallboard, one side is exposed to a fire, and the heat generated by the fire is first transferred to the exposed surface by radiation and convection, and radiation is the primary method. Then it conducts along the thickness of the protective layer and the unexposed steel profile, and the heat is distributed around the cavity by radiation and convection.

Finally, conduction occurs through the unexposed layer and heat is released to the environment through radiation and convection, where convection dominates at lower temperatures.

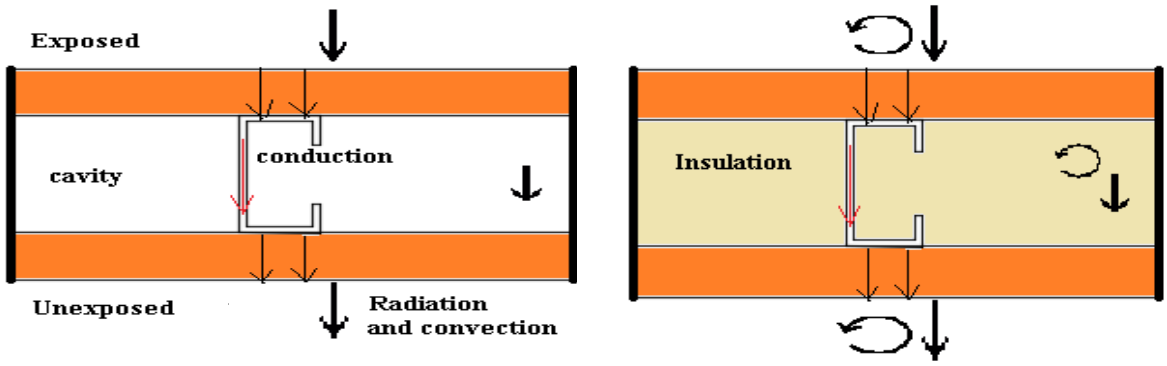

Figure 3.4:Typical thermal actions on uninsulated and cavity insulated single stud LSF walls.

Due to the evaporation of water when the temperature reaches 120 ° C and the radiation effect in the porous structure as the temperature increases, internal convection occurs in the plasterboard. However, internal convection is a phenomenon that can be reasonably simulated with an appropriate specific thermal value.

Additionally, it is common architectural practice to insert porous media into wall cavities (such as mineral insulating layers), where conduction, convection, and radiation will occur. However, in the case of porous media (such as plaster and insulating materials), its effective thermal conductivity can explain the effects of radiation and convection in its voids, then heat conduction is mainly caused by conduction.

Additionally, complexity of integrity, such as sheath loss, weakening of gypsum board joints and removal of the insulation layer from the cavity, will affect the way heat is transferred through the wall, thus affecting its heat transfer. Temperature distribution. If user input data is provided, these effects will be greatly simplified.

According to the previous analysis, the net heat flow to the outside of the exposed or unexposed surface of the LSF partition wall is due to the combination of convection and radiation.

Therefore, the combination EN 1991-1-2 [52] Sections 3.9(a) and 3.9(b) state that the net heat flux of the exposed or non-exposed surface of a building element $\dot{h}net$ [W / m²] is

$$\dot{h}_{net} = \dot{h}_{net,cv} + \dot{h}_{net,r} \quad (3.9)$$

$$\dot{h}_{net,r} = \alpha_{cv} \left(T_g - T_m \right) \quad (3.9\ (a))$$

$$\dot{h}_{net,r} = \alpha_{cv} \left(T_g - T_m \right) + \phi\, \varepsilon_f \varepsilon_m\, \sigma \left({T_g}^4 - {T_m}^4 \right) \quad (3.9(b))$$

CHAPTER 4

4. Introduction

This chapter presents the assembly, design and characteristics of the tests required to determine the fire resistance in wall specimens, recommended by the standards.

4.1.Standards to be used

The standards used to obtain the fire resistance of non-loadbearing LSF walls are: EN 1363-1 (fire test - general requirements), EN 1364-1 (fire test of non-loadbearing walls) and Eurocode 3 (EN 1993-1-2) Steel design Structure-general rules: design of fire protection structures).

4.1.1. EN 1363-1

The EN 1363-1 establishes the general principles for determining the fire resistance of different elements of construction, when subjected to standard fire exposure conditions [1]. A specially designed furnace is required to subject the test specimen to the test conditions. The system to control the temperature of the furnace, the equipment to control and monitor the pressure of the hot gases within the furnace, the frame in which the element can be inserted and submitted to appropriate heating, pressure and support conditions. The arrangement for loading and restraint of the test specimen should be appropriate including control and monitoring of the load equipment for measuring temperature in the furnace and in the test specimen. For some cases, the system for measuring the deflection of the test specimen is required.

Also, in some cases, specific devices are required to evaluate the integrity and for establishing compliance with the performance criteria. For very special cases, the equipment for measuring the oxygen concentration of furnace gases is also required. This standard for testing also specifies the design and tolerances about systems, including some sketches about the sensors, such as the disk thermocouples and plate thermocouples. The performance criteria used to validate the tests of fire resistance of non-load bearing walls are the insulation criteria (I). By definition this is the time, in completed minutes, for which the test specimen continues to maintain its separating function during the test without developing temperatures

on its unexposed surface, which increase the average temperature above the initial average temperature by more than 140°C or increase at any location (including the roving thermocouple) above the initial average temperature by more than 180 °C [1].

The performance criteria "insulation" shall automatically be assumed not to be satisfied when the "integrity" criterion ceases to be satisfied. The integrity criteria (E), in this case, concern about the time of flame or smoke pass through the unexposed side by some crack.

It's important clarify that the main performance criteria given by this standard is the loadbearing criteria or stability. The load bearing resistance (R) is the ability to support its test load without exceeding specified criteria with respect to the extent of deflection or rate of deflection.

The assessment shall be made on the basis of limiting vertical contraction (C=h/100 [mm]), or limiting rate of vertical contraction (dC/dt=3.h/1000 [mm/min]). The measurement of the horizontal deformation is also mandatory. This study concerns about the fire resistance of nonloadbearing walls, reason why this criterion is not analysed.

4.1.2. EN 1364-1

The EN 1364-1 contain the procedures to perform the experimental tests to measure the fire resistance of a non-loadbearing wall to resist the fire propagation from one side to another [2]. For this experiment, more information about the requirements are specified. A rigid frame with high stiffness and low thermal expansion is requested to fix the specimen.

According to [2] the dimension of the specimen should be defined in accordance to the following rule: if the width or the height of the construction element is smaller than 3 m, the specimen should be testes in its actual size. If one of the dimensions of the construction element is bigger than 3m, the dimension should not to be less then 3m in the test.

Anyway, the wall dimensions in this investigation were restricted by the furnace aperture, and is highly recommended that the maximum size of the wall coincide with this size, in this case 1m, this standard also gives information about the instrumentation. The control of the furnace temperature should be made by plate thermocouples in its interior, with the biggest surface turned to the furnace wall. The recommendation is to put 5 thermocouples to measure the average temperature, one in the center of the specimen, and the another 4 in the centre of each fourth part of the wall [76]. The recommendation to measure the maximum temperature is to use 7 more thermocouples.

4.1.3. EN 1993-1-2:

Eurocode 3 (EN 1993-1-2) applies to the design of steel buildings. It complies with the principles and requirements of safety and serviceability of structures. EN 1993-1-2 deals specifically with the design of steel structures for accidental conditions in the event of fire [22]. The load-bearing must be assumed that the function of a steel member is maintained after a time t in a given fire, if the condition of equation (4.1) is satisfied. $E_{fi,d}$, d is the design effect of actions for the fire design situation, according to EN 1991-1-2 and $R_{fi,d,t}$ is the corresponding design fire resistance of the steel member at time t.

$$E_{fi,d} \leq R_{fi,d,t} \tag{4.1}$$

For class 4 cross-sectional elements other than tensile elements, it can be assumed that this relation is satisfied, if at time t, the temperature of the steel at all cross-sections is not greater than a critical temperature, recommended as $\theta_{crit} = 350^{\circ}C$. This criterion may be too careful and dangerous for specific cases, because this simple method is independent of the load ratio. Just in case load conditions need to be applied. The flow chart using Eurocode 3 Part 1.2 [45] is given in Figure 4.1

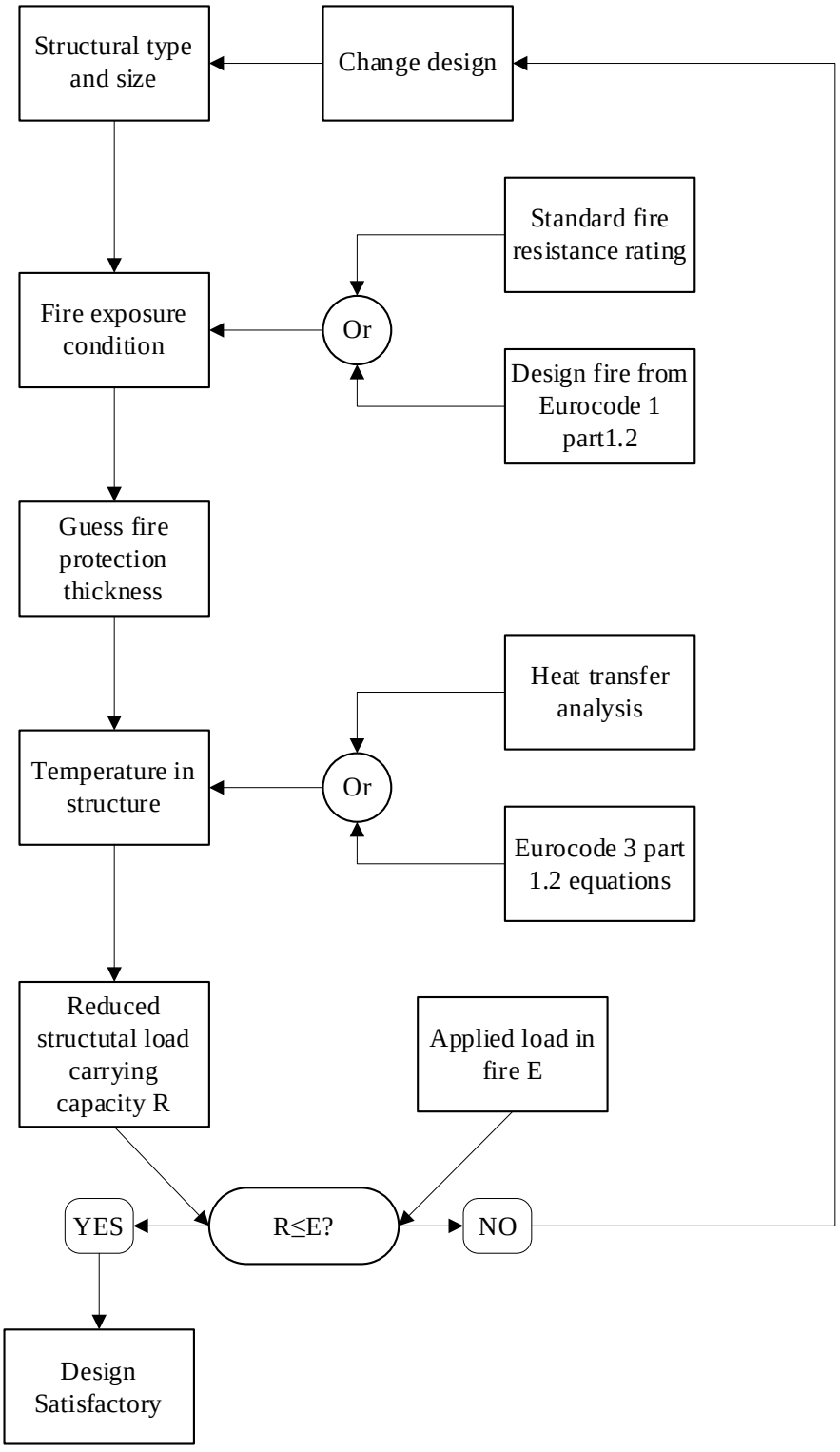

Figure 4.1:Design Flow Chart Using Eurocode 3 Part 1.2 [45] .

4.2.Wall specimens: Experimental test

the studs used are C92x35x15x1,15 steel grade S280GD. The material configuration of the wall is: Single gypsum board, Cavity insulated and single plasterboard lined LSF wall. This constructive solution was chosen to evaluate the fire performance examination. It was also evaluated with Glass Fibre to assess the fire resistance of the insulating material inside the cavity, see table 4.1.

Table 4.1: Represents details of Test Specimen Configurations in the Current Study[76]

Specimen	Insulation Cavity	Plate Layer (mm)	Spacing Studs
Test 1	No	1 X 13 (Gypsum Plasterboard)	600mm
Test 2	Glass Fibre	1 X 16 (Gypsum Plasterboard)	600mm

A large-scale experimental study was conducted at the Fire Research Laboratory of the Queensland University of Technology (QUT) in Brisbane, Australia, to assess the fire resistance of LSF wall components. [76] performed a total of five (2) large-scale fire tests. Table 4.1 gives detailed information about the samples of non-loadbearing LSF walls tested by them under a constant load of 10 kN /m^3 stud during the fire resistance test.

However, the influence of LSF wall parameters (such as plasterboard thickness, cavity insulation and wall structure) on fire resistance was investigated. The exterior (plasterboard) uses insulation material and the cavity (Glass Fibre) uses internal insulation material.

The plasterboards could be fixed following 2 configurations, see Figure 4.2.

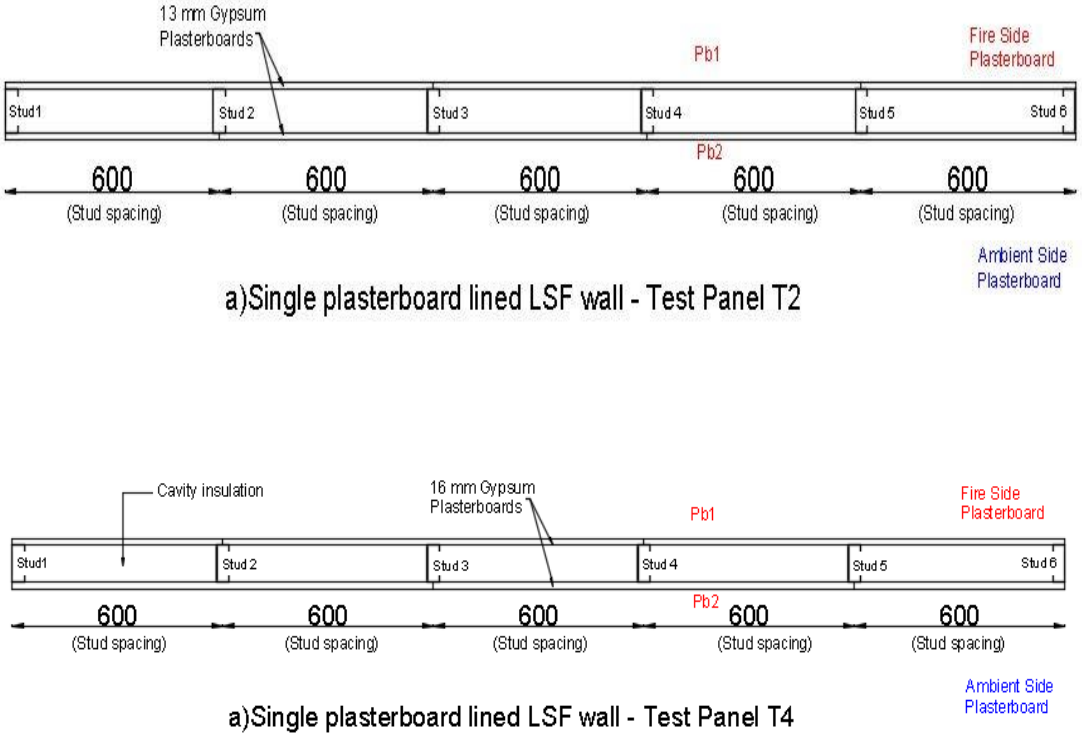

Figure 4.2:Position of the screws in the plasterboards with 6 studs [76].

4.2.1. Specimen 2: Test 2:

The specimen 2 was made with one plasterboard, with a total thickness of 13 mm of plasterboard in each side. The pink plate was used in this case too, and additional thermocouples were inserted between the plasterboards, as presented in Figure 4.3, 4.4, 4.5.

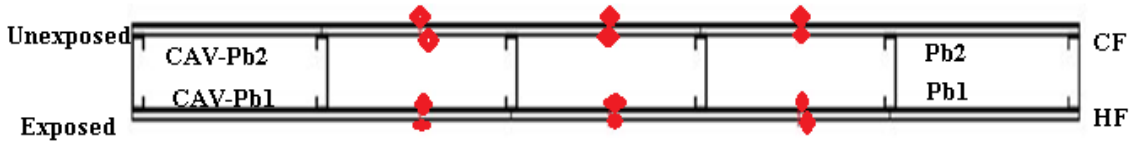

Figure 4.3:Thermocouples Position on Specimen 2,[76].

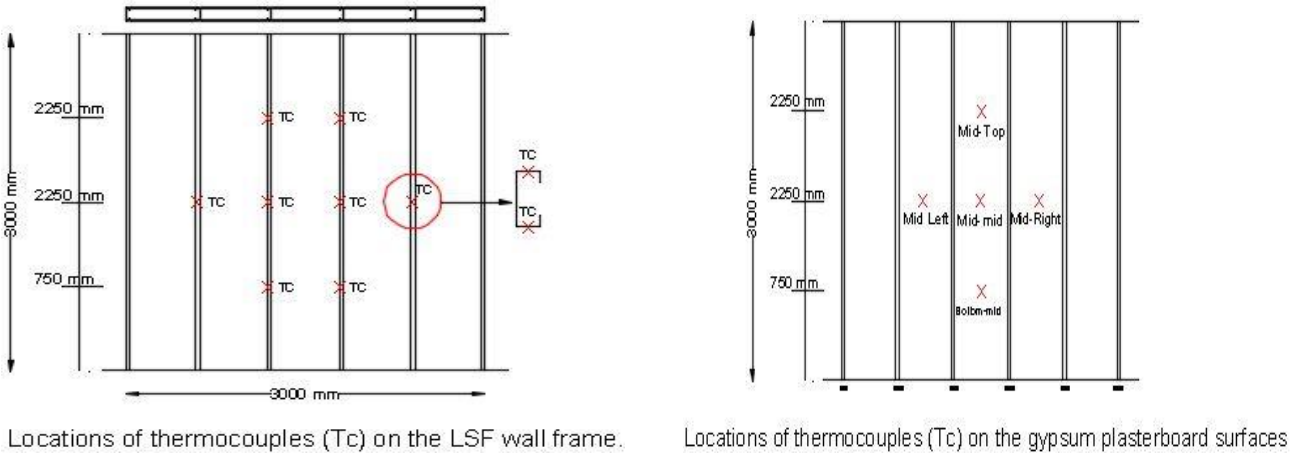

Figure 4.4:Thermocouples Position[76].

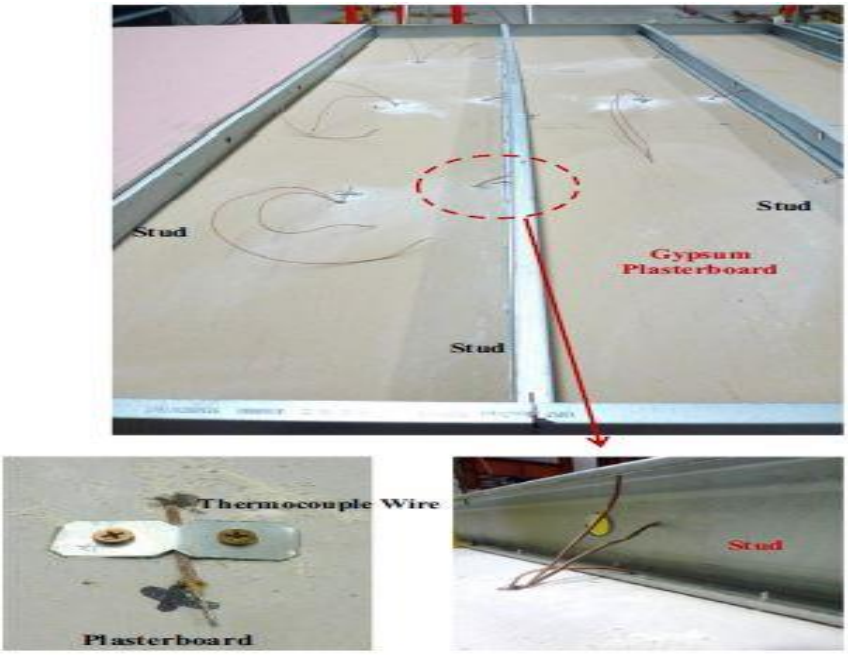

Figure 4.5:Thermocouple fixings on LSF wall test panel[76].

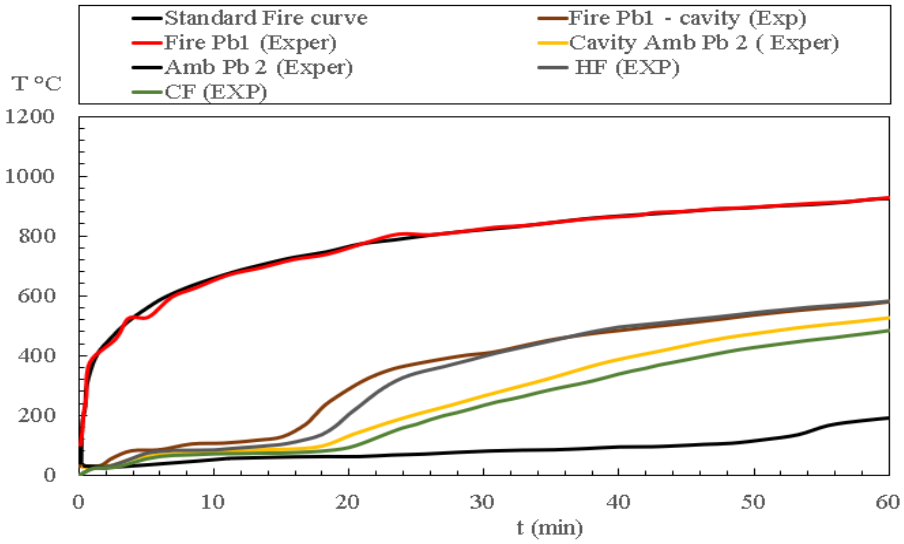

Figure 4.6:(a) Average plasterboard temperatures

The figure 4.6 shows the average and the maximum temperature evolution of the thermocouples across the time. With linear regression, some failures were estimated.

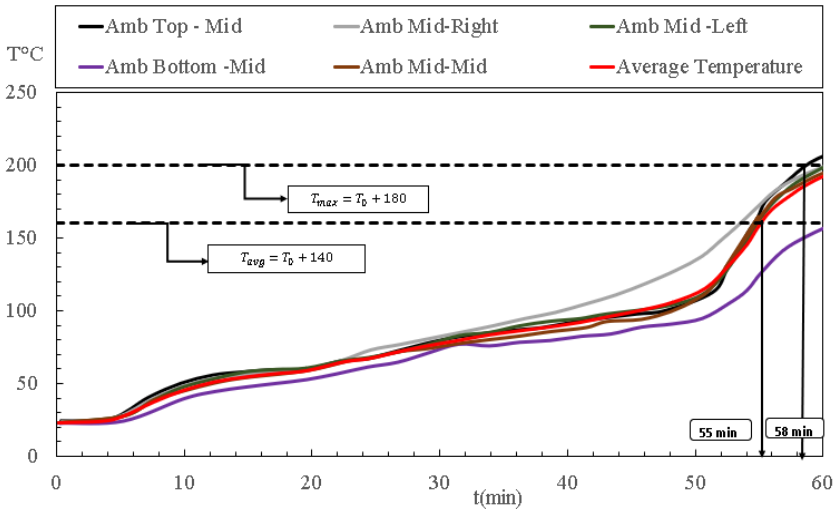

Figure 4.7:(b) Ambient plasterboard temperatures

The figure 4.7(a), shows the temperature evolution in point of vue the average and the maximum temperature on the unexposed side.

4.2.2. Specimen 4: Test 4:

The specimen 4 has single layer of plasterboard, but the cavity is filled with glass Fibre. The Glass Fibre used in this case has density of 10kg/m3. The thermocouples are distributed by the specimen as presented in the figure 4.8.

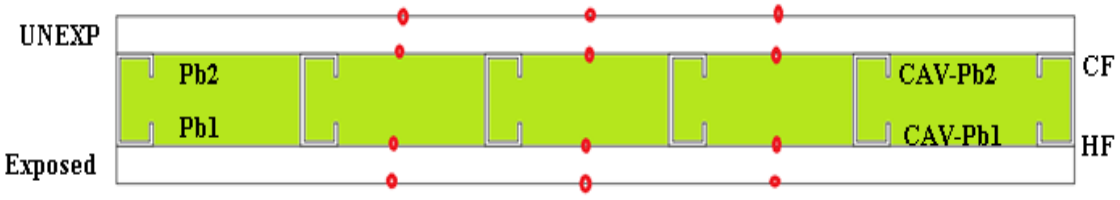

Figure 4.8:Thermocouples Position on Specimen 4

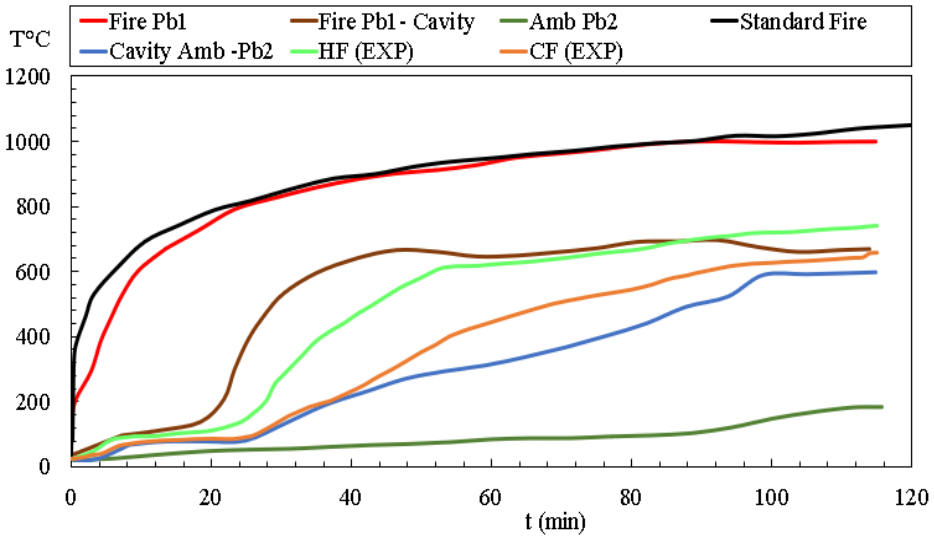

Figure 4.9(a): Average plasterboard temperatures on Specimen 4

The figure 4.9 shows the average temperature measurements. This specimen has one single layer plate and the cavity is filled with glass fibre.

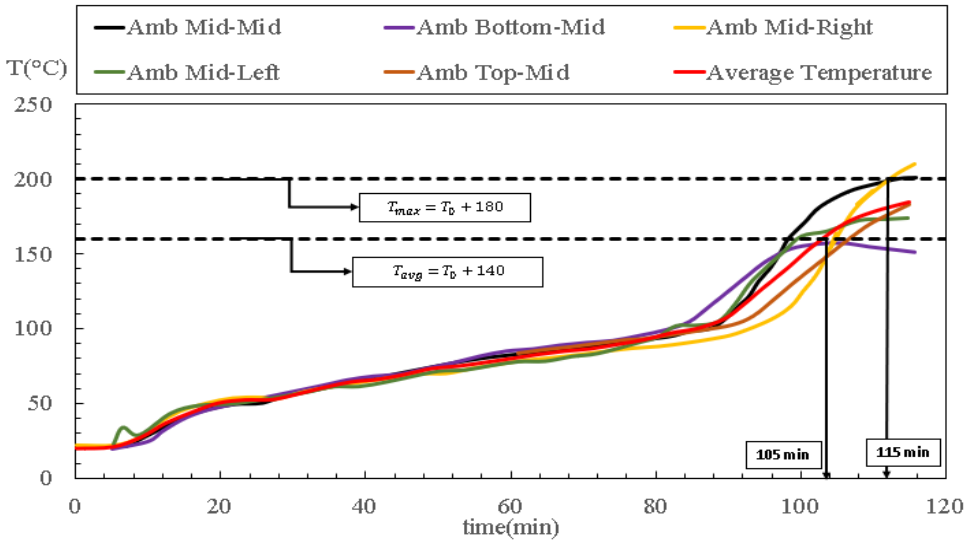

Figure 4.10(b): Ambient plasterboard temperatures on Specimen 4

The figure 4.10 (b), shows the temperature evolution in point of vue the average and the maximum temperature on the unexposed side.

4.3. Material Properties

The thermal properties of materials have a significant impact on the results of numerical simulation of structural members under fire conditions. In this regard, since the thermal model estimates that the thermal performance is closer to reality, better results can be obtained. Nonlinear transient heat transfer analysis requires the calculation of the specific heat, thermal conductivity, and density of the material at each time step. Specific heat can be defined as "the energy required to raise the temperature of a unit mass of matter by one degree in a specific way." Thermal conductivity is "a measure of the thermal conductivity of a material" The density of a material is defined as the mass per unit volume. These thermal properties vary depending on the standards used, and the thermal properties of each material of interest are briefly discussed. The thermal properties are decisive to simulate the performance of the non-loadbearing wall. The thermal properties are temperature dependent for all the materials involved. Steel presents typical evolution for the specific heat with a maximum value that accounts to the allotropic transformation. The thermal conductivity depends on temperature and specific mass is considered constant, [22]. The thermal properties of Gypsum considered in this investigation were proposed by Sultan et al. [56] for the specific heat, thermal conductivity and for the specific mass. The material properties of the glass fibre were assumed as proposed by Keerthan et al [58], but considering the density equal to 15.42 kg/m3.

4.3.1. Gypsum Plasterboards

Sultan [56] , conducted test at NRCC to obtain the thermo-physical properties of type X Gypsum Board. Measurements were carried out at a heating rate of 2°C/min as it provided the maximum specific heat at approximately 100°C. The author has given the results in the form of equations for Specific heat, thermal conductivity and density. The equations are represented in the form of table (4.2), (4.3), and the specific heat and thermal conductivity of the plasterboards used in this study followed the recommendations of Sultan [56], as shown in Figure 4.11. In their research, the authors analysed the fire resistance of load-bearing wall elements made of type X fire-resistant plasterboard at 20 ° C. The bulk density at 20 ° C used in this study is 576 kg / m³. Moreover, the emissivity is considered equal to 0.8, constant. Thermophysical Properties of type X Gypsum Board:

Table 4.2:Gypsum plasterboard thermal properties for the relevant temperature range [56].

Type of gypsum plasterboard	**Temperature range (T) (°C)**	**Property value**
Type X	$20°C \leq T \leq 78\,°C$	$C_g = 6.146\,T + 1.377$
	$78°C \leq T \leq 85°C$	$C_g = 150\,T - 9.858$
	$85°C \leq T \leq 97°C$	$C_g = 262\,T - 1.9501$
	$97°C \leq T \leq 124°C$	$C_g = 476\,T - 40311$
	$124\,°C \leq T \leq 139°C$	$C_g = 154.507 - 1.097\,T$
	$139\,°C \leq T \leq 148°C$	$C_g = 16.601 - 105\,T$
	$148\,°C \leq T \leq 373°C$	$C_g = 1.189 - 1.27\,T$
	$373°C \leq T \leq 430\,°C$	$C_g = 714$
	$430\,°C \leq T \leq 571°C$	$C_g = 1.151 - 1.014T$
	$571\,°C \leq T \leq 609$	$C_g = 1.877\,T - 501$
	$609\,°C \leq T \leq 662°C$	$C_g = 44.2\,T - 26.300$
	$662\,°C \leq T \leq 670°C$	$C_g = 3.000$
	$670\,°C \leq T \leq 685°C$	$C_g = 103.570 - 150\,T$
	$T \geq 670°C$	$C_g = 571$

Table 4.3:Gypsum plasterboard thermal properties for the relevant temperature range, Sultan [56] .

Type of gypsum plasterboard	**Thermal property**	**Temperature Range (T) (°C)**	**Property value**
Type X	Density (Kg/m3)	$20°C \leq T < 80°C$ $T \geq 80$	698 576
Type X	Thermal conductivity (W/m.K)	$20°C \leq T < 100°C$ $100°C \leq T < 400°C$ $400°C \leq T < 800°C$ $T \geq 800°C$	$K_g = 0.25$ $K_g = 0.12$ $K_g = 0.00035\,T - 0.01$ $K_g = 0.0013\,T - 0.77$

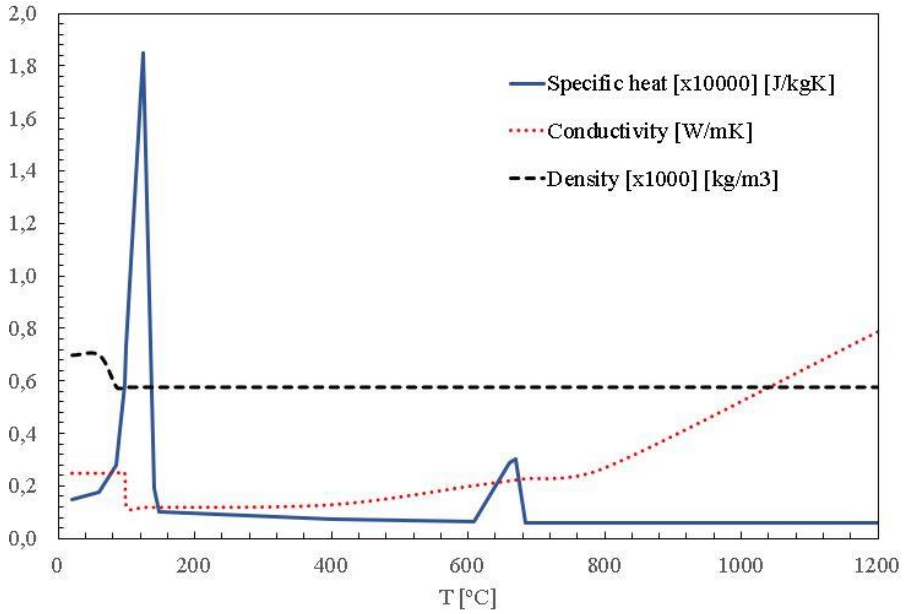

Figure 4.11: Effective thermal properties of gypsum plasterboard. Adapted from Sultan [56].

Figure 4.11 show the Two peaks in the specific heat curve indicate the dehydration of Gypsum, which delay in the temperature rise of protected steel studs in the stud wall assembly. The area under the peak gives the energy consumed per Kg of Gypsum Board to drive out the water of crystallization and free water from its core.

At this stage (around 100°C) there is a drop in density and thermal conductivity of the board. There is a steady rise in thermal conductivity beyond 400°C .

Thermal conductivity values above 400°C get affected by the presence of shrinkage cracks in the boars which depend upon the type and composition of board and the nature of fire ,Buchnan [59] .

Conductivity increases on account of radiative heat transfer caused due to the opening of cracks in the gypsum boards at high temperatures and also due to ablation, a process in which layers of calcined gypsum due to their cohesionless nature tend to fall off the board. Raking is more severe in fir with greater initial temperature gradient. According to Manzello et al. [60], cracks will be propagated in the order of opening at plasterboards joint, cracks at screw point along the stud and transverse cracks. Manzello et al. [61] study recommends incorporating plasterboard contraction and crack formation in thermal models.

The plasterboards play an important role in providing lateral stability to the steel studs. They provide adequate restraint against buckling and flexural buckling of the stud .They provide adequate restraint against buckling and flexural buckling of the stud about the minor axis .When

the assembly is expose to fire , this ability of the plasterboard to provide lateral restraint reduces due to the calcination of the gypsum board on the fire exposed side , whereas the plaster board on the ambient side of the assembly continues to provide lateral support as it is less affected by temperature.

Sultan [62], reported that fall-off of plasterboard occurs when the unexposed face of the board reaches about 600°C , Buchanan and Gerlich [63]. The temperature which the gypsum boards lose their restraining capacity depends on the type of boards used.

However, according to Ranby [64] a common temperature of 550°C was proposed. In the numerical study of Katila [65], the boundary condition providing lateral restraints at both flanges were assumed to be valid until 66°C.Thermal properties of gypsum plasterboards are required to determine the extent to which the plasterboards offer lateral support to the cold-formed steel studs at elevated temperatures resisting buckling about the minor axis.

4.3.2. Glass fibre

The material properties of the glass fibre were assumed as proposed by Keerthan et al. [58] in their investigation about the thermal performance of different insulation materials [58] but considering the density equal to 15.42 kg/m3. The thermal conductivity increases expressively after 200 ºC as to include the effects of ablation and account for porous radiation and convection. The emissivity is 0.9 constant. See figure 4.13 , table 4.4 .

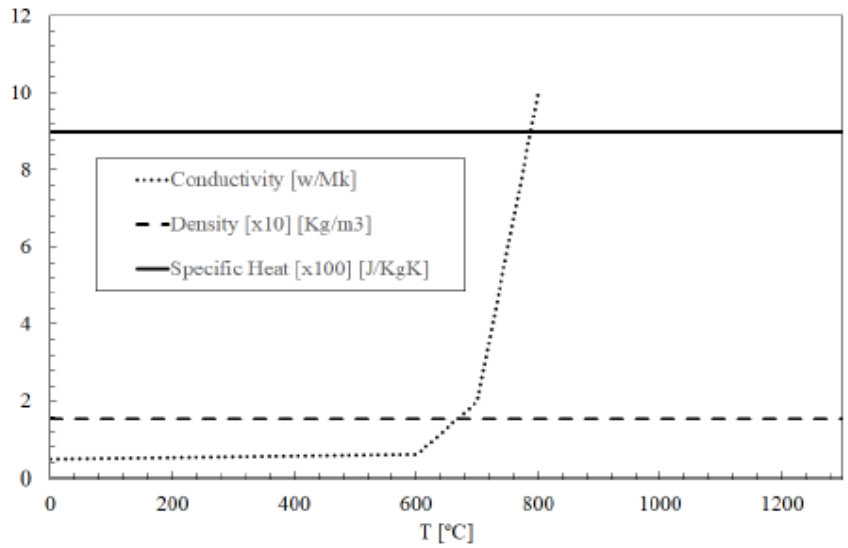

Figure 4.12:Thermal properties of glass fibre insulation. Adapted from. Keerthan et al [58].

Table 4.4: Glass fibre thermal properties for the relevant temperature range Advanced Material, Keerthan et al [58]

T(°C)	Specific mass (Kg/m3)	Conductivity (W/m/K)	Specific heat (J/Kg/K)	Emissivity
20	15.4	1	900	0.9
80	15.4	0.5	900	0.9
199	15.4	0.5	900	0.9
200	15.4	0.1	900	0.9
299	15.4	0.1	900	0.9
300	15.4	0.1	900	0.9
399	15.4	0.1	900	0.9
400	15.4	1.5	900	0.9
499	15.4	1.5	900	0.9
500	15.4	2	900	0.9
699	15.4	2	900	0.9
700	15.4	3	900	0.9
1200	15.4	3	900	0.9

These insulators are made in the form of thick rectangular plates and installed on the wall. Physical experiments show that when the porosity of this insulating material increases, i.e. when the number of glass fibres decreases, the effective heat transfer coefficient of the material also decreases. In fact, the thermal conductivity of glass is greater than that of air. But this phenomenon continues only up to a certain degree of porosity. If the porosity exceeds this level, the heat transfer coefficient of the insulating material begins to increase again with the porosity. This shows that the quality of fiberglass insulation can be improved by reducing the uneven density of glass fibre as much as possible.

4.3.3. Carbon Steel:

For carbon CFS elements, their thermophysical properties are given by EN 1993-1-2 [22] and are represented in figure 4.13. The emissivity of carbon steels is ε_f = 0.7 at all temperatures, as stated by EN 1991-1-2 [52], the specific heat of carbon steel Ca(J/kgK) is temperature dependent and shall be determined from the following equations.

$20°C \leq \theta \leq 600°C$ $\quad c_a = 425 + 7.73 \times 10^{-1}.\theta_a - 1.69 \times 10^{-3}.\theta^2{}_a + 2.22.10^{-6}.\theta_a{}^3$

$600°C \leq \theta \leq 735°C$ $\quad c_a = 666 + 13002/(738 - \theta_a)$

$735°C \leq \theta \leq 900°C$ $\quad c_a = 545 + 17820/(\theta_a - 731)$

$900°C \leq \theta \leq 1200°C$ $\quad c_a = 650$

It can be noticed that the specific heat of steel has an abrupt variation for temperatures between 700 °C and 800 °C. This is due to the allotropic phase transformation, which can affect the temperature development on steel components.

The EN 1993 – 1-2 [22] states that the thermal conductivity of carbon steel λ_a (W/mK) varies with temperature and should be calculated according to the following equations.

$$\lambda_a = 54 - 3.33 \times 10^{-2}\theta_a \qquad \text{For } 20°C \leq \theta \leq 800°C \qquad (4.2\text{ a})$$

$$\lambda_a = 27.3 \qquad \text{For } 800°C \leq \theta \leq 1200°C \qquad (4.2\text{ b})$$

In the equations above, θ_a is the steel temperature (°C). Figure 4.13 represents the variation of this thermal property with temperature.

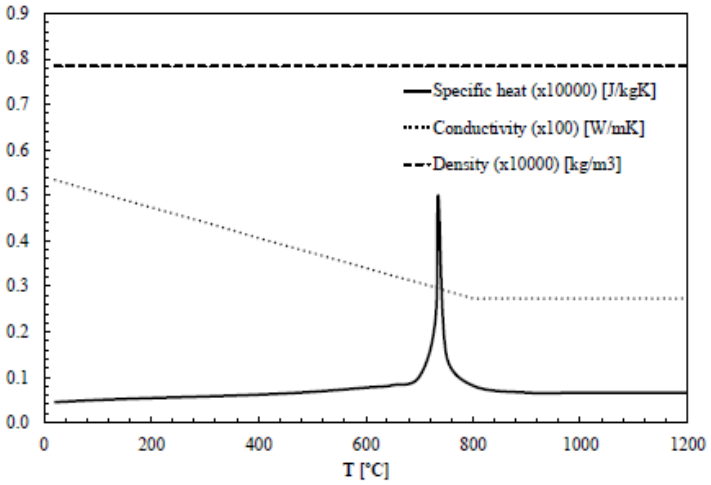

Figure 4.13: Thermal properties of Steel. Adapted from EN1993 [22].

4.4. Findings Relevant to this Research

Researchers attempted to improve the fire resistance of the wall system by using different types of insulating materials in the wall cavity. However, their observations are contradictory. Sultan and Lougheed [66] observed that, compared to uninsulated wall components, the use of rock fibres or cellulose as an insulating cavity improves fire resistance by about 30 minutes. Only rock fibre used as a non-loadbearing cavity insulation wall component can improve fire resistance, while the component using cellulose fibre actually has lower fire resistance Feng et al. [67] It was observed that the fire resistance of non-loadbearing wall panels was improved by using cavity insulation.

Since other researchers have not been able to conclude that the use of cavity insulation has an effect on the fire resistance of wall samples, more detailed experimental studies are needed. Fully understand the advantages and disadvantages of traditional methods of building walls using cavity insulation and recommend new wall designs to improve fire resistance. In the study conducted by Kodur et al. [68] and Alfawakhiri [69] showed that studs are essentially perfect and have failed at this precise stage. All the frames studied are crossed, and the bending failure mode is assumed to be through this lateral restraint, Gerlich [70] tested a frame with a central row of teeth to avoid low torsion and axle buckling.

Feng et al. [71].A study was conducted using a stud with a repair hole in the centre of the web. The studs are supported laterally by four flat rods fixed horizontally, two on each side of the frame, and studs without perforations or frames without side supports are not tested. Therefore, more research is needed to investigate the behaviour of half-timbered panels without perforations and / or supports. Gerlich's research [70] is limited to 300 and 450 grades of steel. The studies by Kodur et al. [68] and Alfawakhiri [69] involved the use of cold-formed steel nails. Feng et al. The yield strength is 230 MPa , extended their field of research to S350 steel of 1.2 mm and 2 mm thickness.

Therefore, it can be concluded that previous studies on the performance of high temperature LSF stud wall panels are limited to lower grade steels, so more research on high grade LSF steel wall systems is needed. superior. In the studies by Kodur et al. [68], Alfawakhiri [69] and Feng et al. [71], It is assumed that the temperature of the flange and lip of lip groove studs on the hot and cold sides is uniform . These observations indicate that it is necessary to study the actual temperature distribution through and along the poles in the event of a fire, and it is

recommended to simplify the temperature distribution for numerical and theoretical studies of wall systems. LSF.

Due to the lack of experimental results and the complexity of the problem, most of the numerical models tested previously have not been fully verified. In addition, the high temperature calculation method developed previously is extremely complicated. Therefore, more research is needed to recommend simplified temperature profiles for numerical and theoretical research and to develop simple models. In Gerlich's [70] study, the test performed on only three samples contained too many variables. Multiple variables between trials make it difficult to draw specific inferences, and this study only used one coat of coating.

Regarding the effect of multi-layered plasterboard, there is very limited data on the influence of joints in plasterboard and the density and thickness of the insulating material of the cavity on the fire behaviour. Wall components. Therefore, a series of fire tests must be performed to establish the fire resistance of gypsum board, load-bearing wall components and load-bearing wall components using insulating materials of different densities and thicknesses. in consideration. In most of the previous experiments, it was noted that the actual standard time temperature heating curve in the furnace could not be satisfactorily controlled.

In addition, the instrument is not detailed enough to fully understand the wall thickness and the temperature gradient in the direction of the wall thickness, and does not fully record the furnace pressure information. In most cases, negative pressure in the oven will cause the temperature of the edge pad to drop relative to the centre pad, resulting in uneven thermal expansion of the pad. Also, commonly observed bolt loads using steel beams cannot guarantee that the loads on all bolts are equal.

Due to the uneven expansion of the studs, the prediction of the collapse load is not accurate further complicating the problem. In order to overcome all these problems, it has been found that it is necessary to construct a special furnace which can accurately provide the heating process and the equipment required to monitor and control the pressure of the furnace. Select the appropriate instrument to measure the change in temperature of the wall specimen, customize the load frame to allow load to be applied to each stud, and maintain a constant load to ensure free thermal expansion during the procedure test .

Additionally, as most of the research is conducted outside of Australia, it represents the specific materials and construction methods used in those countries / regions, and since there is no custom-built loading frame, loads can be applied to each column and maintain a constant load.

To ensure free thermal expansion during testing. Additionally, since most of the research is done outside of Australia, it represents the specific materials and construction methods used in those countries, and since there is no custom-built loading frame, allows load to be applied to a single column and maintain a constant load. Ensure free thermal expansion during the test.

In addition, since most of the research is conducted outside of Australia, it represents the specific materials and construction methods used in those countries, and since there is no research on load-bearing walls in LSF. In Australia, it is important to conduct these studies to assess the performance of the Australian LSF half-timbered wall system and to provide recommendations for improving its fire resistance.

CHAPTER 5

5. Numerical Simulation

Small- and large-scale standard fire tests are expensive and time consuming. As an alternative,advanced computational methods based on computer-aided digital technology can effectively assess the thermal and structural performance of various complex engineering limit-value problems related to field variables, complex domains and irregularities in the fields. conditions to the limits. The non-linearity and the geometrical defects of the material are limited, in this case, the analytical solution of closed form cannot be obtained directly, it is the case when the composite structure LSF loaded and unloaded is exposed to fire.

In fire safety engineering, the Finite Element Method (FEM) has been gradually used to evaluate the thermal and structural performance of LSF walls at elevated temperatures in order to achieve a safe and economical design. By exposing the wall models to a standard time-temperature curve and applying appropriate initial conditions and limits, the transient thermal response and fire resistance of these walls can be predicted.

In addition, the actual thermal performance of the material in the appropriate temperature range must be specified. However, the modelling of integrity problems and mass transfer phenomena is still limited, and the current practical methods for solving these problems are mainly based on the results of the observation of the user's fire tests and on the effective thermal properties of the material. Additionally, since almost no information is provided on the fire behaviour of the LSF stud wall, a numerical assessment is required to identify simulation parameters, routines and model assumptions that affect its thermal model and resistance . Fire can dramatically improve performance design standards and specifications.

Therefore, this chapter explores the main aspects of the process of developing 2D models in standard fire scenarios to simulate thermal behaviour and predict the fire resistance of LSF frame wall insulation. In other words, it is a special numerical task to develop an accurate model to predict fire resistance and to verify the two-dimensional finite element model for fluid interaction.

This chapter presents the numerical verification of the experimental tests. It also covers the resources and limitations of ANSYS®Multiphysics, which is used for FEM-based transient heat transfer analysis.

5.1. FEM for Heat Transfer Phenomena

Steady and transient heat transfer phenomena involving complex geometries, varying material properties, and irregular boundary conditions are common in fire safety engineering. For such problems, which are governed by second order continuous differential equations, it is generally difficult to develop approximate functions for the variable field of interest. Consequently, by discretizing the problem zone and its governing equations, the FEM allows the local representation of the complex domain and its limits.

The geometry [94], node position and element coordinate system are shown in Figure 5.1 for PLANE55 geometry.

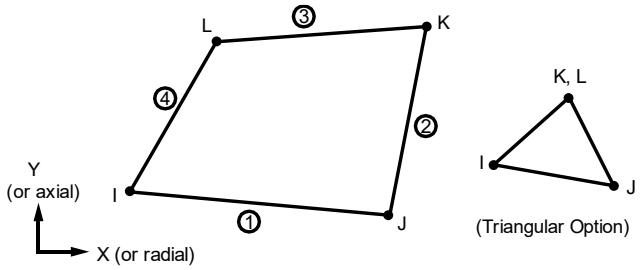

Figure 5.1: Geometry PLANE55 [94].

This element is defined by the properties of four nodes and expressed in terms of approximating functions (also called interpolation or shape functions). The direction of the element's natural coordinate system is that described by the nodes of the element.

The element load is described in node load. Convection or heat flow (but not both) and radiation can be entered as a surface charge on the element's surface, as indicated by the number circled in the geometry of PLANE55, [94].

5.1.1. Thermal Models of stud LSF Walls

ANSYS®Multiphysics is an FEM-based software package that can perform geometric design and thermal analysis on stable or transient linear and non-linear heat transfer problems (including 1D, 2D or 3D domains). The program provides a set of elements with finite lines, surfaces or volumes. These elements have a varying number of nodes with different degrees of freedom and interpolation functions, depending on the object of analysis.

The complex boundary conditions of the material and the associated thermal properties can be used in the form of tables or of functional quantities depending on the temperature [72]. In transient analysis, the ANSYS® solver manages three main modes of heat transfer. Convection is referred to as the external surface charge of a solid element or conductive shell. If necessary the film coefficient can be defined as a temperature related parameter. For radiation effects,using the radiosity solver method, the generalized radiation interaction between two or more surfaces inside the enclosure can be treated as 2D or 3D elements with degree of freedom temperature, where the change temperature in each enclosure is defined as a Space Function node. The enclosure can be composed of multiple gray diffuse radiating surfaces with known emissivity, where the emissivity of each material pattern varies with temperature. Use the hemicube method to calculate the view factor between 3D shell surfaces. The calculated heat flux will be used as the boundary condition for the conduction analysis of the entire finite element model. For the new node temperature of each time step, determine the new surface heat flux condition and find the temperature of node of the following time step for the whole of the model.

5.1.2. 2D Finite Element Model:

PLANE55 [94], can be used as a plane element or as an axisymmetric annular element with 2D thermal conductivity. The element has four nodes, and each node has only one degree of freedom, namely temperature. This element is suitable for two-dimensional thermal analysis in steady or transient conditions. This element can also compensate for the flow of mass transfer heat from a constant velocity field. If you want to perform structural analysis on a model that contains temperature elements, you must replace this element with an equivalent structural element (such as PLANE182).

ANSYS® provides a graphical interface that allows users to define geometric entities based on the geometric characteristics of the problem, such as key points, lines, areas, and volumes. In this study, the 2D -dimensional LSF wall is made of three or four isotropic materials: Gypsum plasterboard, steel, air and cavity insulation (Glass Fibre), each with its own set of thermal characteristics and assigned elements. For each material model, the lines are subdivided into appropriate line segments, which will define the size and density of the mesh.

The area is obtained from the line. The 2D finite element model of the LSF composite frame wall and the type of finite element assigned to each material model. In this survey, mesh size and density were determined on the basis of sensitivity analysis and previous numerical studies [60]. (a) Steel mesh (SHELL131 finite elements), (b) Gypsum plasterboard layer mesh).

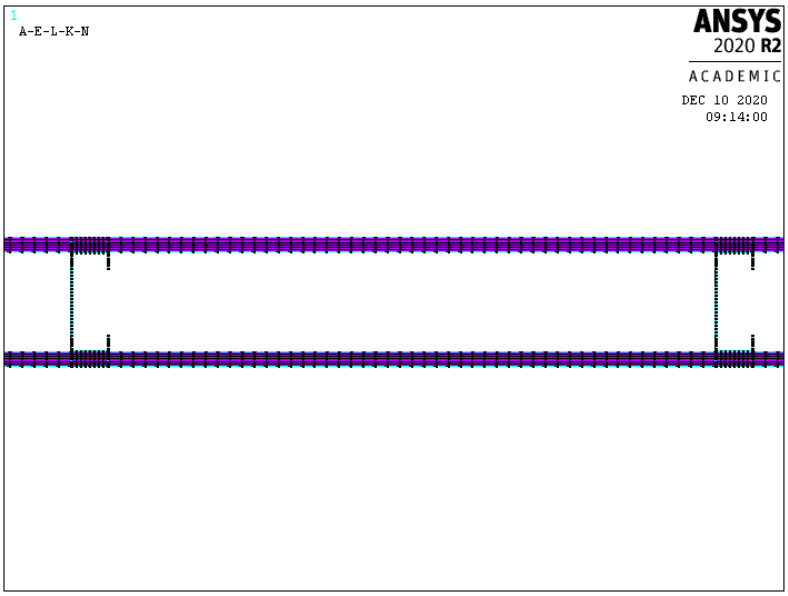

Figure 5.2: Finite element mesh of LSF wall model (model specimen 2).

This method was developed in the ANSYS Multiphysics, and use the average temperature of the cavities obtained from the experiment. A mixed boundary condition of radiation and convection was applied on lines inside the cavities, being the convective coefficient assumed as an average of the convective coefficients of the fire side and unexposed side. The emissivity in the cavity was assumed equal to 1.

- **Test 4: 1 Layer 16mm Gypsum Pb and Glass Fibre** 15.42 **Kg/m²**

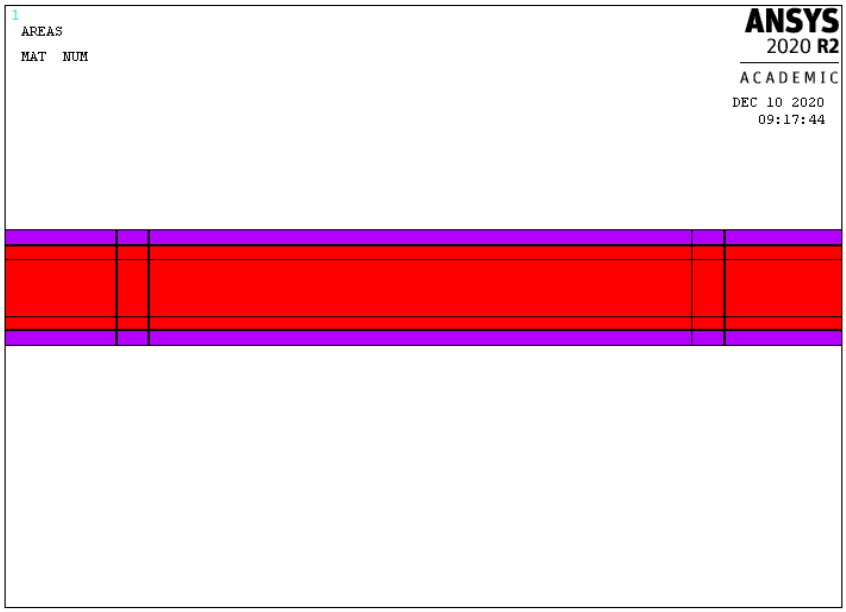

Figure 5.3: Finite element create areas of LSF wall model (model specimen 4).

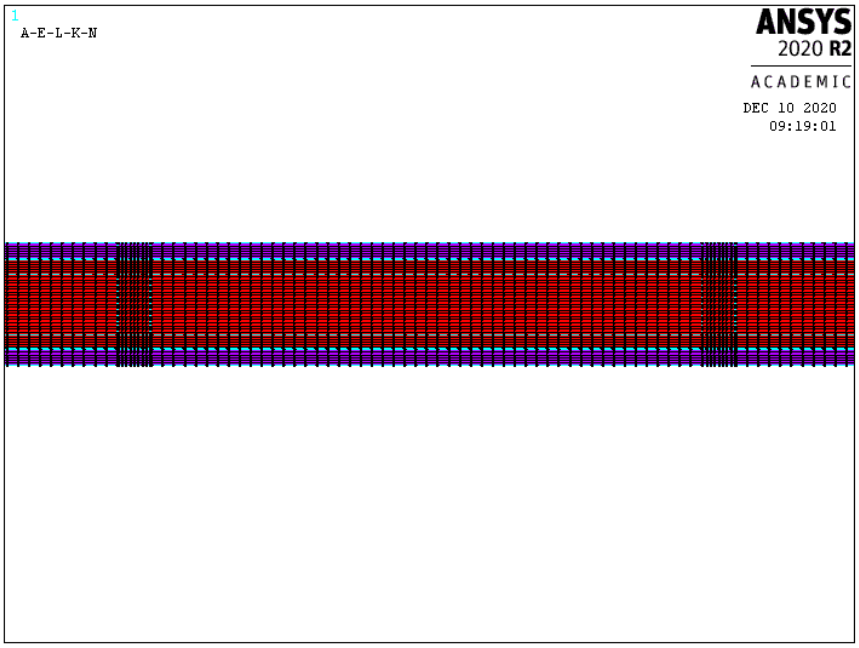

Figure 5.4:Finite element mesh of LSF wall model (model specimen 4)

The solid model used ANSYS MULTIPHYSICS to solve transient and nonlinear thermal analysis, using full option solution method. The same time step was used with similar convergence criterion for the heat flow. Figure 5.4 represents the mesh of CASE 2D. The mesh was defined based on a convergence test.

5.1.3. Initial and Boundary condition:

Regarding the standard fire exposure, EN 1991-1-2 [24] states that for the exposed face of building elements, when the following situations occur, it is acceptable to use αcv = 25 [W / m²K] using the ISO 834 [17] fire protection standard, For the unexposed surface, assuming radiation and convection work together, αcv is equal to 9.0 [W / m²K]. In addition, the fire is considered to be a black body, which means εf = 1.0, εm depends on the type of material.
For composite wall panels under standard fire conditions, the initial temperature is specified in accordance with ISO 834 [17], which means T0 = 20 ° C is applied to all nodes. EN 1991-1-2 [24] does not specify the parameters of heat transfer between the surface and the cavity. Therefore, when convection and radiation occur in the LSF wall cavity, the boundary conditions of convection and radiation should be targeted to these areas, as shown below.
Therefore, according to previous numerical studies [60], for a row of exposed studs, the film coefficient in the gypsum board-cavity interface and the steel surface facing the cavity is set at αcv = 17 [W / m²K]. See figure 5.5.

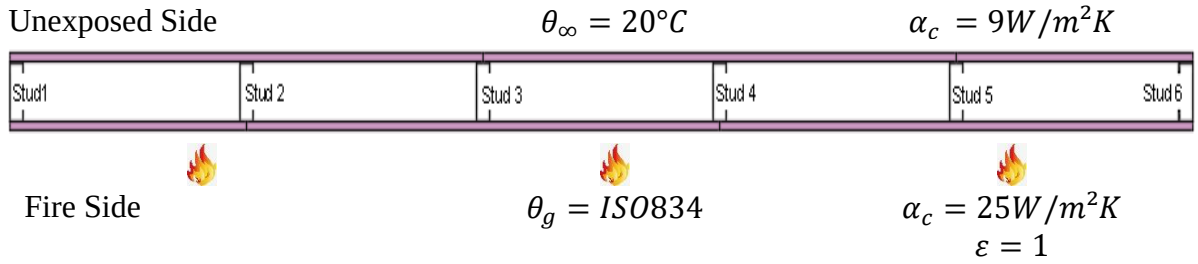

Figure 5.5: Boundary Conditions.

5.1.4. Interpolation function

In numerical analysis (and in its discrete algorithmic application for numerical computation), interpolation is a mathematical operation allowing to replace a curve or a function by another curve (or function) simpler, but which coincides with the first one in one finite number of points (or values) given at the start.

Depending on the type of interpolation, besides the fact of coinciding in a finite number of points or values, the curve or the constructed function can also be requested to verify additional properties. The choice of starting points (or values) is an important element in the interest of the construction.

The simplest type of curve interpolation is linear interpolation, which involves "joining the points" given by line segments. Given two points (x1,y1) and (x2,y2), the value at an intermediate point (x,y) is given by

$$y=(x-x2)/(x1-x2)y1+(x-x1)/(x2-x1)y2. \quad (5.1)$$

5.2.Numerical Validation and Discussion

Use a finite element model to define part of the cross section of a non-loadbearing wall. The model uses PLANE 55 finite elements with a two-dimensional thermal behaviour. The element has four nodes with only one degree of freedom (the temperature of each node). The unit has a linear interpolation function and uses four points to develop a fully integrated Gaussian method on the quadrilateral. The grid is defined on the basis of the convergence test.

The solution uses incremental and iterative methods to solve nonlinear transient thermal problems. Convergence is based on the calculation of internal heat flow; the minimum reference value is 1E-6 and the tolerance value is 0.001. The time step is defined as 60 s, at least 5 s to reach convergence.

The fire resistance of non-loadbearing walls depends on the calculation of unexposed walls surface temperature. The temperature is not uniform, depending on the amount of steel included in each type of non-load-bearing wall. Performance standards used for these structural elements consider the average temperature $\boldsymbol{T_{ave}}$ and the highest temperature$\boldsymbol{T_{max}}$.The calculation of the maximum temperature and the average temperature depends on the distribution of the nodes over the entire length of the unexposed surface.

Figure 5.6 and figure 5.8 illustrate the comparison between the experimental and numerical results for the temperature development in Model Specimens 2(test 2) and Model Specimens 4 (test 4), respectively expressed in terms of average and maximum temperatures. The data were collected at selected nodes throughout the finite element mesh see final temperature distribution at Fig. 5.7 and 5.9.

Figure 5.6 show the comparison between the experimental and numerical results for the temperature development in Model Specimens 2 (test 2) respectively, expressed in terms of average and maximum temperatures.

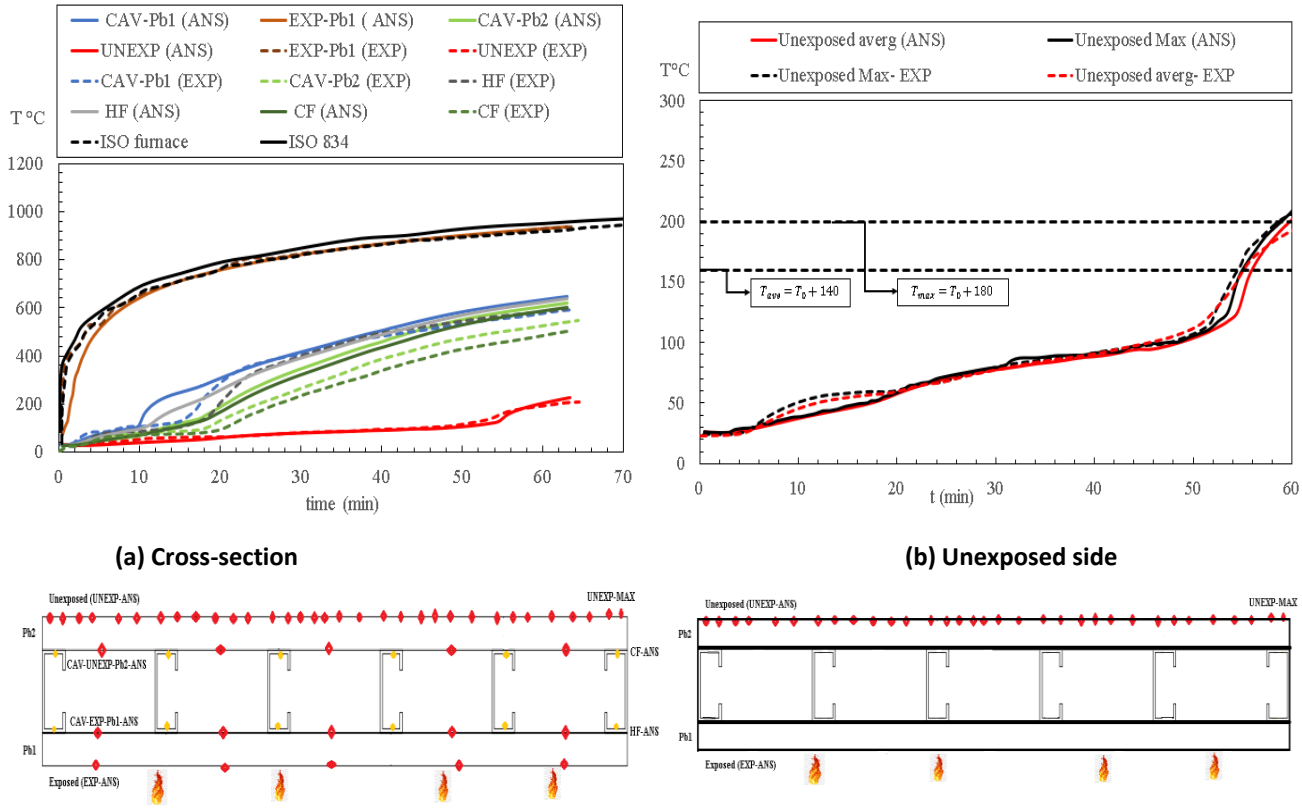

Figure 5.6:Numerical and experimental results for Model Specimen 2

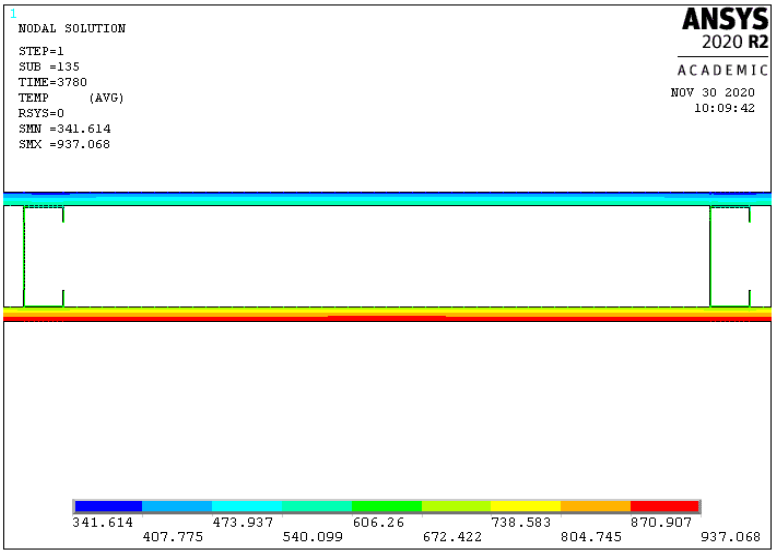

Figure 5.7:Numerical simulation for Model Specimen 2, **t=63 min**

The thermal properties used to solve this numerical simulation; the steel properties were retrieved from EN 1993-1-2 [22] and the gypsum properties were retrieved from the work developed by Mohamed Sultan. [56]. Accordingly, the numerical results are higher than the experimental ones and we can justify this by the temperature development on the exposed surface of the models, it is noteworthy that the furnace temperature used to represent ISO 834 standard fire curve (dashed) is lower than the curve employed in the simulations.

However numerical simulation gives a significant difference between PB-EXP and PB-EXP-ANS in Model Specimen 2 (test 2) and this justifies the higher conduction resistance of the air in comparison to these materials. Moreover, a great significant difference between the UNEXP-ANS and UNEXP-EXP such a behaviour can be justified by using a perfect contact between the elements.

Concerning the average and maximum temperatures on the unexposed side of both, good agreement was obtained during the simulation period, such behaviour can be justified by the perfect contact between the elements.

Figure 5.8 show the comparison between the experimental and numerical results for the temperature development in Model Specimens 4 (test 4) respectively, expressed in terms of average and maximum temperatures.

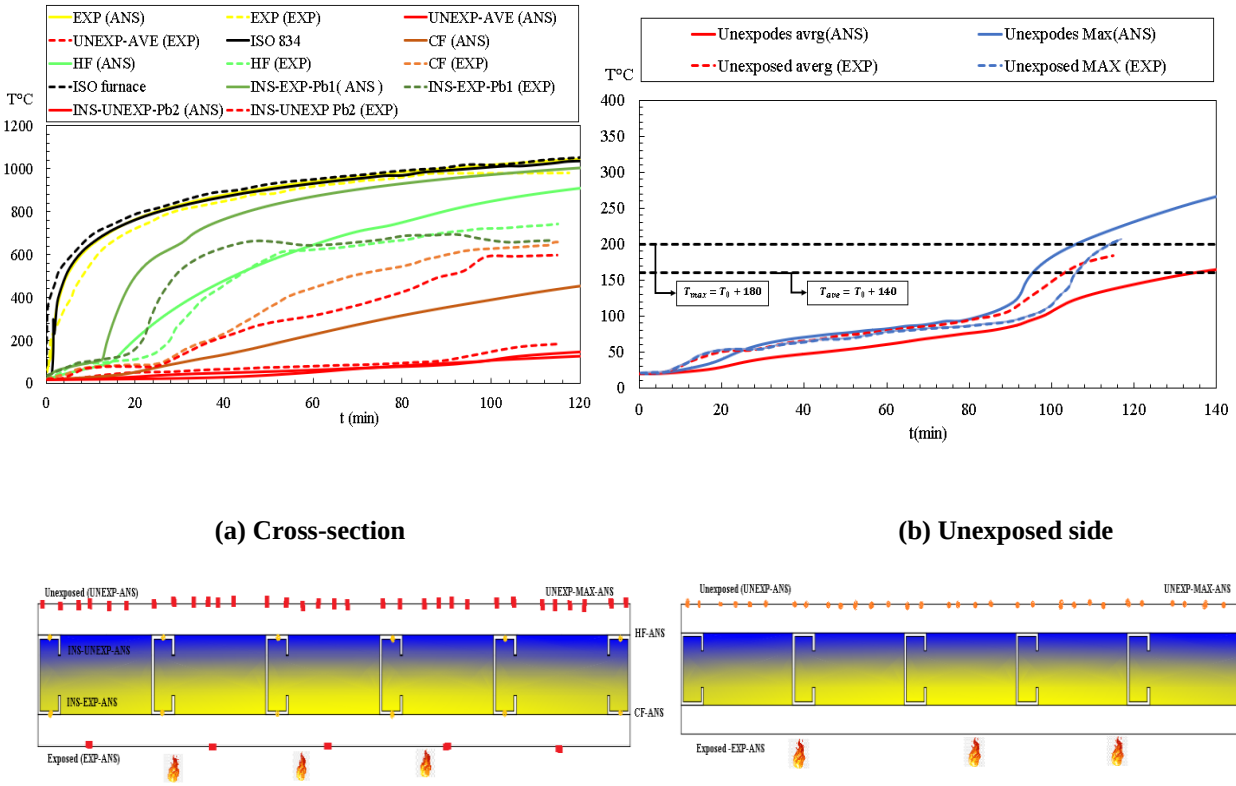

Figure 5.8:Numerical and experimental results for Model Specimen 4

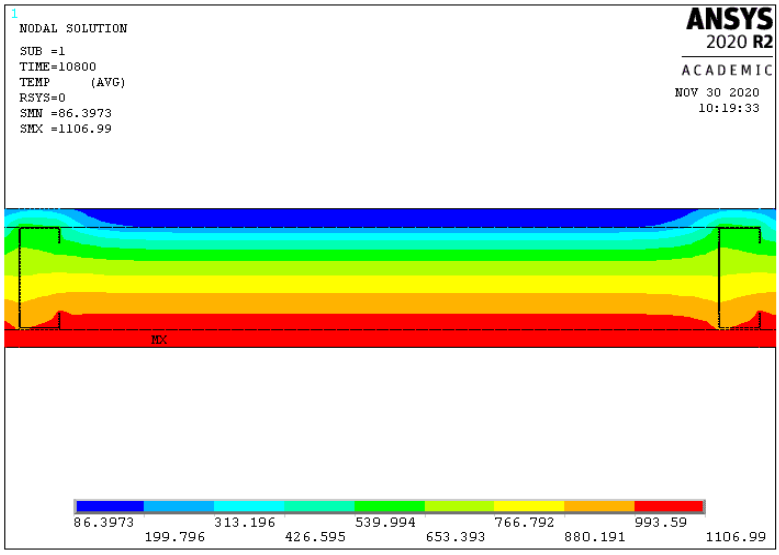

Figure 5.9:Numerical simulation for Model Specimen 4, t= 180min

As for the models with wall cavity insulation the thermal properties used to solve this numerical simulation; the steel properties were retrieved from EN 1993-1-2 [22] and the gypsum properties were retrieved from the work developed by Mohamed Sultan. [56], the glass Fibre developed by Keerthan et al [58].

Referring to Model Specimen 4, as cavity are filled with glass fibre insulation However numerical simulation give unsignificant difference between the CF-EXP-ANS and CF-EXP such behaviour can be justified that the using material properties [58] different from the experimental test.

In terms of average and maximum temperatures there is a difference between experimental and numerical results were noticed for Model Specimens 4, with cavity insulation. This is due to the using material properties of the glass fibre developed by Keerthan et al [58] different from the material properties used in experience test 4 [76] .

5.3. Summary and Conclusions

Table 5.1 presents the comparison between the experimental and numerical fire resistance obtained for the LSF walls concerning Tave and Tmax insulation requirements. the specimens tested by the author were used to validate the numerical models, two different specimens from the tests developed by [76] were also used in for validation. The relative error is the method adopted to validate the mathematical model, the relative errors related to the maximum temperatures (T_{max}) and the average temperature (T_{avg}) on the unexposed side of the Model Specimens 2 and 4 and it is presented in (5.2) .

$$RE = \frac{T_{experimental} - T_{numerical}}{T_{experimental}} \ (\%) \qquad (5.2)$$

Table 5.1:Comparison between the experimental and numerical fire resistance of the specimens

Model Specimen N°	Experimental		Numerical		Relative Error %	
	Fire resistance (T_{ave}) (min)	Fire resistance (T_{max}) (min)	Fire resistance (T_{ave}) (min)	Fire resistance (T_{max}) (min)	(T_{ave}) (min)	(T_{max}) (min)
Model Specimen 2	55	58	56	59	1.81 %	1.7 %
Model Specimen 4	106	115	134	106	26.4 %	7.8%

Model Specimen 2 T_{ave} fire resistance is slightly overestimated, with an absolute relative error of 1.81%. However, with the exception of Model Specimen 2, the results of the finite element thermal analysis are more conservative than the experimental tests. The potential sources of error are related to the method of resolution and to the numerical error of the selected finite element mesh, to the characteristics of the materials used and to the parameters independent of temperature.

The root means square error are (RMS %) related to the maximum temperatures T_{max} and the average temperature T_{ave} , the exposed side and the cavity insulation, and it is presented in the equation (5.3)

- **the root means square error (RMS %) see table 5.2 equation (5.3)**

$$\boldsymbol{RMS}\ \% = \sqrt{\frac{\boldsymbol{1}}{\boldsymbol{n}}\ \boldsymbol{X}\ \sum_{\boldsymbol{i=1}}^{\boldsymbol{n}}\ \left(\frac{\boldsymbol{T_{numerical} - T_{experiment}}}{\boldsymbol{T_{experimental}}}\right)^2}\ \ \boldsymbol{X}\ \ \boldsymbol{100}\ \ (\%) \qquad (5.3)$$

Table 5.2: The root means square error (RMS %) between the experimental and numerical fire resistance of the specimens

(UNEXP-MAX-ANS) **test 2**	(UNEXP-AVE-ANS) **test 2**	(CAV-Pb1-ANS) **test 2**	(CAV-Pb2 - ANS) **test 2**	(EXP-ANS) **test 2**	(UNEXP-MAX-ANS) **test 4**	(UNEXP-AVE - ANS) **test 4**	(EXP-ANS) **test 4**
8.37 %	**8.54 %**	**16.5 %**	**21.04%**	**14.98 %**	**21.87%**	**26.13%**	**10.47 %**

CHAPTER 6

6. Parametric analysis

The parametric analysis considers the variation of the density of the insulation and the thickness of the cavity. This parametric analysis kept a few distances fixed in the model. The fire resistance was determined considering the insulation criterion (I).

A parametric study comprising 2 Layers of Gypsum plaster boards heights 2 X 13mm. for the time 36000s this parametric analysis is presented in figure 6.1 ,6.2 and 6.3 .

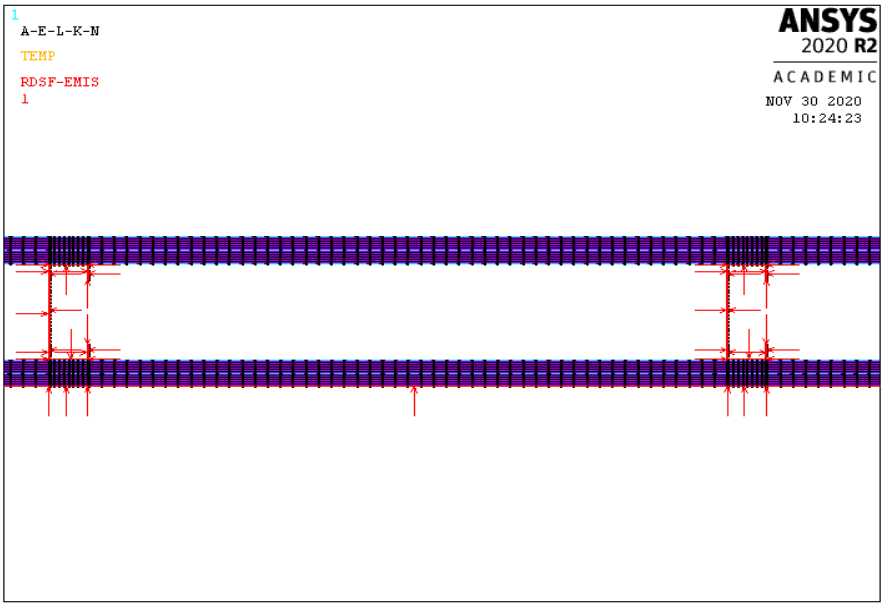

Figure 6.1:Numerical Model 1 Specimen 2

(a) Cross-section **(b) Unexposed side**

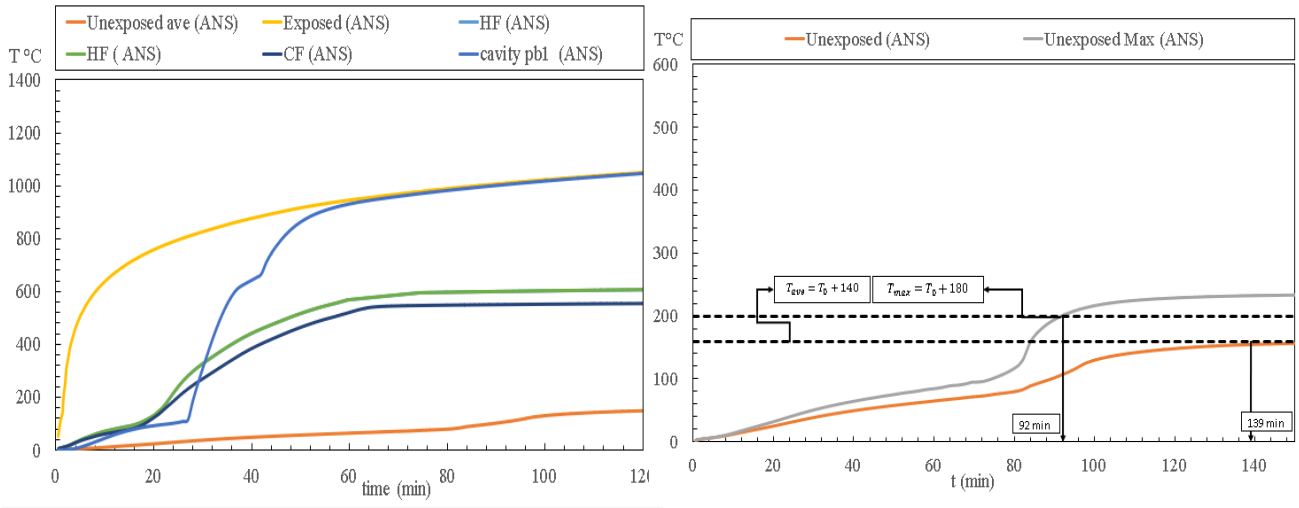

Figure 6.2:Numerical results for Model 1 Specimen 2.

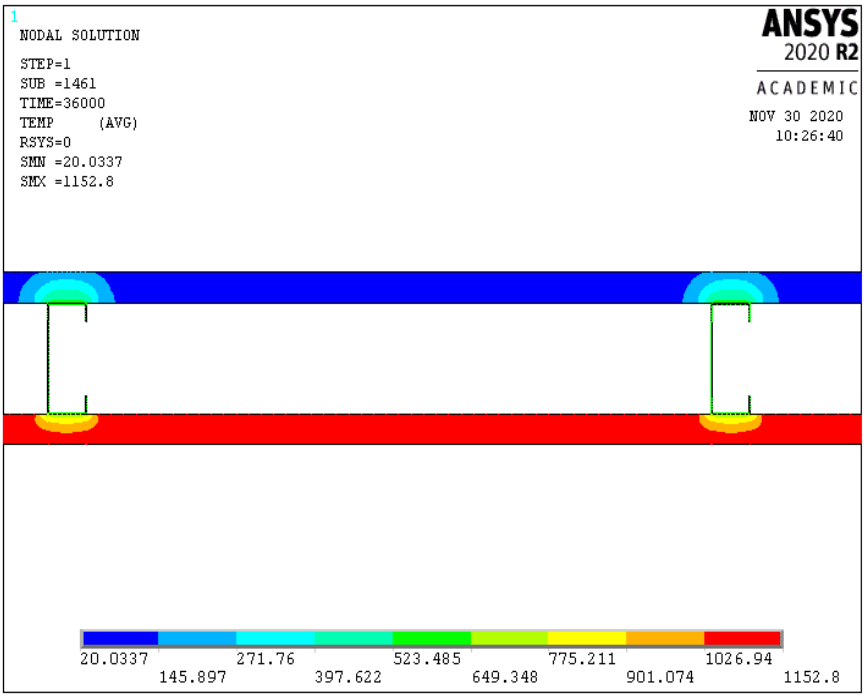

Figure 6.3:Numerical results for Model 1 Specimen 2, t=600min

Table 6.1:Characteristics and fire resistance of the wall assemblies used for parametric analysis. Model 1

Case	TH_ cavity [Mm]	Plate layer [mm]	Density Gypsum Plasterboard[kg/m3]	Fire resistance [min] (I) (T_{ave})	Fire resistance [min] (I) (T_{max})
1	92	2 X 13 mm	576	139 min	92 min

The using of two gypsum plates with 13 mm thickness each, increase the fire resistance of non-loadbearing walls .The fire resistance depends on the material used for the simulation of the structure.

This justify that we have moisture effect of gypsum because of using the material properties of gypsum developed by Mohamed Sultan [56], which may be different from the material properties used in test 2 by [76], so to avoid the effect of moisture of Gypsum boards : if we increase the specific heat (Cp) of the gypsum we will have a big temperature plateau . However, as we know sheathing and cavity insulation materials are significant elements of LSF walls due to their critical influence in the thermal, structural, and acoustic performance of the assembly. Apart from its sealing function, gypsum-based sheathing supplies fire protection for either load or non-load-bearing walls, due to its insulating properties, moisture content and chemically-bonded water, working as thermal rated fire barriers for the steel frame and other load and non-load wall components [73].

The thermal properties used to solve this numerical simulation; the steel properties were retrieved from EN 1993-1-2 [22] and the gypsum properties were retrieved from the work developed by Mohamed Sultan [56].

It can be noted that the fire resistance of LSF walls increases with the number of thicknesses of the protective layers. It was clearly noteworthy that when we doubled the number of plasterboards the fire performance of two coats of LSF wall gypsum (model 1) was better than using a single coat (test 2, specimen 2) to assist the wall crack.

For the model 2 we increase the thickness of the cavity with the modification of the dimension of the stud C100X50X10X1.5 [74] means increasing the thickness of the glass fibre using the material properties of glass Fibre developed by Keerthan et al [58].

The increase in the thickness of the fiberglass is the most important factor influencing the FRL (I) fire resistance of the non-load-bearing wall for more (3 hours), it means that it takes a long time to reach the gypsum crack in the wall this parametric analysis is presented in figure 6.4 and 6.5 and 6.6

As we know for the insulation of the cavity, mineral fibrous materials (glass fibre), gives improved acoustic behaviour, due to their high melting point, high porosity and low thermal conductivity, prove an exceptional insulation integrity and performance at elevated temperatures, preventing the spread of fire along the wall cavity for a certain temperature range.

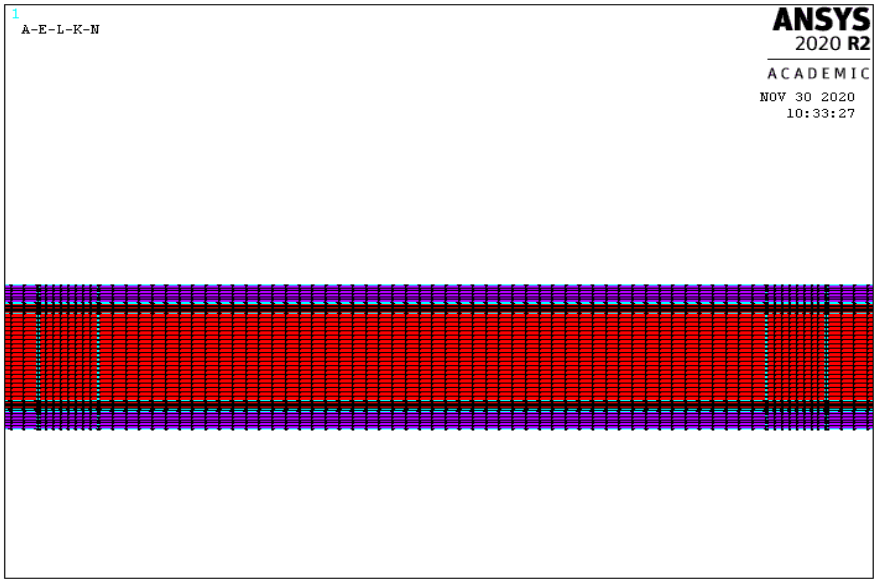

Figure 6.4:Numerical Model 2 Specimen 4.

(a) Cross-section **(b) Unexposed side**

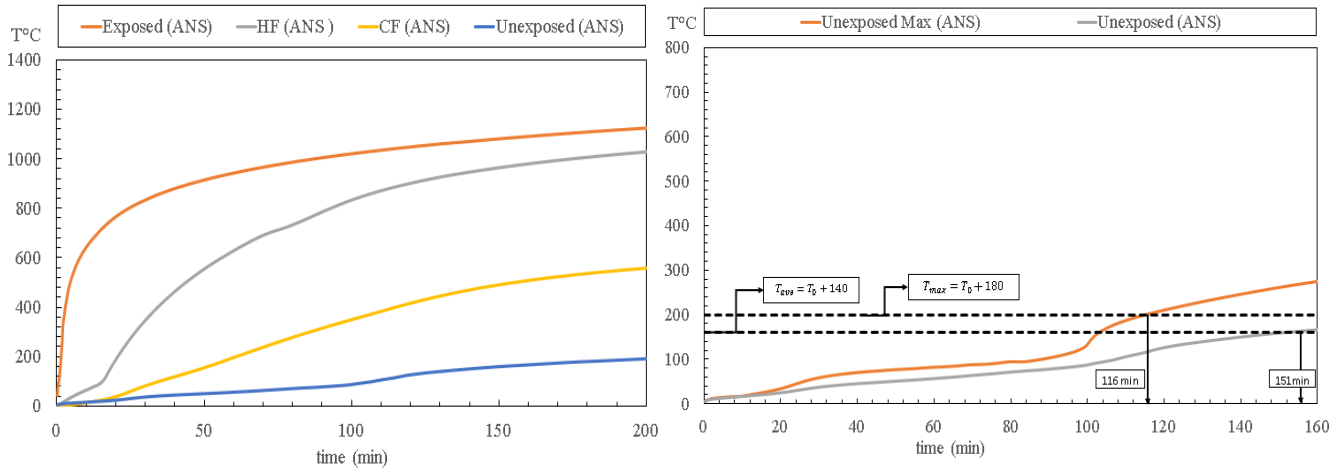

Figure 6.5:Numerical results for Model 2 Specimen 4

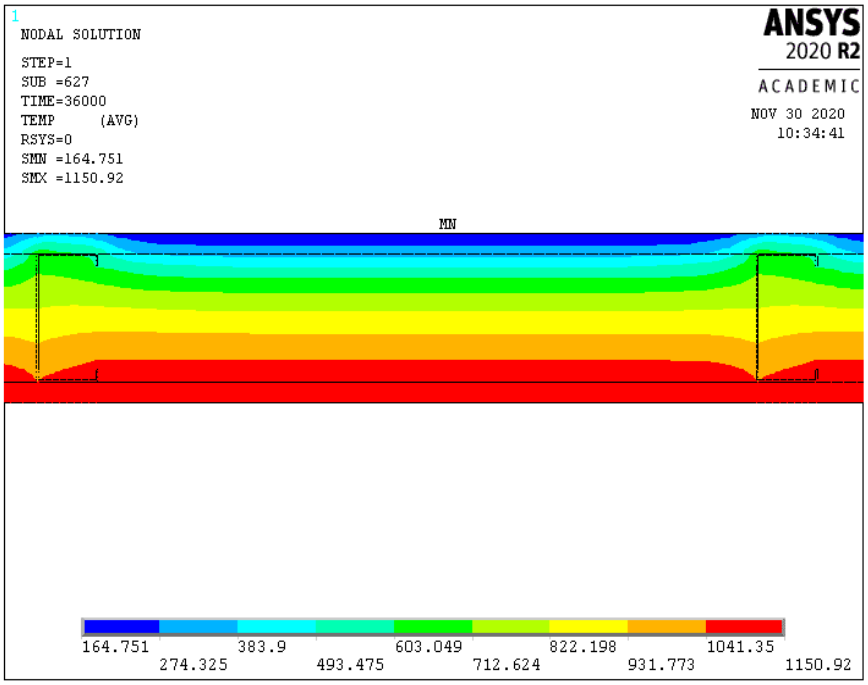

Figure 6.6: Numerical results for Model 2 Specimen 4, t=600min

Table 6.2:Characteristics and fire resistance of the wall assemblies used for parametric analysis.

Case	TH_ cavity [mm]	Density Gypsum Plasterboard[kg/m 3]	Density Glass Fibre [kg/m3]	Fire resistance [min] (I) (T_{avg})	Fire resistance [min] (I) (T_{max})
2	100	576	10	151 min	116 min

Table 6.3:Characteristics and fire resistance of the wall assemblies used for parametric analysis.

Parametric Analysis Model 1		Parametric Analysis Model 2	
Fire resistance (T_{ave}) (min)	Fire resistance (T_{max}) (min)	Fire resistance (T_{ave}) (min)	Fire resistance (T_{max}) (min)
139 min	92 min	151 min	116 min

6.1.Discussion of the Results

Two analysis were performed in this section: one on the variation of the protective layer of the structure (2 layers Gypsum plasterboards), another one on the performance of the increasing of the cavity insulation. Parametric analysis and numerical test have been proposals to provide knowledge of the effect of varying certain parameters to increase fire resistance in LSF walls.

6.1.1. Influence of the variation of the protection Layer

One analysis was performed in this section: about the variation of the thickness of the gypsum. (one with 1 layer, the other with 2 layers).

As the Table 6.4 shows, the time needed Time to reach $\boldsymbol{T_{ave}}$ and $\boldsymbol{T_{max}}$ increases with increasing the number of Layers.

Table 6.4:Influence of the variation of the material of the protection layer.

Cases.	Plate Layer	Fire resistance (I) (Numerical simulation)		Fire resistance (I) (Experimental test)	
		Fire resistance (T_{ave}) (min)	Fire resistance (T_{max}) (min)	Fire resistance (T_{ave}) (min)	Fire resistance (T_{max}) (min)
1	1 X 13 mm	56 min	58 min	56 min	59 min
2	2 x 13 mm	139 min	92 min	-----	-----

6.1.2. Influence of cavity thickness due to the dimension of the stud

The parametric analysis based on different dimensions of the stud for the same wall configurations. The table (6.5) presents the fire resistance of the cases for thickness of cavity equal to 92mm and 100 mm.

Table 6.5:Influence of cavity thickness due to the dimension of the stud .

		Fire resistance (I) (Numerical analysis)		Fire resistance (I) (Experimental analysis)	
Cases.	Dimension of the stud	Fire resistance (T_{ave}) (min)	Fire resistance (T_{max}) (min)	Fire resistance (T_{ave}) (min)	Fire resistance (T_{max}) (min)
1	C92X35X15X 1.15	106 min	115 min	134 min	106 min
2	C100X50X10X 1.5	151 min	116 min	------	

The increasing of the thickness due to the modification of the stud dimension provides better thermal insulation because when we increase the thickness of the cavity insulation, this fact justifies the increase of the fire resistance (I).

The fire resistance of non-loadbearing walls depends on the calculation of unexposed walls surface temperature. The temperature is not uniform, depending on the amount of steel included in each type of non-load-bearing wall. Performance standards used for these structural elements consider the average temperature T_{ave} and the highest temperature T_{max}. The calculation of the maximum temperature and the average temperature depends on the distribution of the nodes over the entire length of the unexposed surface.

CHAPTER 7

Conclusion

Numerical simulation of two-dimensional cross sections generally allows the temperature of all materials to be calculated, especially the temperature of unexposed surfaces. This method requires defining the geometric model and the meshing process, which can be time consuming.

This work presented a study across the fire effects on a non-loadbearing walls made with Light Steel Frame (LSF) structure, to improve the knowledge using different configurations and materials. Two specimens with 2 different configurations developed by [56].

Two parametric analysis were performed to evaluate the influence of some parameters in the fire resistance.

In this matter, a comprehensive numerical study using ANSYS® Multiphysics was carried out to predict the fire resistance of LSF walls and identify the relevant parameters of the numerical simulation approach increasing the thickness of the protection layer, among the LSF structure influence, increase the thickness insulation of the cavity, were the most relevant parameters in the fire resistance of the LSF nonloadbearing walls.

Insulating the cavity can also significantly improve fire resistance, but the impact of this solution is proportional to the thickness of the cavity.

The increase of the cavity in to the thickness brings the increase of the fire resistance (I) in fact the relation between the fire resistance and thickness of the cavity has a linear trend.

Recommendations for Further Studies:

Providing experimental data and modelling techniques is particularly useful developing design models and using them in construction practice engineering tools are very important for accurately representing various physical phenomena. In this case, more research needs to be done to better understand fire behaviour. LSF wall expand the knowledge regarding the thermal and structural behaviour of these assemblies:

- Includes various construction materials and their thermal and their thermal and structural response, contribution or deterioration of the fire resistance of the LSF walls, including various sections of cold formed steel.
- Experiment and analyse the thermal properties of materials used to identify possible differences between data.
- Develop different investigations for numerical and experimental research curves, including natural fire models.
- Perform a set of parameter analysis to identify a wide range of parameters, affect the fire resistance of L SF wall, such as insulation, the thickness, geometry and characteristics of studs, Gypsum board and other protective materials, different types of cavities insulation and their position in the assembly.
- Develop a simplified design method to predict the fire resistance of LSF walls supported by parametric analysis, experimental tests and previous research.

References:

[1] E. 1363-1, Fire resistance tests - part 1: General requirements. Brussels: European Committee for Standardization, 2012.

[2] E. 1364-1, Fire resistance tests for non-loadbearing elements. part 1: Walls. Brussels: European Committee for Standardization, 1999.

[3] E. L. S. C. Association, European lightweight steel-framed construction. Belgium, 2004.

[4] T. A. for Specialist Fire Protection (ASFP), Fire rated non-loadbearing partitions - "the purple book", 1st. Surrey: ASFP Publication, 2003, isbn: 1870409213.

[5] P.J. Grubb, M.T. Gorgolewski, R.M. Lawson, Building Design Using Cold Formed Steel Sections: Light Steel Framing in Residential Construction, SCI Publ. P301. (2001) 97.

[6] S. Gunalan, Structural Behaviour and Design of Cold-formed Steel Wall Systems Under Fire Conditions, Queensland University of Technology, 2011.

[7] LSK,European Lightweight Steel-framed Construction, (2005) 92.

https://constructalia.arcelormittal.com/files/european%20lightweight%20steelframed%20construction--627c1249e5c97aecee4a7eb06658b457.pdf

[8] CSSBI, The Lightweight Steel Frame House Construction Handbook, Can. Sheet Steel Build. Inst. (2005) 151.

[9] M.A. Sultan, V.R. Kodur, Light-Weight Frame Wall Assemblies: Parameters for Consideration in Fire Resistance Performance-Based Design, Fire Technol. 36 (2000) 75–88. doi:10.1023/A:1015446207222.

[10] P. Keerthan, M. Mahendran, Thermal Performance of Composite Panels Under Fire Conditions Using Numerical Studies: Plasterboards, Rockwool, Glass Fibre and Cellulose Insulations, Fire Technol. 49 (2013) 329–356. doi:10.1007/s10694-012-0269-6.

[11] M. Feng, Y. Wang, J. Davies, Thermal Performance of Cold-Formed Thin-Walled Steel Panel Systems in Fire, Fire Saf. J. 38 (2003) 365–394. doi:10.1016/s0379-7112(02)00090-5.

[12] P. Kolarkar, M. Mahendran, Experimental Studies of Non-Load Bearing Steel Wall Systems Under Fire Conditions, Fire Saf. J. 53 (2012) 85–104. doi:10.1016/j.firesaf.2012.06.009.

[13] M.A. Sultan, A Model for Predicting Heat Transfer Through Noninsulated Unloaded Steel-Stud Gypsum Board Wall Assemblies Exposed to Fire, Fire Technol. 32 (1996) 239–259. doi:10.1007/bf01040217.

[14] F. Alfawakhiri, M.A. Sultan, Fire Resistance of Loadbearing LSF Assemblies, 15th Int. Spec. Conf. Cold- Form. Steel Struct. (2000) 545–561.

[15] Y. Dias, P. Keerthan, M. Mahendran, Predicting the Fire Performance of LSF Walls Made of Web Stiffened Channel Sections, Eng. Struct. 168 (2018) 320–332. doi:10.1016/j.engstruct.2018.04.072.

[16] K. Poologanathan, M. Mahendran, Numerical Modelling of Load Bearing LSF Walls Under Fire Conditions, in: Struct. Fire-SIF'2012 Proc. 7th Int. Conf. Struct. Fire, Zurich, Switzerland, 2012: pp. 205–214.
[17] Standards Australia, AS 1530.4 - Methods for Fire Tests on Building Materials, Components and Structures, (2005) 151.

[18] M. Rusthi, P. Keerthan, M. Mahendran, A. Ariyanayagam, Investigating the Fire Performance of LSF Wall Systems Using Finite Element Analyses, J. Struct. Fire Eng. 8 (2017) 354–376. doi:10.1108/JSFE-04-2016-0002.

[19] W. Chen, J. Ye, X. Li, Thermal Behavior of Gypsum-Sheathed Cold-Formed Steel Composite Assemblies Under fire Conditions, J. Constr. Steel Res. 149 (2018) 165–179. doi:10.1016/j.jcsr.2018.07.023.

[20] W. Chen, J. Ye, X. Li, Fire Experiments of Cold-Formed Steel Non-Load-Bearing Composite Assemblies Lined With Different Boards, J. Constr. Steel Res. 158 (2019) 290–305. doi:10.1016/j.jcsr.2019.04.003.

[21] International Organization for Stardardization, ISO 834-1 Fire-Resistance Tests - Elements of Building Construction Part 1: General Requirements, (1999).

[22] European Commitee for Standardization, EN 1993-1-2 Eurocode 3: Design of Steel Structures Part 1-2: General Rules - Structural Fire Design, (2005) 78.

[23] European Lightweight Steel-framed Construction. Luxemburg: LSK. Arcelor.; 2005.

[24] J. Gerlich, P. C. R. Collier, and A. H. Buchanan, "Design of light steel-framed walls for fire resistance", *Fire and Materials*, vol. 20, no. 2, pp. 79–96, 1996.

[25] Y. Telue and M. Mahendran, "Design of cold-formed steel wall frames lined with plasterboard on one side under axial compression", International Journal of Steel Structures, vol. 6, no. 1, pp. 1–12, 2006.

[26] S. L. Manzello, R. G. Gann, S. R. Kukuck, K. Prasad, and W. W. Jones, "Performance of a non-load-bearing steel stud gypsum board wall assembly: Experiments and modelling", Fire and Materials, vol. 31, no. 5, pp. 297–310, 2007.

[27] S.-H. Park, S. L. Manzello, M. F. Bundy, and T. Mizukami, "Experimental study on the performance of a load-bearing steel stud gypsum board wall assembly exposed to a real fire", Fire Safety Journal, vol. 46, no. 8, pp. 497–505, 2011.

[28] A.D. Ariyanayagam, Fire Performance and Design of Light Gauge Steel Frame Wall Systems Exposed to Realistic Design Fires, Queensland University of Technology, 2013.

[29] B. Baleshan, Numerical and Experimental Studies of Cold-formed Steel Floor Systems under Standard Fire Conditions, Queensland University of Technology, 2012.

[30] J. Vallée, Reliability of Fire Barriers, Lund University, 2016

[31] Santos P, Martins C, Simões da silva L. Thermal performance of lightweight steel-framed construction systems. Metallurgical Research & Technology 2014;111:329–38.

[32] Santos P, Simões da Silva L, Ungureanu V. Energy Efficiency of Light-weight Steelframed Buildings. 1st ed. European Convention for Constructional Steelwork (ECCS), Technical Committee 14 - Sustainability & Eco-Efficiency of Steel Construction, ISBN 978-92-9147-105-8, N. 129; 2012.

[33] B. Baleshan, "Numerical and experimental studies of cold-formed steel floor systems under standard fire conditions", PhD thesis, Queensland University of Technology April 2012.

[34] N. D. Kankanamge and M. Mahendran, "Mechanical properties of cold-formed steels at elevated temperatures", Thin-Walled Structures, vol. 49, no. 1, pp. 26–44, 2011.

[35] P. Kolarkar and M. Mahendran, "Experimental studies of non-load bearing steel wall systems under fire conditions", Fire safety journal, vol. 53, pp. 85–104, 2012.

[36] D. Kontogeorgos, K. G.Wakili, E. Hugi, and M. Founti, "Heat and moisture transfer through a steel stud gypsum board assembly exposed to fire", Construction and Building Materials, vol. 26, no. 1, pp. 746–754, 2012.

[37] S. Kesawan and M. Mahendran, "Fire tests of load-bearing lsf walls made of hollow flange channel sections", Journal of Constructional Steel Research, vol. 115, pp. 191–205, 2015.

[38] M. Rusthi, P. Keerthan, A. D. Ariyanayagam, and M. Mahendran, "Numerical studies of gypsum plasterboard and mgo board lined lsf walls exposed to fire", in Proceedings of the Second International Conference on Performance-based and Life-cycle Structural Engineering (PLSE 2015), The University of Queensland, 2015, pp. 1077–1084.

[39] A. D. Ariyanayagam and M. Mahendran, "Fire tests of non-load bearing light gauge steel frame walls lined with calcium silicate boards and gypsum plasterboards", Thin-Walled Structures, vol. 115, pp. 86–99, 2017.

[40] V. Jatheeshan and M. Mahendran, "Fire resistance of lsf floors made of hollow flange channels", Fire Safety Journal, vol. 84, pp. 8–24, 2016

[41] S. Kesawan, M. Mahendran, A Review of Parameters Influencing the Fire Performance of Light Gauge Steel Frame Walls, Fire Technol. 54 (2018) 3–35. doi:10.1007/s10694-017-0669-8.

[42] L. Gunawan, Numerical Models to Simulate the Thermal Performance of LSF Wall Panels, Queensland University of Technology, 2011.

[43] P. Keerthan, M. Mahendran, Numerical Studies of Gypsum Plasterboard Panels Under Standard Fire Conditions, Fire Saf. J. 53 (2012) 105–119. doi:10.1016/j.firesaf.2012.06.007.

[44] D.A. Kontogeorgos, M.A. Founti, Gypsum Board Reaction Kinetics at Elevated Temperatures, Thermochim. Acta. 529 (2012) 6–13. doi:10.1016/j.tca.2011.11.014.

[45] E. 1993-1-2, Eurocode 3: Design of steel structures. part 1-2: General rules - structural fire design. Brussels: European Committee for Standardization, 2005.

[46] R. Karwa, Heat and Mass Transfer, Springer, Singapore, 2017.

[47] T.L. Bergman, A.S. Lavine, Fundamentals of Heat and Mass Transfer, 8th ed., John Wiley & Sons, Inc., Hoboken, New Jersey, 2017.

[48] A.H. Buchanan, A.K. Abu, Structural Design for Fire Safety, 2nd ed., John Wiley & Sons, Ltd., Chichester, United Kingdom, 2017.

[49] European Commitee for Standardization, EN 1991-1-2 Eurocode 1 : Actions on Structures - Part 1-2 : General Actions - Actions on Structures Exposed to Fire, (2002) 59.

[50] W. Y.C., Steel and Composite Structures: Behaviour and Design for Fire Safety, Spon Press and Taylor & Francis, London, United Kingdom, 2005.

[51] P. Nithiarasu, R.W. Lewis, K.N. Seetharamu, Fundamentals of the finite element method for heat and mass transfer, 2nd ed., Wiley & Sons, Ltd., Chichester, United Kingdom, 2016. doi:10.1002/0470014164.

[52] European Commitee for Standardization, EN 1991-1-2 Eurocode 1 : Actions on Structures - Part 1-2 : General Actions - Actions on Structures Exposed to Fire, (2002) 59.

[53] W. Y.C., Steel and Composite Structures: Behaviour and Design for Fire Safety, Spon Press and Taylor & Francis, London, United Kingdom, 2005.

[54] T.L. Bergman, A.S. Lavine, Fundamentals of Heat and Mass Transfer, 8th ed., John Wiley & Sons, Inc., Hoboken, New Jersey, 2017.

[55] D.A. Kontogeorgos, M.A. Founti, Gypsum Board Reaction Kinetics at Elevated Temperatures, Thermochim. Acta. 529 (2012) 6–13. doi:10.1016/j.tca.2011.11.014.

[56] M.A. Sultan, A Model for Predicting Heat Transfer Through Noninsulated Unloaded Steel-Stud Gypsum Board Wall Assemblies Exposed to Fire, Fire Technol. 32 (1996) 239–259. doi:10.1007/bf01040217.

[57] S. Lundberg, “Material aspects of fire design. talat lectures 2502 (training in aluminium application technologies, leonardo da vinci project tas/wp (pp. 21)”, EAA
- European Aluminium Association, Queensland University of Technology 1997.

[58] P. Keerthan and M. Mahendran, “Thermal performance of composite panels under fire conditions using numerical studies: Plasterboards, rockwool, glass fibre and cellulose insulations”, Fire technology, vol. 49, no. 2, pp. 329–356, 2013.

[59] Buchanan,A.H.(2001),structural Designe for fire safety,Johny Wiley Sons,HK .

[60] Manzello, SL.Gann, R.C. Kukush, S.R. Prasad, K. and Jones, W.W .(2005),real Fire performance of Partition Assemblies, National Institute of Standards and Technology (NIST), USA.

[61] Manzello, S.L. Gann, R.G. Kukuch, S.R. Lenhert, DB.(2006), Influence of Gypsum Board Type (X or C) on real Fire Performance of Partition Assemblies, National Institute of Standars and technology (NIST), USA.

[62] Sultan, M.A. (1996), A Model for Predicting Heat Through Non-insulated Unloaded Steel-Stud Gypsum Board Wall Assemblies Exposed To Fire, Fire Technology, Vol. 32, No. 3, pp. 239-259 .

[63] Gerlich, J.T. Collier, P.C.R. and Buchanan, A.H.(1996), Design of steel-framed Walls for Fire Resistance, Fire and Materials, Vol.20,No. 2, pp. 79-96

[64] Ranby,A.(1999), Structural Fire Designe of Thin Walled Steel Section, Licentiate Thesis, Department of Civil and Mining Engineering, Lulea University of Technology Stockholm, Sweden.

[65] Outinen, J. Kaitila, O. Makelainen, P. (2000), A Study for the Development of the Design of Steel Structures in Fire Condition, Proceedings of 1^{st} International Workshop of Structural in Fire, Copenhagen, Denmark

[66] Sultan, M.A. and Lougheed, G.D. (1994), The Effect of Insulation on the Fire Resistance of small-scale Gypsum Board wall Assemblies, Proceedings of the Fire and Materials Third International conference and Exhibition, Washington, DC, Interscience communications Limited, London, UK, pp. 11-20

[67] Feng, M. Wang, Y.C and Davies, J.M, (2003), Thermal Performance of Cold-Formed Thin-walled Steel panel systems in Fire Safety Journal, Vol.38,pp.365-394.

[68] Kodur, V. K.R. Sultan, M. A. Latour, J. C. Leroux,P. ad Monette, R. C.(1999), Experimental Studies on the Fire Resistance of Load-bearing Steel walls, Internal Report, IRC, NRC, Ottawa, Canada.

[69] Alfawakhiri, F.(2001), Behaviour of Cold-formed-Steel-Framed Walls and Floors in Standard Fire Resistance Tests, PhD, Thesis, Department of Civil and Environmental Engineering, Carleton University, Ottawa, Ontario, Canada.

[70] Gerlich, J.T. (1995), Design of Load-bearing light Steel Frame Walls For Fire Resistance, Fire Engineering Research Report 95/3. School of Engineering, University of Canterbury , New Zealand .

[71] Feng, M. Wang, Y .C .(2005), An Experimental Study of loaded Full-Scale Cold-Formed Thin Walled Steel Structural Panels Under Fire Conditions, Fire Safety Journal, Vol.40, pp.43-63.

[72] I. Guve, E. Madenci, The Finite Element Method and Applications in Engineering Using Ansys, 2nd ed., Springer, New York, NY, 2015.

[73] E. Yandzio, R.M. Lawson, A.G.J. Way, Light Steel Framing in Residential Construction, SCI Publ. P402. (2015) 125.

[74]European,lightweight,steel,Framed,construction,(2005),(https://constructalia.arcelormittal.com/files/european%20lightweight%20steel,framed%20construction,627c1249e5c97aecee4a7eb06658b457.pdf)

[75] ABNT NBR 14432:2001 ,Exigências de resistência ao fogo de elementos construtivos de edificações – Procedimento, NBR 14432: 2000 ,(2001)

[76] Anthony Deloge Ariyanayagam and Mahen Mahendran, 'Experimental Study of Non-Load Bearing Light Gauge Steel Framed Walls in Fi Re', Journal of Constructional Steel Research, 145 (2018), 529–51 <https://doi.org/10.1016/j.jcsr.2018.02.023>.

[77] Kolarkar, Prakash& Mahendran, Mahen Performance thermique des murs à ossature d'acier revêtus de plaques de plâtre. À LaBoube, R& Wei-Wen, Y (Eds.) Recherches (2008) et développements récents dans la conception et la construction en acier formé à froid. Missouri University of Science & Technology, États-Unis, pp. 517-530 .

[78] https://galusaustralis.com/2020/08/856712/global-light-gauge-steel-framing-market-2020-with-covid-19-impact-analysis-metek-uk-hadley-group-emirates-building-systems-icarus-lsf .

[79] https://www.engenhariaeconstrucao.com/2011/07/vantagens-do-sistema-lsf.html.

[80] http://futurecon.co.za/wp-content/uploads/2016/09/Architects-Pack-Approved-March-2017.pdf

[81] B.C. Son, H. Shoub, Fire Endurance Tests of Double Module Walls of Gypsum Board and Steel Studs, Washington, D.C., 1973.

[82] ISBN 3-456-80526-8 .Series 342.43'088 80-461252 MARC Klippstein , Eberhard . Soziale Erziehung mit .testing in the United States (Klippstein 1978) revealed average steel temperatures at wall failure under E119 test conditions ranging from 740 ° F to over 1,000 .

[83] Sultan, S. (2010) Analysis of Procrastination among University Students (2010). Procedia-Social and Behavioral Sciences, 5, 1897-1904 .

[84] SCI (1993) Computerised analysis tools for assessing the response of .ASCE Journal of Structural Engineering (SCI , Publication 112) ,James RT and Partners (1993) .

[85] Zhao and Xu, 2002; Shi et al., 2002; Wang et al., 2003; Zhao et al., 2002, 2003, 2004; Ding et al., 2004; Luo et al., 2005; Xu et al., 2005; Jiang et al., 2008a). Second method is dynamic downscaling. The regional climate models with the high .

[86] Belmiloudi, Aziz, and Gregory Le Meur. "Mathematical and numerical analysis of dehydratation of gypsum plasterboards exposed to fire." Applied Mathematics and Computation 163.3 (2005): 1023-1041.

[87] Gunawan, L. (2011). Modèles numériques pour simuler les performances thermiques des panneaux muraux LSF (Thèse de doctorat, Queensland University of Technology).

[88] https://www.indiamart.com/proddetail/solar-cold-form-sections-11725143512.html .

[89]https://www.google.com/search?q=Applications+of+Coldformed+Steel+Products+&tbm=isch&ved=2ahUKEwiU4suIkNztAhVHYxoKHZD5B8AQ2-cCegQIABAA&oq=Applications+of+Coldformed+Steel+Products+&gs_lcp=CgNpbWcQDFDdtgVY3bYFYMu-BWgAcAB4AIABdIgBdJIBAzAuMZgBAKABAaoBC2d3cy13aXotaW1nwAEB&sclient=img&ei=IQnfX9TNHMfGaZDzn4AM&bih=663&biw=1366&hl=fr .
[90]https://www.sciencedirect.com/science/article/pii/S0143974X15300390 .

[91]https://www.researchgate.net/figure/Behaviour-of-LSF-wall-studs-when-subjected-to-fire-from-one-side-a-neutral-axis-shift_fig2_275555659 .

[92]https://www.arabnews.fr/node/14976/monde-arabe

[93]https://www.google.com/search?q=Steel+Stud+Wall+System+&tbm=isch&ved=2ahUKEwiuoDunNztAhVQ8IUKHRYnDHIQ2cCegQIABAA&oq=Steel+Stud+Wall+System+&gs_lcp=CgNpbWcQAzIECCMQJzIECAAQHlDDaljDamDda2gAcAB4AIABdIgBdJIBAzAuMZgBAKABAaoBC2d3cy13aXotaW1nwAEB&sclient=img&ei=ixbfX6IF9DglwSWzrCQBw&bih=663&biw=1366#imgrc=KecX8uN_Ic_9pM&imgdii=H_sdYKqCaAPBGM .

[94]https://www.mm.bme.hu/~gyebro/files/ans_help_v182/ans_elem/Hlp_E_PLANE55.html

[95]https://www.google.com/search?q=glass+fiber+&tbm=isch&ved=2ahUKEwiC2Yzs5dztAhUQ4RoKHfYSAEoQ2-cCegQIABAA

Annexes

Interpolation Test 2		*Function and*	*Calculation of*	*Error*	RMS% ERROR	
EXP-CAV-Pb1 (EXP and ANS)						
TIME	Min	**TEMP (Interpol EXP)**	**TEMP (Interpol (ANS)**		RMS %	Relative Error %
30	0,5	28	29		0,001276	3,571428571
41,09088	0,684848	29,87564228	30,23609954		0,000146	1,206525576
43,8636	0,73106	38,96124445	42,82042337		0,009811	9,905173661
46,63632	0,777272	51,99169969	65,03901237		0,062976	25,09499161
50,7954	0,84659	64,52203958	81,17707236		0,066631	25,81293599
54,95448	0,915908	74,15621272	82,69082055		0,013246	11,50895861
61,19311	1,019885	81,28787524	84,23834328		0,001317	3,629653303
67,43173	1,123862	87,09646578	92,507		0,003859	6,212116844
86,14759	1,435793	93,25754793	100,7756567		0,006499	8,061662518
95,92189	1,598698	98,4431754	104,3978101		0,003659	6,048804001
105,6962	1,761603	115,2799336	105,6263103		0,007013	8,374070833
115,4705	1,924508	174,8227989	107,537411		0,148131	38,48776495
120,2448	2,004081	204,9154849	111,4639365		0,207981	45,60492267
125,0192	2,083653	223,9675217	115,390462		0,235021	48,47893071
129,7936	2,163226	237,1946155	121,1332391		0,239423	48,93086472
144,1166	2,401943	247,3066279	127,2117214		0,235818	48,56113543
158,4397	2,640661	256,803952	149,5391325		0,174466	41,7691467
172,7627	2,879379	266,8061228	178,3894631		0,109819	33,13891706
189,0154	3,150256	278,7630506	221,4429236		0,042281	20,56231157
207,6998	3,461663	292,672006	256,8139041		0,015011	12,25197531
222,5588	3,709314	306,1935764	285,0943469		0,004748	6,890813903
237,4179	3,956965	319,7180492	312,7658899		0,000473	2,174465685
258,2734	4,304556	332,3730701	331,9582767		1,56E-06	0,124797525
280,3899	4,673165	344,5961451	350,1504387		0,00026	1,611826971
302,5064	5,041773	355,9849758	361,2109162		0,000216	1,468022732
329,4758	5,491263	367,0280851	371,5220453		0,00015	1,22441862
343,1846	5,719743	377,4528905	379,4340003		2,75E-05	0,524862801
356,8934	5,948223	387,4330579	387,3459553		5,05E-08	0,022481972
370,6022	6,176703	397,1136144	395,2579103		2,18E-05	0,467298031
384,311	6,405183	406,4410765	401,3671665		0,000156	1,248375299
415,9765	6,932941	415,306587	406,6397381		0,000435	2,086855624
447,642	7,4607	424,1472598	413,4668258		0,000634	2,518095728
481,808	8,030134	433,1516006	423,2322181		0,000524	2,290048678
515,9741	8,599568	442,3152351	432,9976105		0,000444	2,106557472
555,476	9,257933	451,5816525	442,271405		0,000425	2,061697478
594,5688	9,90948	461,0494491	451,4658359		0,000432	2,078651917
633,6616	10,56103	470,3172124	458,7499647		0,000605	2,459456601
668,2828	11,13805	479,391881	465,5975872		0,000828	2,877456712
702,904	11,71507	488,3047384	472,3770017		0,001064	3,261843567
738,3953	12,30659	496,5129272	477,4296776		0,001477	3,843454727
773,8866	12,89811	504,207223	482,4823536		0,001857	4,308718415
809,3779	13,48963	513,2022743	487,6644828		0,002476	4,976164907
844,8691	14,08115	521,4260775	492,9118254		0,00299	5,468512852
880,3604	14,67267	529,7562051	498,040335		0,003584	5,986880348
915,8517	15,2642	538,2725409	502,7450611		0,004356	6,600277201
951,343	15,85572	546,4139849	507,4497871		0,005085	7,130893222
986,8343	16,44724	554,2022173	512,6002026		0,005635	7,50664891
1022,326	17,03876	561,6889778	517,843201		0,006093	7,806059682
1057,817	17,63028	568,909123	523,2449336		0,006443	8,02662281
1093,308	18,2218	575,6780394	528,8847676		0,006607	8,128375329
1119,301	18,65501	581,991162	534,5246017		0,006652	8,15589023
1145,293	19,08822	587,9292383	539,4439129		0,006801	8,246796094
1172,43	19,54049	593,5762844	544,3559461		0,006876	8,292167263
1199,786	19,99643	599,0826045	548,7693362		0,007053	8,398385779
1226,382	20,4397	604,3917258	552,8216401		0,00728	8,532559847
1252,292	20,87154	609,4909947	556,7782928		0,00748	8,648643274
1278,202	21,30337	614,2998254	560,271233		0,007735	8,795150212
1304,113	21,73521	618,8622767	563,7641732		0,007927	8,90312846
1333,333	22,22222	623,3871556	568,4808387		0,007758	8,807739524
1362,831	22,71385	627,9742787	573,5776129		0,007503	8,662244238
1392,495	23,20825	632,5977705	578,7004		0,007259	8,520006393
1422,745	23,71242	637,2014375	583,9004		0,006997	8,364864611

1453,85	24,23083	641,6447604	588,2065691		0,006936	8,328314139
1484,955	24,74924	645,9730478	591,7104952		0,007056	8,400126419
1516,079	25,26798					
1547,204	25,78673			SUM	1,743745	
1579,718	26,32863				0,165064	
1612,054	26,86756			RMS %	16,50637	
1643,849	27,39748					
1675,644	27,9274					
1707,439	28,45732					
1739,234	28,98723					
1771,029	29,51715					
1805,331	30,08886					
1839,352	30,65587					
1872,242	31,20403					
1905,131	31,75218					
1938,02	32,30034					
1970,91	32,8485					
2003,799	33,39665					
2036,688	33,94481					
2068,5	34,475					
2099,68	34,99467					
2129,877	35,49795					
2160,073	36,00122					
2190,27	36,5045					
2220,309	37,00516					
2250,349	37,50582					
2281,331	38,02218					
2313,886	38,56476					
2346,441	39,10734					
2384,631	39,74386					
2422,822	40,38037					
2465,415	41,09025					
2500,826	41,68044					
2536,238	42,27063					
2571,88	42,86466					
2603,765	43,39608					
2635,649	43,92749					
2667,534	44,4589					
2699,419	44,99032					
2731,304	45,52173					
2763,189	46,05315					
2795,074	46,58456					
2826,958	47,11597					
2858,843	47,64739					
2890,728	48,1788					
2922,613	48,71022					
2954,498	49,24163					
2986,383	49,77304					
3018,267	50,30446					
3050,152	50,83587					
3082,037	51,36729					
3113,922	51,8987					
3145,807	52,43011					
3177,692	52,96153					
3209,576	53,49294					
3241,461	54,02435					
3273,346	54,55577					
3305,231	55,08718					
3337,116	55,6186					
3369,001	56,15001					
3400,885	56,68142					
3432,77	57,21284					
3464,655	57,74425					
3496,54	58,27567					
3528,425	58,80708					
3560,31	59,33849					
3592,194	59,86991					
3624,079	60,40132					
3655,964	60,93274					
3687,849	61,46415					
3719,734	61,99556					
3751,619	62,52698					

3780	63					

Test 2 For the Unexposed side					
Error RMS% for T ave 160°C		(EXP and ANS)			
Time ref	TEMP Interpolation **T ave (Exp)**	Interpol **T ave (ANS)**		RMS%	Relative Error %
0	22,876	24		0,002414196	4,913446407
60	23,13361906	26,0492102		0,015884227	12,60326423
120	23,43994375	25,82286618		0,01033491	10,16607575
180	23,74626843	25,96728176		0,008748057	9,353104595
240	24,81815291	26,8135495		0,006464271	8,04006888
300	26,9916966	28,23406151		0,002118546	4,602767017
360	30,6180495	29,96829358		0,000450345	2,122133598
420	34,69816695	31,8197065		0,006881886	8,295713296
480	38,52656707	33,71627781		0,015589126	12,48564206
540	41,94076568	35,61864038		0,022722363	15,07393869
600	45,27243077	37,46781299		0,0297191	17,23922848
660	47,68012308	39,23840001		0,031346385	17,7049104
720	50,08781538	40,92440204		0,033469589	18,29469557
780	51,85552308	42,5615554		0,032122717	17,92281155
840	53,21748889	44,16562882		0,028931231	17,009183
900	54,47909477	45,75685714		0,025632801	16,01024698
960	55,47209023	47,42355598		0,021051572	14,50915986
1020	56,4650857	49,31794361		0,016021562	12,65763082
1080	57,32145279	51,64131076		0,009819379	9,909277859
1140	58,15275787	54,58290753		0,003768421	6,138746419
1200	59,55225068	57,84117568		0,000825547	2,873233121
1260	61,61339932	60,87382688		0,000144082	1,200343511
1320	63,67454797	63,57485761		2,45118E-06	0,156562339
1380	65,28511728	66,02361197		0,000127958	1,131183821
1440	66,44869753	68,3038129		0,000779415	2,791800956
1500	68,08500745	70,26777069		0,001027804	3,205938169
1560	70,0957735	71,95847041		0,000706156	2,657359802
1620	72,07673016	73,51118325		0,00039608	1,990175041
1680	73,87903896	75,03782808		0,000246018	1,568495117
1740	75,66432772	76,50820861		0,000124388	1,11529557
1800	77,20069832	77,71181795		4,38331E-05	0,662066081
1860	78,73706891	78,78663927		3,96356E-07	0,062956824
1920	80,29379529	79,93481885		1,99879E-05	0,447078672
1980	81,87520079	81,21239571		6,5534E-05	0,809530933
2040	83,3927948	82,4270324		0,000134117	1,158088537
2100	84,57785564	83,32045429		0,000221021	1,486679161
2160	85,76291649	84,2771121		0,00030014	1,732455528
2220	86,89410827	85,44176532		0,000279356	1,671394043
2280	88,00992866	86,82459951		0,000181391	1,346812992
2340	89,20808611	87,92025738		0,000208405	1,44362332
2400	90,53235476	88,57126861		0,00046923	2,166171591
2460	91,8566234	89,48470664		0,000666773	2,582194593
2520	93,61409744	90,83212815		0,000883125	2,971741824
2580	95,38589231	92,49333025		0,000919596	3,032484145
2640	97,12546528	93,9522766		0,001067396	3,267102678
2700	98,84595139	94,41987205		0,002005029	4,477754802
2760	100,7179853	94,9074809		0,003328232	5,76908321
2820	102,9062115	96,49267135		0,003884297	6,232413015
2880	105,0944376	98,62405672		0,003790533	6,156730149
2940	108,4554343	101,093573		0,004607577	6,787913705
3000	112,2242136	103,8339984		0,005589501	7,476296767
3060	116,8906932	106,9312437		0,007259568	8,520310041
3120	125,4858177	110,6321561		0,014011278	11,83692457
3180	134,5228458	115,1419741		0,020756519	14,40712287
3240	144,5959085	121,6250059		0,025237371	15,88627425
3300	157,9979458	138,440638		0,015321993	12,37820383
3360	169,2400158	160,121027		0,002903269	5,388198944
3420	175,8431711	174,021322		0,000107343	1,036064742
3480	182,140639	184,6964621		0,000196901	1,403214058
3540	187,3408419	193,6081365		0,001119168	3,345396801
3600	191,6966738	201,4011388		0,002562796	5,062406559
3660	194,7782169	208,6327098		0,005059417	7,112958019
3720	197,3239797	215,621026		0,008598095	9,272591362
			SUM	0,459669769	
				0,085418649	
			RMS %	8,54186487	